applied sciences

MDPI

Review

Articular Cartilage: Structure, Biomechanics, and the Potential of Conventional and Advanced Diagnostics

Robert Karpiński [1,2,*], Aleksandra Prus [3], Jacek Baj [4], Sebastian Radej [2], Marcin Prządka [5], Przemysław Krakowski [6,7] and Kamil Jonak [3]

1 Department of Machine Design and Mechatronics, Faculty of Mechanical Engineering, Lublin University of Technology, 20-618 Lublin, Poland
2 Department of Basic Medical Sciences, Faculty of Medicine, John Paul II Catholic University of Lublin, 20-950 Lublin, Poland; sebastian.radej@kul.pl
3 Department of Technical Computer Science, Faculty of Mathematics and Information Technology, Lublin University of Technology, 20-618 Lublin, Poland; a.prus@pollub.pl (A.P.); k.jonak@pollub.pl (K.J.)
4 Department of Anatomy, Medical University of Lublin, 20-059 Lublin, Poland; jacek.baj@umlub.pl
5 Department of Orthopedics and Movement Traumatology, Provincial Integrated Hospital, Szpitalna 45, 62-504 Konin, Poland; marcinprzadka@poczta.onet.pl
6 Department of Trauma Surgery and Emergency Medicine, Medical University of Lublin, 20-059 Lublin, Poland; przemyslaw.krakowski84@gmail.com
7 Orthopaedic and Sports Traumatology Department, Carolina Medical Center, 78 Pory St., 02-757 Warsaw, Poland
* Correspondence: r.karpinski@pollub.pl

Abstract: Articular cartilage (AC) plays an important role in the biomechanics of synovial joints. Its task is to enable smooth movement and transfer of mechanical loads with minimised friction. AC is characterised by unique mechanical properties resulting from its complex structure, in which the dominant components are type II collagen, proteoglycans and water. Healthy articular cartilage shows elasticity in compression, viscoelastic properties, and the ability to relax stresses under the influence of cyclic loads. In response to different loading modes, it shows anisotropic and non-uniform behaviour, which translates into its cushioning and protective function for the subchondral bone. Significant changes occur in the structure and mechanical properties of cartilage with age as a result of mechanical overload or degenerative diseases, such as osteoarthritis. This results in a deterioration of the cushioning and mechanical function, which leads to progressive degradation of joint tissues. Understanding the mechanical properties of AC is crucial for developing effective diagnostic methods. Analysis of changes in mechanical properties contributes to the early detection of pathological changes. The aim of this paper is to review the current state of knowledge regarding the structure and biomechanical properties of articular cartilage, and to analyse conventional and alternative diagnostic methods in the context of their suitability for assessing the state of AC, particularly in the early stages of degenerative processes.

Keywords: articular cartilage; biomechanics; tissue engineering; osteoarthritis; anatomy; diagnostics; friction; wear

check for updates

Academic Editor: Andrea Vescio

Received: 23 May 2025
Revised: 12 June 2025
Accepted: 16 June 2025
Published: 18 June 2025

Citation: Karpiński, R.; Prus, A.; Baj, J.; Radej, S.; Prządka, M.; Krakowski, P.; Jonak, K. Articular Cartilage: Structure, Biomechanics, and the Potential of Conventional and Advanced Diagnostics. *Appl. Sci.* **2025**, *15*, 6896. https://doi.org/10.3390/app15126896

Copyright: © 2025 by the authors. Licensee MDPI, Basel, Switzerland. This article is an open access article distributed under the terms and conditions of the Creative Commons Attribution (CC BY) license (https://creativecommons.org/licenses/by/4.0/).

1. Introduction

Articular cartilage (AC) is a smooth, elastic, and glassy connective tissue that covers the interacting bony surfaces in diarthrodial joints [1–4]. It is one of the most vulnerable elements in the human body to overload and degenerative changes [3]. Articular cartilage includes proteoglycans and collagen, organised into zones containing articular chondrocytes [4–6]. The main function of AC is to facilitate load transfer with a low friction

coefficient, thereby protecting the subchondral bone [7]. It also provides wear resistance as well as shock absorption of up to eight times the body weight [4,8]. Due to constant exposure to mechanical stress, it is susceptible to wear and tear and traumatic injuries. As it is a non-vascular tissue, its ability to regenerate itself is limited [9]. To a large extent, musculoskeletal abnormalities are associated with articular cartilage injuries [2]. In most cases, once articular cartilage is damaged, it is not possible to fully recover its structure, function and also its biomechanical properties, resulting in degeneration and ultimately osteoarthritis (OA) [7,10,11]. People affected by joint cartilage damage struggle with impaired movement of the limbs and trunk, pain and reduced quality of life. Due to the ageing population, more and more people are affected by this problem [12]. Surgical joint replacement is often used to restore cartilage function. However, this solution is associated with the risk of complications and residual pain [13].

A key element in the early detection and monitoring of osteoarthritis progression, a key element is the assessment of AC status. Typical diagnostic methods used in clinical practice include magnetic resonance imaging (MRI), ultrasound, and computed tomography with arthrography (CT-arthrography) [14–17].

MRI is the most commonly used method to assess the condition and structure of the AC. It is characterised by its ability to assess the volume and thickness, as well as integrity of the AC layers, and is a non-invasive method with high spatial and contrast resolution [16,18]. On the other hand, it also has its limitations related to the high cost, especially of advanced imaging protocols, long examination times and sensitivity to patient movement. With MRI, there is only an indirect assessment of the biomechanical properties of the AC [19,20].

CT arthrography is a particularly useful method in joints that are difficult to access for MRI and has a shorter examination time [21]. The method provides a very good visualisation of the AC surface. However, it requires the administration of contrast into the joint cavity and exposure of the patient to ionising radiation, which may be associated with additional pain, infection or allergic reactions, and limits the possibility of repeated examinations [22]. In addition, assessment of the biomechanical properties of the cartilage is not possible.

The diagnosis of degenerative changes according to the Kellgren–Lawrence scale is based on radiography (X-ray) [23]. Factors indirectly assessing the quality of AC are the presence of osteophytes, joint stenosis, joint surface deformities and subchondral bone hypertrophy [24]. The advantages of this imaging modality are low cost, high availability, and low patient exposure to ionising radiation. However, one of its biggest disadvantages is the lack of imaging of the articular cartilage, which only shows the bony changes that result from cartilage damage. Conventional radiography also does not provide information about the surrounding soft tissues [23,25–27].

Ultrasound is a fast, widely available and low-cost imaging modality that allows real-time assessment of the AC surface [17,28]. Unfortunately, it is not useful in assessing the internal structures of the AC, as well as its biomechanical properties, due to its low resolution [28,29]. The examination performed also mainly depends on the experience and skill of the operator [17].

Arthroscopy is a surgical procedure that allows visual assessment of joint structure, including articular cartilage, using a camera that transmits images to a monitor. In the case of AC damage, arthroscopy can provide more precise information. During this procedure, the surgeon is able to see and evaluate the thickness, smoothness of the surface, the presence of cracks, defects or degenerative changes in the articular cartilage. In addition, it allows AC samples to be taken for histopathological analysis, which aids in the diagnosis of certain diseases of the knee joint. Arthroscopy serves mainly as a therapeutic tool; as a surgical

procedure, it can involve the risk of complications, such as infection, bleeding, infection of the joint, or damage to nerves or blood vessels.

Due to the limitations of the above-mentioned methods, there is growing interest in so-called alternative diagnostic methods to assess the mechanical and biochemical properties of AC. Magnetic resonance elastography (MRE) is a method that illustrates the distribution of tissue stiffness based on shear wave propagation [30]. On the other hand, advanced MRI techniques in the form of T1ρ- or T2-mapping or dGEMRIC (delayed gadolinium-enhanced MRI of cartilage) make it possible to detect changes in the collagen, proteoglycan and water content, parameters that are associated with early degradative changes in AC [31,32]. Real-time assessment of AC mechanical susceptibility and monitoring of OA progression is possible using ultrasound elastography [33]. A significant method to provide information regarding changes in the mechanical properties of the joint surface is vibroarthrography (VAG), which involves recording the vibrations emitted by the joint during movement [34]. The use of VAG is particularly useful in the evaluation of early changes in OA. Optical techniques can also be used, such as optical coherence tomography (OCT), which involves imaging with a resolution comparable to in vivo histology of the AC microstructure [35]. On the other hand, the use of Raman spectroscopy makes it possible to obtain information on the molecular composition of AC, such as the distribution of proteoglycans and collagen, which can be used as a biomarker of degeneration [36]. Another continuously developed approach is modal analysis, which makes it possible to assess the dynamic mechanical properties of AC, which in turn may be altered by tissue degeneration [37]. Although alternative methods of AC diagnosis are in the experimental research phase, they nevertheless show potential for the detection of early degenerative changes.

The aim of this paper is to analyse the mechanical parameters of AC and to assess their changes during degradation processes such as osteoarthritis. The suitability of classical as well as alternative diagnostic methods to detect and monitor changes in the structure, biomechanical and biochemical properties of AC is presented. The aim of the study is also to indicate possible directions for the development of diagnostics based on mechanical parameters and their correlation with the patient's clinical condition, which requires the synthesis of knowledge from various disciplines, such as anatomy and biomechanics.

Unlike many earlier reviews that focus narrowly on the biological composition or imaging diagnostics of articular cartilage, the present study offers a comprehensive and interdisciplinary perspective that integrates cartilage microstructure, mechanical properties, and both conventional and alternative diagnostic techniques. Particular emphasis is placed on methods capable of assessing the biomechanical and biochemical state of articular cartilage at early stages of degeneration. A distinguishing feature of this review is the critical synthesis of measurement techniques (e.g., indentation, elastography, vibroarthrography) in relation to specific mechanical parameters (e.g., Poisson's ratio, tensile modulus, shear loss angle), which are often discussed in isolation in previous literature. Furthermore, this work highlights the translational potential of high-resolution diagnostics in supporting regenerative medicine and biofabrication approaches, paving the way toward more personalised and mechanobiology-informed treatment strategies. This integrative view contributes to bridging the gap between fundamental cartilage biomechanics and clinical decision-making.

The article focuses on the mechanical parameters of articular cartilage and their changes during osteoarthritis, as well as typical and alternative diagnostic methods. The article is divided into sections that systematically discuss the most important issues related to the topic of AC. They include the Introduction, introducing the problem and the aim of the work. Then, the Anatomy of Articular Cartilage is presented, describing its structure and functions. The next section is Biomechanics of Articular Cartilage, focusing on the

analysis of mechanical properties and behaviour under load. The Articular Synovial Parameters section discusses the composition and importance of synovial fluid in the context of joint function. The next section is Degradation of Articular Cartilage, including degradation processes leading to its damage. Then, Alternative Methods of Articular Cartilage Diagnosis describes modern approaches to assessing the condition of AC, and ends with the Summary and Conclusions.

2. Anatomy of Articular Cartilage

Articular cartilage can be characterised as an elastic, smooth and glassy tissue with a thickness of 2 to 4 mm [2,38,39]. However, it has no blood vessels, lymphatics or nerves, and nutrition comes from the synovial fluid. The primary function of articular cartilage is to distribute the load over as large a surface area as possible with minimal frictional resistance and high wear resistance. Another function is to protect the underlying bone by providing flexibility and resistance to compressive forces [40].

AC exhibits complex biomechanical behaviour compared to classical models used in materials mechanics. Its properties depend on factors such as loading, deformation rate, and biological and chemical conditions. The non-linearity of articular cartilage is due to its multilayered structure, as well as the dynamic interaction between the interstitial fluid and structural components. To understand the non-linearity of AC, it is necessary to take an interdisciplinary approach to the issue, combining anatomy, mechanics and physiology. From an anatomical point of view, it is important to consider the layered structure, as well as the differing functions of the different cartilage zones. The mechanical approach takes into account, among other things, anisotropic and viscoelastic properties. In terms of physiology, the influence of biological factors should be analysed. Particularly relevant are fluid circulation, chondrocyte nutrition and degenerative processes. AC can therefore be described as one of the most complex biological materials due to its biomechanical properties. Understanding its non-linearity provides the basis for developing new, effective diagnostic and therapeutic strategies in orthopaedics and tissue engineering.

2.1. Zonation and Regional Organisation

The structure of articular cartilage consists of a dense extracellular matrix (ECM) with a sparse distribution of highly specialised cells called chondrocytes. It is composed of water, proteoglycans, collagen, along with other less common non-collagenous proteins and glycoproteins [2,4,41–43]. The combination of such ingredients influences water retention in the ECM, which in turn contributes to maintaining its mechanical properties. Chondrocytes contribute to the zonal structure of articular cartilage. It is divided into four distinct zones: I superficial zone, II middle zone, III deep zone, and IV calcified zone. A schematic cross-sectional diagram of healthy articular cartilage is shown in Figure 1 [44]. Each of the above-mentioned zones exhibits different biomechanical and biochemical properties. Depending on the tissue layer, the proteoglycan concentration and water content are variable. The amount of proteoglycans is higher from the superficial to the deep zone, while the water concentration decreases from the superficial to the deep zone [4,43,45].

The superficial zone has a protective function for the deeper layers against shear stresses. It accounts for approximately 10–20% of the thickness of the articular cartilage [2,4]. In this layer, there are numerous flattened and smaller chondrocytes with a higher density as opposed to cells deeper in the matrix. The collagen fibres are arranged very tightly, with their position aligned parallel to the articular surface. The zone is mostly water and a small amount of proteoglycans. The superficial zone, otherwise known as the tangential zone, directly borders the synovial fluid. It is responsible for the tensile properties of the articular cartilage, which is what allows it to resist the shearing, compressive and tensile

forces exerted by the articulation. A characteristic feature of the superficial zone is its deformability and lower stiffness compared to the other zones.

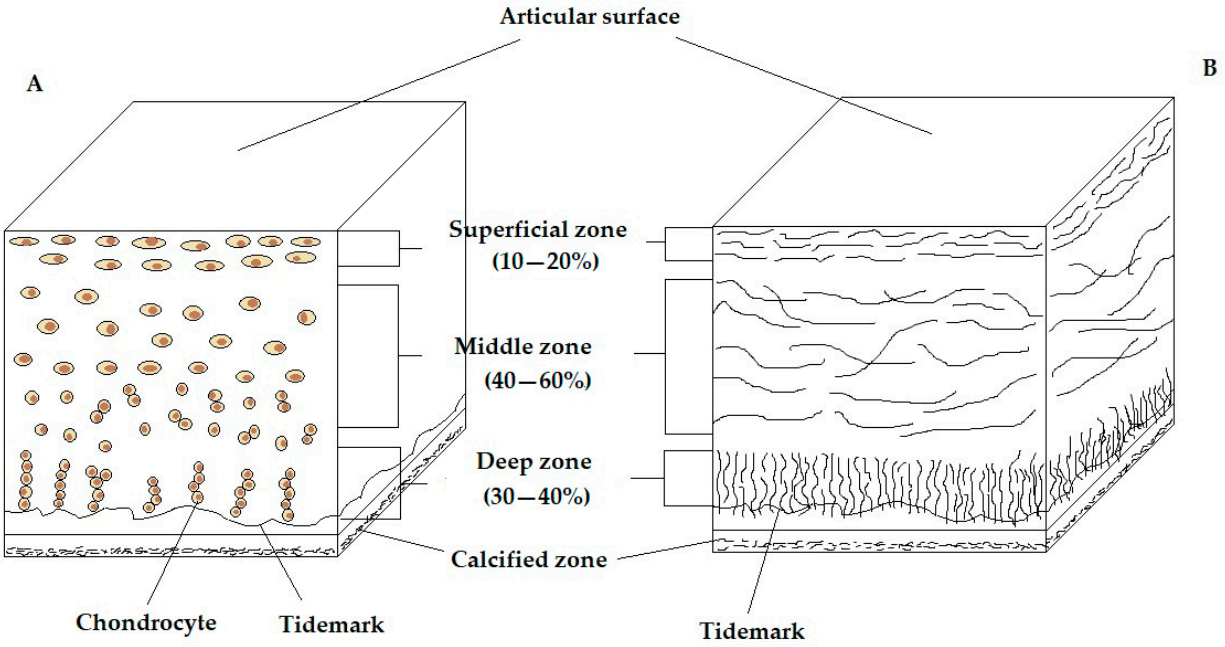

Figure 1. Schematic, cross-sectional diagram of healthy articular cartilage; (**A**)—cellular organisation in the zones of articular cartilage, (**B**)—collagen fibre architecture.

The middle zone, otherwise known as the transitional zone, accounts for 40–60% of the articular cartilage volume. It consists of proteoglycans and thicker collagen fibres organised obliquely. Chondrocytes are spherical and have a low density. This zone is responsible for resisting compressive forces.

The third zone is the deep zone, which accounts for approximately 30% of the articular cartilage volume. Due to the perpendicular alignment of the largest diameter collagen fibres radially to the articular surface, it provides the greatest resistance to compressive forces. It also features the lowest water concentration and the highest proteoglycan content. The position of the chondrocytes is in a columnar orientation, perpendicular to the joint line and parallel to the collagen fibres.

There is a tidal mark between the deep and calcified zones, separating the lime-poor cartilage from the lime-rich cartilage. It consists of strands of fibrils that are attached to collagen fibres anchored in a lime-poor layer, which prevents the cartilage from detaching from the bone [46].

The deepest zone is the calcified zone. It is characterised by numerous recesses, protrusions and interlacing, which contribute to the high resistance to shear forces and prevent the cartilage from detaching from the underlying bone. The calcified zone secures the cartilage to the subchondral bone through the collagen fibres of the deep zone, which are anchored to the subchondral bone. Chondrocytes in this zone are hypertrophied, and the cell population is sparse.

The matrix is also made up of regions that differ in their proximity to chondrocytes, as well as in the composition, diameter and organisation of collagen fibrils. These regions include pericellular, territorial and interterritorial regions. The pericellular matrix is mainly composed of proteoglycans, glycoproteins and other non-collagenous proteins. It is a thin layer that adheres to the cell membrane and surrounds the chondrocyte. The pericellular matrix may be responsible for initiating signal transduction in cartilage under load-bearing conditions [2,47]. The pericellular matrix is surrounded by a territorial matrix, consisting

primarily of fine collagen fibres [48,49]. This region has a protective function for cartilage cells against mechanical stress. It also influences the resilience of the articular cartilage structure, as well as the ability of the cartilage to withstand significant loads [50]. The largest of the regions is the interarticular region, which is most responsible for the biomechanical properties of the articular cartilage [51]. In this region, the large collagen fibrils are randomly oriented bundles. They are arranged parallel to the surface of the superficial zone, perpendicular to the joint surface in the deep zone and obliquely in the medial zone. There is also a large amount of proteoglycans in this region.

2.2. Chondrocytes

Chondrocytes can be characterised as highly specialised and metabolically active cells. They are the resident cell type in articular cartilage [2]. Their share of the total articular cartilage volume is approximately 2% [52]. Chondrocytes produce enzymes that regulate extracellular matrix synthesis and growth factors [53]. When deposited in the ECM, they form articular cartilage [54]. The classic markers of the chondrocytic phenotype are the main components of the ECM, which include collagen II (COL2) and aggrecan (ACAN) [55].

In healthy articular cartilage, the chondrocyte population represents resting and differentiated cells whose function is to maintain a dynamic relationship between the anabolism and catabolism of the ECM [56,57]. Mature chondrocytes are stored in lacunae in isogenic groups of a few cells in the territorial matrix in the vitreous cartilage in a specific physico-chemical environment [57]. They arise by mitotic division from a single mother cell [2]. The shape of the chondrocytes can be characterised as round or oval. The cytoplasm of chondrocytes has a small, spherical nucleus and contains the Golgi apparatus, mitochondria and lipid droplets [58].

Chondrocytes are formed from bone marrow mesenchymal stem cells (BMSCs) [53]. Aggregated BMSCs have the ability to differentiate into chondroprogenitor cells and then become chondrocytes. The resulting chondrocytes go through differentiation processes so that they develop into hypertrophic chondrocytes. When the cartilage matrix is partially calcified, chondrocytes are gradually replaced by osteoblasts after apoptosis and endochondral ossification [53]. Apoptosis and chondrocyte hypertrophy are natural processes of endochondral ossification, but contribute to the more rapid development of osteoarthritis (OA) if cartilage is damaged [59].

The growth, metabolism, or differentiation of chondrocytes is an extremely complex process. Cytokines and cellular signals interact to maintain cartilage homeostasis and regulate chondrocyte function [60–62]. Therefore, an important aspect is to understand the impact of the interaction of regulatory factors and cellular signals on the growth and development of chondrocytes.

An important influence in the differentiation of bone marrow mesenchymal stem cells into chondrocytes is the SRY-box 9 (Sox9) protein, which acts as a transcription factor [61]. It can be combined with ACAN and COL2, which affect the activation of its own gene expression and induction of chondrocyte proliferation, as well as ECM synthesis [63,64]. Glutamine plays an important role in controlling the expression of chondrogenic genes, protecting the survival of chondrocytes and their proliferation and ECM synthesis [53]. However, this is associated with the stimulation of glutamine metabolism by Sox9 [65]. In order to maintain the chondrocyte phenotype, the Sox9 protein found in significant amounts in chondrogenic and cartilage progenitor cells is essential [66]. The role of Sox9 is also to inhibit the differentiation of chondrocytes into pro-hypertrophic chondrocytes, not participating in the final stage of further differentiation of hypertrophic chondrocytes [67]. For full expression of the chondrocyte phenotype, cooperation between high expression of

the alpha-1 type collagen gene (COL2A1) and high expression of Sox9 is required [57]. The function of the COL2A1 gene is to encode the cartilage-specific molecule COL2 [66].

Another important transcription factor mediating chondrocyte maturation is runt-related transcription factor 2 (Runx2). In proliferating chondrocytes, low expression of Runx2 is observed, which increases in terminally differentiated and hypertrophic chondrocytes [68,69]. The function of Runx2 is to regulate collagen X expression in hypertrophic chondrocytes [70]. The use of Runx2 to regulate chondrocyte differentiation and apoptosis is made possible by its effect on chondrocytes [71]. Osteoarthritis has been observed to be associated with a higher expression of Runx2 in chondrocytes, compared to normal chondrocytes [72]. In contrast, a decrease in this factor contributes to slowing the progression of OA. In conclusion, Runx2 can be described as an important factor in chondrocyte maturation, and it is also involved in the pathogenesis of OA.

Mature chondrocytes are responsible for the production of collagen types II, IX and XI (COL2, COL9, COL11), structural proteins and ACAN [73]. The task of chondrocytes with a natural and intact phenotype is to synthesise lubricin, proteoglycan-4 (PRG4), and a glycoprotein [57]. Chondrocytes have an extremely important lubricating function, thus reducing friction between adjacent cartilage surfaces. The inhibitory effect on inflammatory cytokines and their activation of synovial membrane fibroblast proliferation is demonstrated by PRG4 [74].

Integrins have an important function in cell adhesion and cell-to-cell and ECM interactions [57]. Integrins can be characterised as transmembrane receptors whose function is to recognise specific ECM molecules [2,75,76]. Chondrocytes are characterised by the expression of integrins α1β1, α3β1, α5β1, α10β1, αVβ1, αVβ3 and αVβ5 [77,78]. An important integrin whose role is to bind COL2 in cartilage tissue is integrin α10β1. It also acts as a marker to determine the phenotype of chondrocytes. Integrin α10β1 is a component of the cell–matrix interaction required for cartilage development and MSC chondrogenesis [77,79]. Chondrocytes express the types of integrins that bind to ECM molecules [80]. The hyaluronan receptor CD44 is an isotopic membrane receptor of chondrocytes [81]. The binding of chondrocytes and HA affects the homeostasis of the cartilage environment, and if this binding is blocked, the ECM is damaged and degraded [80,82].

Cell metabolism is also regulated by the release of soluble factors [57]. The transforming growth factor-beta (TGF-β) superfamily plays a key role in pathological and physiological phenomena by influencing tissue cell growth and differentiation, and adhesion [83]. This group of activins includes more than 30 proteins and bone morphogenetic proteins (BMPs) [84]. They take part in the maintenance of homeostasis, immune events and embryogenesis [85,86]. TGF-β is involved in the formation of cartilage, as well as bone tissue [87].

TGF-1 is one of the most extensively studied growth factors [88]. TGF-2 has also been the subject of research into disorders and the treatment of cartilage defects [89]. It is involved in the activation of mitogen-activated protein kinase (MAPK) in chondrocytes [50]. BMPs belong to the TGF-β family, showing stimulatory effects in the process of chondrogenesis. Their role is also to support the condensation step at the onset of chondrogenesis. In addition, BMPs affect the expression of COL2 and Sox9 [58].

Chondrocytes can vary in number, shape and size depending on the zones in which they are located. In the superficial zone, they are smaller, denser, and their shape is flatter compared to the chondrocytes found deeper in the matrix. Chondrocytes do not normally form intercellular contacts for intercellular communication or direct signal transmission. Their response is related to factors such as growth factors, piezoelectric forces, mechanical loads, and hydrostatic pressure [90]. Due to the limited replication potential of these cells, the intrinsic healing capacity of cartilage is limited.

2.3. Collagens

The most structural macromolecule in the ECM is collagen, accounting for 60–85% of cartilage's dry weight [2,4]. The orientation of collagen fibrils varies depending on the zone of the articular cartilage [91]. Collagen types I, II, IV, V, VI, IX and XI are found in the ECM, but type II accounts for 90–95% of the total collagen, with the remaining types constituting a minor part, participating in the formation of fibrils and fibres associated with proteoglycan aggregates [2,4,43,92]. Intramolecular and intermolecular connections between fibrils influence the elasticity of the collagen network. In addition, proteoglycans that are mechanically coupled and bound to water form cross-links, which results in resistance to compressive forces, thereby increasing the tension in the collagen network. Tensile strength is the most important property of collagen fibres. In turn, compressive strength, elasticity and durability are provided by water–proteoglycan compounds.

Collagen II represents the majority of the collagen found in hyaline cartilage [93]. It is the main indicator of differentiation of hyaline cartilage, as the predominant collagen of heterofibrils. Collagen II accounts for approximately 75% of foetal collagen, while its value increases to 90% as the tissue matures [94].

Collagen IX binds to other collagen IX molecules via covalent bonds and also binds to collagen II molecules via cross-linking bonds [95]. This type of collagen is only found in AC and a few other tissues, so it can be used as a marker to differentiate cartilage. With maturation, the expression of collagen IX is increased, which may indicate that it plays an important role in development [96]. In vivo studies have confirmed that collagen IX has an impact on the development and integrity of AC, prevents dysplasia of the bone epiphysis, and influences the development of the cartilage growth plate [97,98].

Collagen XI is a fibrillar collagen that combines with collagen II. It accounts for about 10% of the total collagen in foetal cartilage, while in adult tissue it is only 3% [94]. Collagen XI molecules bind to other collagen XI molecules via cross-links within heterofibrils [95]. This type of collagen has also been shown to reduce fibrinogenesis by inhibiting the growth of collagen II fibrils [99].

Collagen VI is found in the pericellular matrix immediately surrounding the chondrocytes [100]. It contains an Arg-Gly-Asp sequence by which it binds to chondrocyte receptors [101]. The interaction between collagen IV and chondrocytes contributes to mechanotransduction, which implies that replication of this collagen structure is important in order to create a suitable microenvironment for chondrocytes [102]. The collagen VI content constitutes less than 1% of the total collagen in an adult human [94].

Collagen I is produced in various connective tissues, but it is not usually expressed in the articular cartilage of the hyaline joint. Nevertheless, it is found in tissues such as the tendon, ligament, meniscus and disc of the temporomandibular joint. Collagen I is also observed in fibrocartilage, which fills defects in damaged AC [101]. In tissue-engineered AC, the expression of collagen I is undesirable. In vitro culture of chondrocytes can affect dedifferentiation and collagen production [103]. This allows collagen I to act as a marker of the differentiation state of chondrocytes in tissue engineering procedures [101].

Collagen X is found exclusively near bone. Immunohistological studies have shown the presence of collagen X in the hypertrophic and calcifying cartilage zone [104]. Also, this type of collagen is expressed on the articular surface of maturing cartilage through certain cells, as well as in AC with osteoarthritis [105–107]. However, the presence of collagen X in tissue-engineered structures may indicate chondrocyte hypertrophy. A summary of the types and molecular structure of collagen in articular cartilage is shown in Table 1, based on [108].

Table 1. Types and molecular structure of collagen in articular cartilage.

Classification	Type	Molecules	Concentrations [%]
Fibrillar	II	3 × α1(II)—triple helix	90–95
	XI	α1(XI), α2(XI), α3(XI)	3–5
	V	α1(V), α2(V), α3(V)	<1
Fibrillar-associative (FACIT)	IX	2 × α1(IX), α2(IX)—collagen side-bonding	1–2
Microfibrillar	VI	3 × α1(VI)—chondrocyte envelope	1–2
Cross-linking	X	Homo-trimers α1(X)—calcified zone	<1

The properties of the collagen network vary considerably from one AC zone to another. The organisation of collagen fibrils itself is also differentiated by zone, which was first described by Benninghoff [109]. In native tissue, the highest collagen concentration is found in the superficial zone, gradually decreasing further away from the articular surface, resulting in a non-uniform distribution [101]. In the superficial zone, the fibrils are oriented parallel to the articular surface. The middle zone is characterised by larger fibres that form interlaced arches. In contrast, the largest fibrils are located in the deep zone and are perpendicularly oriented to the articular surface. The transition from hyaline cartilage to subchondral bone is contained in the calcified layer. The zonal variation is influenced by the distribution of forces that the cartilage experiences in vivo, which affects the anisotropic arrangement in the native tissue [110,111]. The size of the fibrils, therefore, varies depending on the location. Smaller diameters are noticeable near the surface, in the superficial zone, the fibril diameter is about 30–35 nm, while in the deep zone, it is 40–80 nm [112]. As collagen is mainly responsible for the tensile properties of AC, the collagen content should be taken into account when assessing the tensile properties of tissues, as well as the zonal variation in the orientation of collagen fibres.

Within each of the zones mentioned above, there are different types of matrices, which include the territorial matrix, interterritorial matrix and pericellular matrix. The territorial matrix is located furthest from the chondrocytes and is characterised by less ordered collagen fibrils. The interterritorial matrix, located closer to the chondrocytes, is characterised by more oriented fibres with larger diameters. Closest to the chondrocytes is the pericellular matrix, whose function is to buffer the mechanical forces acting on the chondrocytes [48,113–115].

In summary, the collagen network of AC is mainly composed of collagen II, IX, and XI fibrils. Enzymatic and nonenzymatic cross-linking connect the fibrils, with the exception of collagen IX cross-linking. The cross-linking process can affect collagen retention, AC biomechanics, and collagen susceptibility to proteases. Collagen molecules associate laterally or linearly as the tissue matures, resulting in the formation of fibrils and fibres. Collagen has been shown to be characterised by variability in AC (number of fibres and their orientation) depending on the zone.

2.4. Proteoglycans

Proteoglycans are highly glycosylated protein monomers that consist of a protein core with attached glycosaminoglycans [116,117]. They are the second largest macromolecular group in the ECM after collagen, accounting for 10–15% of the wet weight. There are several types of proteoglycans in articular cartilage, such as aggrecan, decorin, biglycan and fibromodulin [2]. Aggrecan is the largest and most abundant proteoglycan, characterised by its ability to interact with hyaluronan. This interaction allows the formation of large aggregates of proteoglycans through linker proteins [118]. Aggrecans, together with collagen, form a porous, strong, fibre-reinforced composite material. No covalent bonds between

collagen and proteoglycans were found; however, the size of the proteoglycan aggregates is an extremely important factor affecting their retention in cartilage [117,119]. The location of the aggrecan is in the interfibrillar space of the ECM cartilage. Its presence influences the osmotic properties of the cartilage, making it capable of resisting compressive loads. Decorin, biglycan and fibromodulin are similar molecules due to their protein structure; however, they differ in their composition and function as glucosaminoglycans. Biglycan is located in the immediate vicinity of chondrocytes, allowing interaction with collagen VI. Fibromodulin and decorin interact in the matrix with fibrils of type II collagen.

Proteoglycans consist of repeating carboxyl and sulphate groups along their chains [117]. When placed in an aqueous solution, these groups become negatively charged, causing a high solid charge density in the cartilage through their tight packing [120].

With a higher concentration density of negatively charged proteoglycans, swelling pressure increases, which in turn leads to tensile stress on the surrounding collagen network [117,121]. The swelling pressure also promotes the maintenance of a high degree of hydration in the articular cartilage. The degree of hydration of cartilage is determined by the balance between the expanding total swelling pressure, which is exerted by proteoglycans, and the restraining tensile force that develops in the surrounding collagen network [117,121–123]. If the collagen network of the articular surface is damaged, thereby disturbing this balance, it will contribute to increased tissue hydration, as a result of which the ability of the articular cartilage to bear loads will change [117,124,125].

2.5. Water

Water is the most abundant component of articular cartilage, accounting for 80% of its wet weight, of which 30% is associated with the interfibrillar space in collagen, and the remainder occurs in the matrix pore space [2,126,127]. The relative water concentration reduces to around 65% in the deep zone [41]. The transport and distribution of nutrients to the chondrocytes is made possible by the flow of water through the articular cartilage and articular surface. A significant amount of interfibrillar water occurs in the form of gels. Compression of the solid matrix or application of a pressure gradient in the tissue serves to move water through the ECM [123,128]. Against such a flow through the matrix, the frictional resistance is very high, resulting in very low tissue permeability. Due to a combination of matrix water pressure and frictional water flow, two primary mechanisms are created that affect the cartilage's ability to withstand significant loads [2].

2.6. Metabolism

The matrix of the adult articular cartilage is separated by the subchondral plate from the subchondral vascular spaces. Diffusion from synovial fluid affects AC nutrition. The cartilage matrix restricts materials in terms of size, molecular configuration and charge [2]. The average pore size in the ECM is approximately 6.0 nm [129]. Due to the lack of direct nutrient supply from the lymphatic or blood vessels, mainly anaerobic metabolism affects the chondrocytes.

The development, maintenance as well as repair of the ECM is the task of chondrocytes via a group of degrading enzymes. The role of chondrocytes is to synthesise matrix components, proteins and glycosaminoglycan side chains. Factors surrounding chondrocytes in the mechanical and chemical environment affect their metabolic activity. Pro-inflammatory cytokines are characterised by anabolic and catabolic effects that function in the synthesis and degradation of matrix macromolecules [130].

Chondrocytes influence the synthesis, maintenance and secretion of proteoglycans into the ECM. A number of growth factors and regulatory peptides are involved in the regulation of proteoglycan metabolism, including transforming growth factor-β, interleukin-1

and tumour necrosis factor-α. However, further studies are needed to expand the knowledge of the molecular mechanism by which these peptides and growth factors affect proteoglycan metabolism.

The ECM surrounds chondrocytes, thereby protecting them from harmful biomechanical forces. ECM metabolic homeostasis contributes to balancing the degradation of macromolecules with their replacement by newly synthesised products. It is estimated that proteoglycan turnover can last up to 25 years, while the half-life of collagen is estimated to be from several decades to 400 years [94,131].

The main proteinases involved in cartilage turnover are metalloproteinases (gelatinase, stromelysin and collagenase) as well as cathepsins (B and D). The function of gelatinase is to degrade denatured collagen types II and IV, and also has significant activity against collagen types V, VII, X, XI, elastin and fibronectin [132,133]. Stromelysin is responsible for the degradation of the aggrecan protein core. In turn, the function of collagenase is to degrade spiral native collagen fibres in one place [2]. Metalloproteinases are secreted as latent proenzymes that require extracellular activation. Cathepsins are active in the process of aggrecan degradation.

Movement and joint loading are necessary to maintain both the proper structure and function of the AC. A lack of physical activity affects cartilage degradation [41]. Dynamic loads and systematic movement are extremely important to ensure proper AC metabolism. Changes in cartilage metabolism may occur as a result of diseases, such as osteoarthritis, which is caused by a physiological imbalance between synthesis by chondrocytes and degradation [134].

Understanding the unique physiological properties of AC is intrinsically linked to its structure, more specifically its zonation and regional organisation, cellular composition and ECM composition. This is the key knowledge required to further analyse the biomechanical parameters of AC, which will be discussed in detail in the next section.

3. Biomechanics of Articular Cartilage

Articular cartilage can be described as a thin layer of specialised connective tissue that is characterised by specific viscoelastic properties. The main function of AC is to provide a smooth and lubricated surface for low-friction articulation. It also facilitates the transfer of loads to the underlying subchondral bone [2]. A special feature of articular cartilage is its ability to withstand high cyclic loading with little or no signs of damage or degenerative changes [2,92,135,136].

The AC consists of two basic phases: a solid phase that is porous and permeable, consisting of collagen fibres, proteoglycans, glycoproteins and chondrocytes, and a liquid composite phase consisting of interstitial fluid containing water and ions such as sodium, potassium, calcium and chloride [3,137,138]. The solid phase accounts for about 15–32% of the total cartilage mass, with the proportion reduced to 10% in diseased cartilage immediately prior to its destruction [139]. The liquid phase accounts for about 68–85% of the total mass. The resistance to compression of articular cartilage is provided by the relationship between aggregates of proteoglycans and interstitial fluid, and more specifically, by the negative forces of electrostatic repulsion [14,120,140].

The immediate increase in interstitial fluid pressure is associated with the initial and rapid application of contact forces to the joint during loading. The effect of such a local increase in pressure is that interstitial fluid flows out of the ECM, generating high frictional resistance on the matrix [120,138,141–143]. Interstitial fluid flows back into the tissue when the compressive load ceases. Due to the low permeability of the AC, interstitial fluid is not quickly squeezed out of the matrix [141,144]. The cartilage under the contact surface is

limited by the opposing bones and surrounding cartilage, which has the effect of reducing mechanical deformation.

Articular cartilage is viscoelastic, and its behaviour is dependent on the time and exposure to constant load or deformation [2,145]. The viscoelasticity of cartilage is associated with a flow-dependent and a flow-independent mechanism [8,146]. The flow-dependent mechanism is related to the interstitial fluid, as well as the frictional resistance that is associated with this flow [128,137,138,147]. The displacement of cartilage is a function of time, which is related to the inability of the fluid to immediately escape from the matrix [45]. The increase in interstitial fluid pressure is influenced by the application of joint contact forces during joint loading. In the case of deformity, fluid flow occurs through the layers of cartilage, as well as the surface of the joint, resulting in fluid flowing out of the ECM. Fluid can also flow through layers of tissue if a pressure differential is applied to a section of cartilage. Initially, the displacement is quite rapid and corresponds to a larger or smaller flow of fluid from the cartilage [4,5,148]. The fluid flow slows down as the rate of displacement decreases, and its value approaches a constant value [45]. Displacement is constant at equilibrium, and the fluid flow is stopped. The flow-independent component of viscoelasticity is due to the intrinsic viscoelastic behaviour of the collagen-proteoglycan matrix [149,150]. The fluid pressure is an important component of the total load support, which has the effect of reducing the stresses acting on the solid matrix. In the articular cartilage, aggregated molecules swell against the collagen skeleton, which is its mechanical response. The compression resistance of articular cartilage is provided by the association between proteoglycan aggregates and interstitial fluid, due to the negative forces of electrostatic repulsion [2,4,49]. In an aqueous environment, the aggregated proteoglycan molecule spreads under the influence of mutual repulsion of negative charges, occupying a large volume [45]. During compression, negatively charged areas on the aggrecan are pressed against each other, increasing the mutual repulsive force of each other. As a result, the stiffness of the compressed cartilage increases [2,45,151].

AC is also subject to the phenomena of creep and relaxation. Under constant compressive stress, the tissue deforms or creeps until an equilibrium value is reached [138]. In articular cartilage that has been deformed and is subjected to constant stress, the stress value increases, reaching a maximum, and then gradually decreases in the process of relaxation until an equilibrium state is reached. AC cannot be described by a single Young's modulus due to its predisposition to stiffen with increased strain. Therefore, the tissue modulus depends on the time at which the forces were measured during the stress relaxation test. Such a method was used in the preliminary studies of mechanical tests performed on AC [145]. Currently, a known strain is used, after which the maximum measured force is reached immediately, followed by a slow relaxation of the strain. Force and/or stress values are recorded when equilibrium is reached. This process is repeated over the entire range of strain values, while the equilibrium modulus is denoted as the dependence of the slope of the curve on the strain [2,152–154].

The shear-resistant properties of articular cartilage are mainly responsible for its complex composition and organisation through the middle zones of cartilage. Randomly distributed collagen fibres under tension affect the cartilage's shear response [155,156]. The precise molecular arrangement of collagen fibres provides resistance to tensile forces. Intramolecular and intermolecular cross-links provide stabilisation and tensile strength to collagen fibres.

The mechanical properties of AC are affected by heterogeneity, anisotropy, and multiscale. To assess the mechanical behaviour of AC, most mechanical tests are carried out in vitro using AC biopsies [12]. In the context of biomechanics, AC exhibits specific mechanical characteristics, which can be divided into time-dependent and time-independent behaviour.

3.1. Time-Dependent Behaviour

The articular cartilage exhibits reversible elastic behaviour between the two equilibrium states of deformation. In order to reach the equilibrium state, a so-called transition phase is necessary, during which the strain or stress values are variable. Such a condition demonstrates that AC's behaviour is time dependent.

Viscous behaviour consists of the creeping and relaxation behaviour of the articular cartilage. The changes in stress during the application of a constant strain are called relaxation behaviour, during which there is a gradual adaptation of the reaction force at the point of contact with a simultaneous forced constant displacement. Creep behaviour, during which the shape of a specimen subjected to a constant force gradually adapts, is responsible for the changes in deformation during the application of a constant stress. Two sources of viscous behaviour are known: flow-dependent or porous-elastic [157]. They are related to the porous structure of the articular cartilage and the flow of viscous fluid from the pores contained in the solid phase. As this flow is not instantaneous, resistance forces are induced, increasing the overall reaction force of the tissue. Viscoelastic behaviour and flow-independent viscous behaviour are related to ECM viscosity. COL II fibrils and proteoglycans sliding against each other create friction, which increases the strength of the tissue response [158]. Therefore, during the transitional phase of creep or relaxation, some of the energy required for tissue deformation is lost due to the viscous behaviour of the solid and liquid phases [12]. In contrast, the deformation of the specimen increases or the delivered force decreases.

Time-dependent AC behaviour also shows a velocity dependence. The apparent stiffness of the articular cartilage increases as the load increases, which is related to the viscosity of the solid phase and the ability of the fluid to flow out [159]. Consequently, the AC exhibits different apparent behaviour depending on the loading rate [154,160]. Small values of load rate influence the appropriate reorganisation of the solid matrix without dissipating energy. In contrast, at high load rates, there is insufficient time for the fluid to drain from the solid phase and reorganise the COL II fibres, resulting in time-independent behaviour [160,161]. AC shows incompressible behaviour in the solid state, while visco-elastic behaviour is noticeable during loads with values closer to the physiological range. As the loading rate increases, the dynamic response stress also increases in a nonlinear manner [159,160].

In conclusion, a comparison of the mechanical properties of articular cartilage samples is only possible if usable equilibrium or dynamic data have been achieved at similar loading rates. This is because the dynamic modulus of elasticity is calculated at higher load rates compared to the equilibrium modulus of elasticity determined at low load rates.

3.2. Time-Independent Behaviour

When healthy articular cartilage is removed from mechanical loading, the elastic tissue is able to return to its original shape by withstanding reversible deformation. This behaviour is due to a combination of COL II, proteoglycans and water flowing out and into the tissue during deformation and springback. AC does not exhibit elastic behaviour because it does not show an equal relationship between the force applied to the articular cartilage sample and the deformation during the loading and unloading phases [162]. In contrast, it is possible to identify pseudo-elastic behaviour that depends on the loading conditions. The pseudo-elastic behaviour of the articular cartilage was assessed first during shear, compression, traction and indentation tests [12]. Depending on the stiffness of the specimen, the strain varies for a given stress. As the apparent stiffness of the articular cartilage increases, the strain decreases [163].

The pseudo-elastic behaviour of AC is contributed to by its compressibility and changes in volume during loading. During general deformation, the volume of the solid

and variable phase does not change, from which their incompressibility results. During compression, there is a change in the volume of the articular cartilage, which is influenced by fluid loss.

The osmotic pressure in the tissue affects the natural pre-tensioning of the articular cartilage to the exclusion of mechanical action. Osmotic pressure is generated by water entering the tissue. The main components of the ECM are responsible for maintaining the mechanical balance [164]. Negatively charged proteoglycans affect the separation of molecules, resulting in tissue swelling. As a result of swelling, COL II fibres and their cross-linked copolymers are stretched and their stiffness limits tissue expansion [12]. Increasing the stiffness of the articular cartilage is influenced by the balance between tensile and repulsive forces, leading to pre-tension. A new mechanical equilibrium is created by a change in the balance of forces when an external load is applied.

3.3. Anisotropic, Heterogeneous and Non-Linear Behaviours

The non-linearity of articular cartilage is the result of changes in mechanical behaviour caused by increases in the loading rate and amplitude. The increase in articular cartilage stiffness with an increasing load is defined by stress or strain hardening [161,165]. Tensile stiffness increases as a result of the non-linear behaviour of COL II fibres, as well as changes in their orientation [101,166]. In turn, the recruitment of the cross-linked polymer during stretching affects the structural or geometric nonlinearity. However, there are cases where the stiffness does not change after complete recruitment of the fibre network, indicating a linear behaviour at high strain. Reorganisation of the ECM occurs during compression, which alters the flow of the fluid phase, resulting in a non-linear change in the time-dependent behaviour [167,168].

The difference in the orientation of type II and IV collagen fibres in the three zones influences the anisotropic behaviour of articular cartilage, from which it follows that the orientation should affect the mechanical properties. The heterogeneous behaviour of articular cartilage is also influenced by mechanical changes resulting from the composition and gradients of COL II fibres and proteoglycans in different regions.

Given the above, time-dependent and time-independent behaviours result from the composition and structure of the articular cartilage. Behavioural differences in the tissue are rooted in its depth and distance from the chondrocytes, as well as the main direction of deformation and its state. Various techniques are used, particularly indentation techniques, to illustrate the behaviour at the nano, micro and tissue scales.

3.4. Mechanical Properties of Articular Cartilage

AC is a biphasic tissue characterised by a complex layered structure in which the mechanical behaviour depends on the distribution of collagen, proteoglycans and water. In their work, Mow et al. [51] consider the following key mechanical parameters of AC: aggregate modulus, Young's modulus in compression and tension, and Poisson's ratio.

The aggregate modulus (H_A) is a parameter describing the stiffness of the AC in mechanical equilibrium during compression, when all the load is carried by the solid matrix and the SF flow ceases [51]. This is a key parameter in two- or three-phase AC models, reflecting tissue resistance to volume deformation [122]. For a healthy AC, the values of this parameter range from 0.1 to 2.0 MPa, while the values can increase with the depth of the AC [165]. The high H_A value is related to the high concentration of proteoglycans and negative charges, which, by retaining water, increase the resistance to compression [120].

The compressive Young's modulus (E_C) is a parameter that determines the linear elasticity of AC under compressive loading, which can be determined from indentation

tests or uniaxial compression tests [124]. The value of this parameter depends on factors such as the water content, collagen structure and layer depth, as the surface layer shows greater deformability than the deep layers [169].

The tensile Young's modulus (E_t) shows higher values than in compression, as the network of collagen fibres plays a key role in tension [153]. Depending on the layer and the direction relative to the collagen system, the values of this parameter can be in the range of 5–25 MPa at equilibrium [170]. It has been shown that E_t values can be more than twice as high in the direction following the fibre orientation as opposed to the perpendicular direction [171]. The values of this parameter decrease with age or during the progression of degenerative diseases [154].

The parameter describing the lateral expansion of tissue under compression or stretching in AC is the Poisson's ratio (υ) [172]. The Poisson's ratio is a reflection of the deformation capacity of the AC in response to mechanical loads. Changes in the value of this parameter can be related to degenerative processes. During the course of osteoarthritis of the joint, there is a reduction in elasticity and impaired SF flow, which has a direct impact on υ.

Hydraulic permeability (k) is a parameter describing the ability of AC to allow SF to pass through its porous structure under the action of a pressure gradient [173]. Mow et al. [173] used indentation tests under creep conditions to determine k, obtaining values in the range of 0.44×10^{-15} $m^4/N{\cdot}s$. for femoral condyle cartilage, to 1.42×10^{-15} $m^4/N{\cdot}s$ for patellar sulcus cartilage.

Tensile strength is a parameter referring to the maximum stress the AC is capable of withstanding before breaking in tension [154]. Roth et al. [154] used bovine cartilage in their study and showed that tensile strength increases with age in the deeper layers but decreases in the superficial layers.

To determine the elasticity of AC in equilibrium during tension, the equilibrium tensile modulus (E_{eq}) is used. Williamson et al. [174] showed a significant increase in this parameter with age, which is influenced by the increased collagen content and its cross-linking.

The composite shear modulus (G) is used to characterise the response of AC to shear loads in the dynamic range, taking into account elastic and viscous components. Oscillatory shear tests were used in the studies by Zhu et al. [175], which showed the sensitivity of this parameter to changes in the structure of the extracellular matrix, especially to the degradation of proteoglycans.

Equilibrium shear modulus (G_{eq}) refers to the elasticity of AC in response to long-term shear loading. LeRoux et al. [176] in their studies focused on the properties of alginate gel as a model for AC, showing a strong dependence of G_{eq} on both the alginate concentration and the presence of sodium ions.

The ratio of the viscous to elastic components in the shear response of AC is defined by the shear loss angle (δ). In the work of LeRoux et al. [176], the sensitivity of this parameter to changes in the structure of the extracellular matrix, especially to the degradation of proteoglycans, was demonstrated.

The values of the above-mentioned biomechanical parameters of healthy AC are presented in Table 2 based on the work of Little et al. [177].

Table 2. Biomechanical parameters of healthy AC.

Parameter	Typical Value	Measurement Method	Author
Aggregate modulus (MPa)	0.1–2.0	Confined compression tests, indentation	Mow et al. [51] Mow et al. [128] Jurvelin et al. [172] Mak et al. [178]

Table 2. *Cont.*

Parameter	Typical Value	Measurement Method	Author
Compressive Young's modulus (MPa)	0.24–0.85	Unconfined compression tests	Mow et al. [51] Mow et al. [173] Jurvelin et al. [172]
Hydraulic permeability (m^4/Ns)	10^{-16}–10^{-15}	Confined compression tests, unconfined compression tests, indentation	Mansour [45] Mow et al. [173]
Poisson's ratio	0.06–0.3	Unconfined compression tests, indentation	Mow et al. [51] Jurvelin et al. [172] Moroni et al. [179] Jurvelin et al. [180]
Tensile Young's modulus (MPa)	5.0–25.0	Tensile constant strain rate	Mow et al. [51] Williamson et al. [174] Williamson et al. [181]
Tensile equilibrium modulus (MPa)	5.0–12.0	Tensile stress relaxation	Korhonen et al. [182]
Tensile strength (MPa)	8–25.0	Tensile constant strain rate	Roth et al. [154] Setton et al. [156]
Complex shear modulus (MPa)	0.2–2.5	Dynamic shear	LeRoux et al. [176] Zhu et al. [175]
Equilibrium shear modulus (MPa)	0.05–0.4	Equilibrium shear	Spirt et al. [183] LeRoux et al. [176]
Shear loss angle (°)	10–15	Dynamic shear	LeRoux et al. [176] Moroni et al. [179] Zhu et al. [175]

Various measurement methods were used to determine the parameters described above. The confined compression test is a classic method for testing the mechanical properties of AC, in which a cylindrical tissue sample is axially compressed in a sealed chamber, limiting its lateral expansion [51,128]. This measurement method is one of the key tools used in AC biomechanics to determine material properties that play a key role in the diagnosis of degenerative changes, as well as in the design of biomaterials and numerical models [45,51,128,172,173,178]. In this arrangement, only axial outflow of interstitial fluid is possible through the porous endplates, enabling a detailed study of the time-dependent response (creep and relaxation) of the tissue under controlled hydraulic conditions [51,128]. Mow et al. [128] used this method to experimentally verify the biphasic theory, which describes AC as a poroelastic system composed of a solid phase, which is a collagen-proteoglycan matrix, and a fluid phase in the form of water and dissolved substances. The use of this measurement method made it possible to determine key parameters for understanding mechanotransduction in AC, such as the elastic modulus of the matrix and the hydraulic permeability coefficient. In the next work of Mow et al. [51], the confined compression test was used to discuss the influence of mechano-electrochemical phenomena on the mechanical response of AC. It was proven that this measurement method is particularly useful for investigating the inhomogeneity and anisotropy of AC properties with respect to different depth zones. Jurvelin et al. [172] used this measurement method to evaluate Poisson's ratio values as well as stress modulation within the tissue by examining the mechanical compression between axial strain and lateral displacements of the material. Mak et al. [178] described this measurement method, comparing it to the indentation test. They emphasised its advantage of better control over boundary conditions and fluid flow, which has a beneficial effect on the theoretical analysis. The confined compression test was used by Mow et al. [173] as a reference point to assess the accuracy of the developed numerical algorithm for the indentation test. A significant convergence of the model results

with the experiment conducted in a closed chamber was demonstrated. Mansour [45] described the confined compression test as one of the most repeatable and controllable methods for measuring axial stiffness and flow properties of AC. He indicated its usefulness in analysing SF transport and porosity in the tissue structure.

Another measurement method used is the unconfined compression test, which is one of the basic methods of mechanical testing of AC. It consists of axial compression of a cylindrical tissue sample between rigid plates without lateral restriction of fluid flow and deformation [51,173]. The use of this method enables measurement of the mechanical response of the tissue, taking into account fluid outflow through the lateral surfaces as well as creep and stress relaxation in the axial direction [51,173]. In the work of Mow et al. [51], this method was used to discuss the mechano-electrochemical phenomena occurring in AC during loading. It was emphasised that this measurement method allows for the assessment of the influence of ion transport and osmotic gradients on the mechanical behaviour of AC. The authors emphasised that the use of the unconfined compression test allows for the study of inhomogeneity and anisotropy depending on the tissue zone. Jurvelin et al. [172] demonstrated the utility of this method in combination with optical analysis to determine the Poisson's ratio in adult bovine AC. The acquired data made it possible to calculate the transverse deformation, providing a basis for mechanical calibration of the imaging techniques. Mansour [45] demonstrated that the unconfined compression test is one of the most commonly used tools in tissue biomechanics, which allows for determining axial stiffness and time-dependent response (creep, stress relaxation). He indicated the usefulness of this method for determining the viscoelastic properties of AC. Moroni et al. [179] conducted mechanical studies of tissue scaffolds fabricated using the three-dimensional fibre alignment method using the unconfined compression test. This made it possible to determine the influence of the pore geometry and spatial architecture of the scaffolds on stiffness and damping during cyclic loading.

Another method of testing the mechanical properties of AC is the indentation test. It consists of applying a controlled load or displacement using an indenter of a specific shape in order to make local contact with the sample surface [51,178]. This measurement method is used to assess local tissue properties, such as elastic modulus, stiffness, and biphase parameters [51,178]. Mak et al. [178] developed a theoretical basis for a biphase contact mechanics model for the indentation test, which provided a starting point for analytical solutions to assess the flow and deformation of the solid skeleton during local AC loading. This allowed for a more accurate fit of the models to the experimental results. In the work of Mow et al. [173], numerical and experimental studies were carried out to validate the biphase indentation model, which enabled the precise determination of the Young's modulus and the hydraulic permeability coefficient based on the time response of the AC to the indenter load. Mow et al. [51] determined the usefulness of this method in the analysis of spatial inhomogeneities and anisotropies of cartilage. The indentation test enables the assessment of mechanical properties in small, localised areas, which is crucial when examining different morphological zones of tissue. Jurvelin et al. [172] used this method in combination with optical analysis to determine the Poisson's ratio. Observation of the lateral displacement around the indenter enabled determination of the elastic behaviour of bovine AC. Later, Jurvelin et al. [180] used the indentation test to spatially map the elastic properties of the AC in the dog's knee. The obtained topographic data showed significant regional differences in AC stiffness, confirming the high utility of this method in local and comparative studies. In his work, Mansour [45] demonstrated that the indentation test is one of the methods that provides information on the surface stiffness of tissues with minimal invasiveness. As an advantage, it showed the possibility of performing in situ tests, as well as measuring dynamic and time-dependent behaviour. Moroni et al. [179] used this

measurement method to study the influence of pore geometry on the local stiffness and dynamic response of porous materials that stimulate AC.

In order to investigate the mechanical properties of AC under tensile deformation conditions, one of the basic test methods is the tensile constant strain rate. The specimen is subjected to tensile forces at a predetermined rate, and the stresses and their corresponding strains are measured, allowing parameters such as the tensile modulus, maximum stress, elastic limit and time-dependent response of the tissue to be determined. Using this method, Roth et al. [154] showed that there are changes in tensile properties with age. Tissue from older individuals was less susceptible to stretching, which may be due to collagen reorganisation and changes in collagen density. The team of Williamson et al. [174] used this method at a constant strain rate to assess the mechanical properties of bovine AC. By analysing the relationship between animal age and the tensile properties of the tissue, they found that stiffness also increased with age and correlated with an increase in collagen II content, with a decrease in proteoglycan levels. In their subsequent work, Williamson et al. [181] assessed the development of the mechanical properties of AC cultured in vitro. Their study showed a relationship between the increase in biomechanical parameter values during stretching and the structure and organisation of collagen fibres. Thus, the tensile constant strain rate can be used to monitor tissue maturation and functionality in tissue engineering studies.

Another measurement method mentioned is tensile stress relaxation. It was included in the work of Korhonen et al. [182] to assess the effect of the osmotic environment on the mechanical properties of tissue under axial tension. AC samples taken from the medial condyle of the femur were subjected to axial tension at a constant strain, after which the decreasing stress over time was recorded. The results confirmed that the initial stress level, as well as the rate and extent of stress relaxation, are significantly influenced by the osmotic environment.

The dynamic shear test is a method that is used to assess the mechanical properties of tissues by applying cyclic shear deformations. Its use makes it possible to analyse the elastic and viscoelastic properties of a material [51]. Using this method, Zhu et al. [175] evaluated the effect of enzymatic removal of glycosaminoglycans (GAG) on the viscoelastic properties of AC. Dynamic tests were used to examine the AC response before and after enzymatic digestion, making it possible to determine the contribution of extracellular matrix components to shear deformation resistance. Glycosaminoglycans have been shown to play an important role in suppressing mechanical forces, as a significant reduction in stiffness was observed, as well as an increase in energy loss after GAG removal. Setton et al. [156] focused on studying the effect of ACL transection on the mechanical properties of the knee AC. Specimens were tested in dynamic shear using variable loads at different frequencies to assess the reduction in stiffness after injury. It was demonstrated that ACL transection affected the deterioration of the AC shear properties. Dynamic shear testing was also used in the work of LeRoux et al. [176] to investigate alginate gels as potential scaffolds for tissue engineering. Dynamic tests were performed as a function of the alginate concentration and the presence of sodium ions, assessing the effect of these parameters on the mechanical properties of the gel. The obtained results indicate that the chemical composition and structure of the gel network have a significant effect on the dynamic properties. Moroni et al. [179] used this measurement method, among others, to assess the influence of pore geometry and architecture of scaffolds produced by direct fibre deposition. The material behaviour under variable loading was characterised, and the optimal structural parameters influencing the mechanical properties of the biomaterial, which can be intended for applications in bone and cartilage tissue engineering, were determined.

The last of the mentioned measurement methods is the equilibrium shear test, which is used to determine the mechanical properties of AC by applying a constant shear strain and measuring the stress after reaching the equilibrium state [176,183]. The use of this method makes it possible to isolate the elastic properties of the solid matrix, excluding the influence of time-dependent phenomena. Spirt et al. [183] investigated the nonlinear viscoelastic properties of AC using this method. Samples were subjected to gradually increasing shear strains and then held in a steady state of displacement to determine the variation of the shear modulus with strain. The obtained results indicated a nonlinear nature of the AC response in the equilibrium state. It was also shown that the shear angle has a significant effect on the steady-state stress, which indicates the complexity of this tissue's behaviour and its ability to adapt to different loading conditions. In the work of LeRoux et al. [176], the use of this measurement method made it possible to determine the static shear modulus. It showed a significant dependence on the alginate concentration and the presence of sodium ions, which indicates that ionic interactions are crucial in controlling mechanical properties.

Table 3 provides a comparative summary of selected measurement methods used to assess the mechanical properties of AC, including parameters, advantages and limitations.

Table 3. Comparison of methods for measuring the mechanical properties of AC.

Measurement Method	Measured Parameters	Test Characteristics	Advantages	Limitations	References
Confined compression test	Aggregate modulus, Hydraulic permeability	Cartilage compressed in a cylindrical chamber, without lateral expansion	Measurement of liquid-solid properties (biphasic model)	No mapping of natural anatomical conditions	Patel et al. [184] Mow et al. [128]
Unconfined compression test	Compressive Young's modulus, Hydraulic permeability, Poisson's ratio	Cartilage compressed freely vertically, with possible outflow of fluid and lateral expansion	Simple to carry out, well modelled	Strong dependence of the results on the boundary conditions and sample geometry	Patel et al. [184] Mow et al. [128]
Indentation test	Aggregate modulus, Hydraulic permeability, Poisson's ratio	Local indentation pressure on the cartilage surface	Possibility of in situ and in vivo testing	High sensitivity to tissue heterogeneity and alignment	Patel et al. [184] Jurvelin et al. [172]
Tensile constant strain rate	Tensile Young's modulus, Tensile strength	Cartilage stretching at a constant speed	Mapping of collagen fibre behaviour	Difficulties with sample preparation, risk of damage	Little et al. [177]
Tensile stress relaxation	Tensile equilibrium modulus	Maintaining constant strain and observing stress reduction	Analysis of viscoelastic properties	Long measuring time	Little et al. [177]

Table 3. *Cont.*

Measurement Method	Measured Parameters	Test Characteristics	Advantages	Limitations	References
Dynamic shear test	Complex shear modulus, Shear loss angle	Cyclic shear load application	Dynamic response analysis, testing of viscoelastic properties	Complex apparatus, model-dependent interpretation	Zhu et al. [175]
Equilibrium shear test	Equilibrium shear modulus	Slow deformation until equilibrium is reached	Measurement of elasticity after stabilisation of fluid flow	Long testing time, requires precision	Zhu et al. [175]

3.5. Lubrication Mechanisms in AC

In normal synovial joints, the range of the friction coefficient is $\mu \approx 0.002$–0.02 [185–188]. Measurements of friction on both the AC and whole joint surfaces may depend on the energy dissipation mechanisms occurring during articulation [188]. Such a phenomenon is the result of the viscoelastic deformation of adjacent tissues, such as the synovial membrane, muscles, or ligaments, during joint rotation. Over the years, a number of studies have been conducted on the exact mechanism of lubrication, but to date, no answer has been provided as to why friction is so low in a healthy synovial joint [187,189–193]. The low friction and wear of AC is probably related to the complex structure as well as the composition of the AC surface.

Fluid film lubrication is based on the separation of sliding surfaces by a fluid film of much greater thickness than the surface roughness. Initially, the models describing the SF layer were based on the classical theory of hydrodynamic lubrication known from mechanical engineering, and in later work, these were extended to include the deformation properties of AC during movement [194–196]. The work of Atesheshian, McCutchen, Maroudas and others includes models that take into account the films between the articular surfaces formed by the outflow of interstitial fluid during AC compression [197–203]. Due to the fluid film, contact between the surfaces is reduced, friction and wear are minimised, and interstitial fluid pressure supports much of the cartilage load [188]. Consequently, regardless of the presence of a fluid layer between the sliding surfaces, the actual contact stresses between the AC surfaces may exhibit lower values than the high pressures that are recorded directly at their boundary [204]. This is because the hydrostatic pressure of the interstitial fluid plays a key role in load transfer [202]. Many tribological experiments using AC explants were conducted at physiological strain levels, but at relatively low pressures ($\leq$2 atm) [188]. This value is approximately 100 times lower than the maximum pressures observed in vivo on joint surfaces, regardless of their origin [205,206]. The mechanism of load transfer is realised based on biphasic models, where the AC is treated as an incompressible, porous-permeable matrix composed of a collagen-proteoglycan network in which the interstitial fluid exhibits incompressible fluid behaviour [178,207]. These models are used in mapping the biomechanical response of the AC subjected to loading, as well as in experimental studies using excised specimens [186,208–210]. In their studies, Krishnan et al. showed that during tests conducted at an applied pressure of $\approx$1.5 atm with a sample diameter of 6 mm, the friction coefficient increased from 0.04 to 0.18 within 15 min, with a simultaneous decrease in the interstitial pressure, which confirms the validity of the used model [186,211,212]. Many previous studies have assumed that interstitial pressure is responsible for transferring most of the load between opposing AC surfaces in vivo [213–217].

The actual surfaces of solids are not perfectly smooth; at the microscopic level, various types of irregularities known as surface roughness can be observed. When two such surfaces come into contact, there is an interaction between them that accounts for much of the observed initial static friction coefficient. Experimental studies have shown that, for many materials, the equilibrium static friction coefficient is around 0.3. This value is typical for materials such as dry wood surfaces, steel, as well as AC in a phosphate buffer medium (PSB) without the presence of surface glycoproteins in the form of PRG4 [218]. The value of the static friction coefficient may be higher compared to its equilibrium value due to mechanical interlocking of micro-peaks or adhesive interactions. Local contact stresses can affect the interlocking mechanism, which in turn alters the friction coefficient under cyclic loading and unloading conditions. Increased loads result in both increased frictional forces and greater material wear [191]. As the load increases, the rate of wear also increases. When the value of the initial friction coefficient is higher than the equilibrium value at low slip speed, "stick-slip" friction is possible. This mechanism involves a cyclical transition between the "stick" and "slick" adhesion phases, resulting in an increased rate of surface wear. The equilibrium value of the friction coefficient can be reduced when the spaces between the micro-peaks are filled by the lubricant, reducing the bespoke surface contact. When a lubricant is not subject to rapid extrusion or abrasion, it is referred to as a boundary lubricant. The glycoprotein PGR4, synthesised by AC surface zone chondrocytes, plays a key role in biological systems. PRG4 effectively reduces the equilibrium friction coefficient of AC, lowering its value from 0.3 to 0.1 in the presence of physiological SF [214,219]. PRG4 shows strong binding to denatured, amorphous and fibrillar collagen, which influences its sustained adsorption on the AC surface. When PRG4 is present on both contacting surfaces, it generates significant repulsive forces, which increase with the increasing PRG4 concentration [220]. At the same time, a significant reduction in the coefficient of friction is observed at high concentrations of PRG4, reaching values three or four times lower than in the absence of this component [220]. Other macromolecules such as HA, phospholipids and aggregates also play an important role in the mechanism of boundary lubrication. Previous studies have shown that the presence of these components can have a significant impact on the friction coefficient value, and their removal can lead to disruption of the lubricating function as well as an increase in frictional resistance [191,221–224]. Polymer networks can form structures resembling "polymer brushes" to which hydration layers adhere, according to hydration lubrication theory [218]. The purpose of these structures is to counteract the extrusion of water from the microscopic contact joints while maintaining the fluid shear resting characteristics [203,225]. Such a mechanism can be considered in an osmotic context—as the surface gel is compressed, the local osmotic pressure increases, which causes water to be retained within the gel structure and maintains its hydrated character [226]. A characteristic feature of such a hydrated gel is low shear resistance, making it an effective lubricant under boundary friction conditions. When the key components of the surface gel, such as HA, aggrecan and collagen, are removed, the lubricating properties deteriorate and the contact surfaces wear faster [224]. Therefore, boundary lubrication occurs if surface asperities are in contact and transmit normal forces. The working distance at which boundary lubrication occurs depends on the asperity morphology and the extent of the repulsive forces generated by the PRG4 lubricant components, which at high concentrations can generate repulsion at a distance of up to 0.2 μm [218].

In healthy diarthrodial joints, the AC surfaces allow rolling and sliding relative to each other. Effective lubrication of these surfaces is possible through a combination of hydrodynamic and boundary lubrication, the purpose of which is to reduce friction during movement. Typically, rolling generates less resistance than sliding, although both mechanisms affect energy dissipation within the joint [219]. Differences were observed

at the knee joint in terms of AC surface sliding during the gait cycle. The tibial cartilage and meniscus surfaces exhibit limited sliding, typically measured in millimetres, while the femoral cartilage and meniscus surfaces experience greater sliding during the same cycle [218]. The disproportion in sliding speeds can have a significant impact on the optimal joint structure through differences in the cartilage composition of the shin and femur, and, consequently, on joint function [189]. In mixed lubrication mode, the initial coefficient of friction of AC may be around 0.002–0.02, while in the steady state, the equilibrium kinematic coefficient of friction increases to around 0.05–0.1, depending on the sliding speed, cartilage tissue deformation, or the load ratios attributed to sliding and rolling [227]. It has been empirically found that relative movement between contacting surfaces improves joint lubrication [228]. The viscosity of the SF is crucial not only for the rate at which the fluid is squeezed out of the fracture, but also for the rate at which it is drawn into the fracture via the relative motion between the fluid and the contact interfaces. SF is sucked into the gap at the "leading edge" of the sliding contact mainly due to the tendency of the liquid molecules and dissolved substances to attach to the surface and interact with each other as well as the effect of inertia on the flow [218]. Therefore, higher SF viscosity increases energy losses due to shear, while it promotes hydrodynamic lubrication due to more efficient fluid absorption [227]. The suction of SF into the contact interface at low speeds may explain why physiological SF is initially characterised by a viscosity about 40–50 times greater than water, because the increased viscosity favours its efficient entrainment under low-speed conditions [189]. As the suction speed increases, the viscosity may decrease, thus maintaining a similar level of fluid suction. The nonlinear rheological properties of SF support effective suction regardless of the speed. Appropriate surface roughness may support this process, but the mechanisms of this interaction are not yet well understood [219]. The interaction of friction and lubrication modes is captured on so-called Stribeck curves or Stribeck surfaces [219,227]. In a mixed lubrication model, soft bearings made of a rough, porous material such as AC are characterised by complex interactions. When the roughness of two AC surfaces come into contact with each other, deformation occurs, resulting in changes in the geometry of the contact zone. Deformation can significantly increase the actual contact area due to prolonged loading. The increase in contact area improves AC surface matching and has the effect of lowering nominal contact stresses [219].

The increase in anatomical conformity within the articular surface leads to an increase in the AC contact area, which translates into tribological mechanisms occurring within the synovial joints [123]. Both the increased contact area and the higher degree of geometric conformity result in an increased mean drainage path, both along the articular interface and within the AC matrix [202]. In the context of the knee joint, increased participation of the meniscus promotes improved compliance between the femoral condyles and the articular surface of the tibia [229]. The meniscus plays an important role in load dissipation by reducing local contact stresses in the AC, increasing the effective contact area with the underlying bony matrix [230]. Its presence also contributes to the extension of the SF flow path between the contact surfaces, which extends the duration of the lubricating film [138]. The extension of the SF drainage path correlates with the extended duration of hydrodynamic lubrication, implying that more compliant contact interfaces are characterised by maintaining a low friction coefficient for a longer period [218]. As a result, the average normal stresses are reduced, as well as the friction coefficient over time, which limits the wear of the articular surfaces [231].

McCutchen described a process called "weeping lubrication" [232]. Under mixed lubrication conditions, especially in the presence of porous and rough surfaces, a complex interaction occurs between boundary and hydrodynamic lubrication. Fluid in the AC matrix can migrate to the contact surface, helping to maintain the lubricating film.

3.6. AC Behaviour Under Cyclic Loading

Articular cartilage, as a highly specialised tissue covering the articular surfaces of the bones in the synovial joints, plays an important role in transferring loads and ensuring smooth joint movement [233]. The response of AC to cyclic loading is crucial to understanding the mechanisms leading to damage and degenerative joint diseases [2].

The action of repeated mechanical loading influences changes in the mechanical and structural properties of AC [233]. Studies have shown that with the increase in the number of loading cycles, tissue softening and structural damage in the form of cracks and defects in the extracellular matrix occur [233].

In vitro experiments have confirmed that cyclic loading results in irreversible damage to AC cartilage, even without the participation of biological factors [233]. It follows that mechanical loading can initiate degenerative processes in the tissue.

Cyclic loading also affects the friction properties of joint surfaces. Studies using animal models have found that long-term cyclic loading results in an increase in the coefficient of friction in the joint, which can lead to further AC damage [234].

A schematic representation of the response of AC subjected to cyclic loading is presented in Figure 2 based on the work of Zhang et al. [235]. The graph illustrates the changes in AC deformation in response to repeated loading, revealing the characteristic features of the behaviour of AC under the influence of cyclic forces.

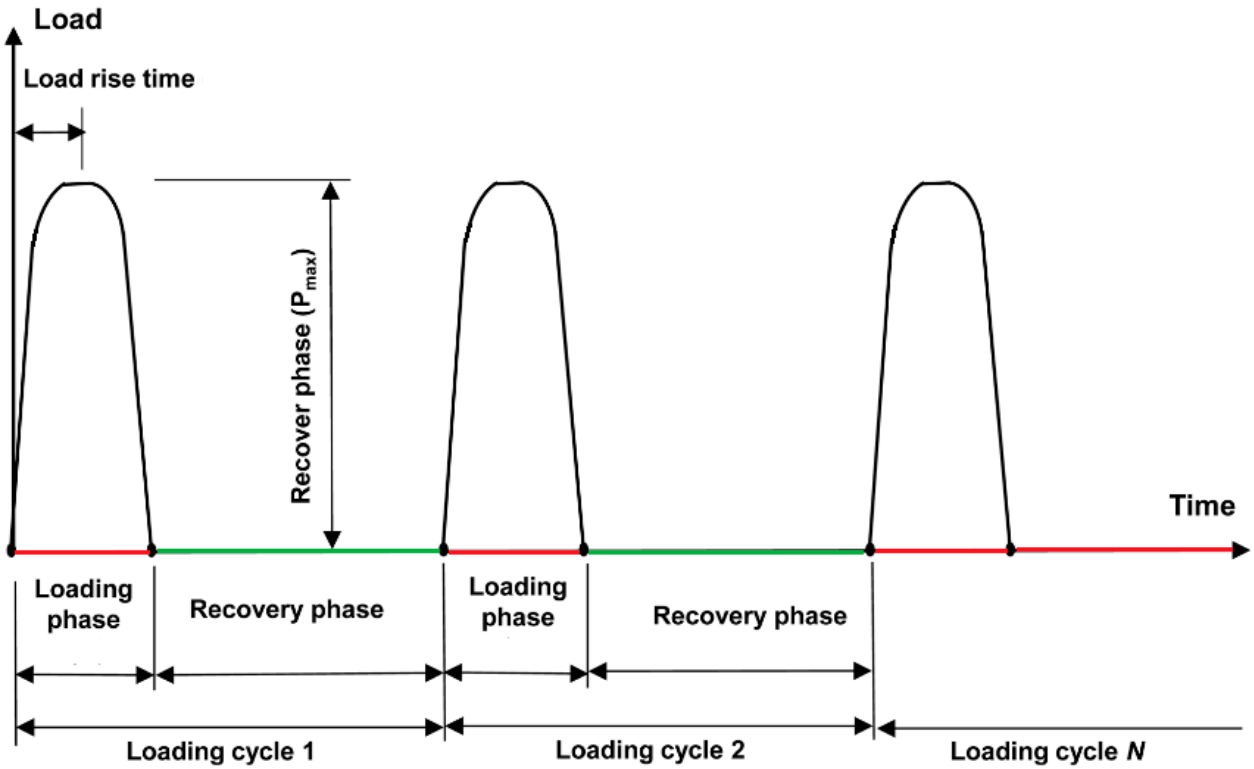

Figure 2. Schematic of deformation response of AC under cyclic loading.

The mechanical properties of AC are a result of its structure and the functions it performs. It is therefore fundamental to understand these aspects in order to further consider the influence of the joint environment, including synovium, on the maintenance of homeostasis and AC properties. This topic will be discussed in the next section.

4. Articular Synovial Parameters

The synovial joint is a complex system consisting of articular cartilage, synovial membrane (SM) and synovial fluid (SF). The interplay between these components affects load transfer, mobility and the protection of bone structures. The parameters of the synovial environment that affect cartilage homeostasis, as well as its ability to regenerate, are an important element [2]. The role of synovial fluid is to act as a lubricant, nutrient and immunoregulator [219,236]. In contrast, the role of the synovial membrane is to produce and regulate the SF composition and, in the case of pathological conditions, can accelerate cartilage degradation through pro-inflammatory mediators [237]. It is therefore important to analyse the biochemical and physicochemical parameters of the synovial fluid to assess the functional status of the joint. Indeed, a change in these parameters may signal degenerative processes (e.g., osteoarthritis), and their precise analysis represents an important role in the pathogenesis of the disease, as well as being a source of diagnostic biomarkers [238–240].

4.1. Composition and Properties of the Synovial Fluid

Synovial fluid is a viscous fluid that is secreted by the inner cells of the synovial membrane and filtered from blood plasma. There is approximately 2.5 mL of SF in a healthy synovial joint [241]. The viscosity of the synovial fluid is a result of its high hyaluronic acid (HA) content. SF is extremely important as its function is to deliver nutrients to the AC, transport waste materials and provide lubrication with reduced friction, covering joint surfaces. Synovial fluids also include components such as proteoglycan 4 (PRG4), surfactant phospholipids (SAPL), collagenases, proteases and prostaglandins [242]. The cellular components of SF also include synovial A and B cells, B and T lymphocytes, neutrophils and monocytes. Synovial fluid may also consist of macrophages, as well as mesenchymal stem cells, especially in pathological conditions. Lubricants are secreted by synoviocytes in the synovial membrane and chondrocytes in the AC. They are accumulated by the semi-permeable synovial lining in the synovial space. If the lubricating system is deficient, AC surface erosion can occur in arthritic conditions [243]. The normal pH value of healthy synovial fluid is in the range of approximately 7.31–7.64 [244,245]. During inflammation, the pH value decreases, which affects the activity of metalloproteinases, resulting in AC degradation. Due to its rheological properties, SF can be characterised as a non-Newtonian fluid with non-linear viscosity.

Hyaluronate (HA) is the most abundant polymeric component in SF, in complex form with proteins, due to its flexible, highly hydrated polymer chain [236,246]. Due to the viscoelastic properties, it is considered one of the key lubricating components in synovial joints [246–248]. The other proteins tested in the presence of HA showed a reduced friction coefficient [249]. In human SF, the concentration of HA is approximately 1–4 mg/mL, while higher values of this component are observed in people under 40 years of age [250,251]. Osteoarthritis sufferers showed a decrease in HA, while the percentage of proteins increased, which correlates with a decrease in synovial fluid viscosity. This results in a reduction of its lubricating properties. To maintain adequate SF viscosity, HA is injected intra-articularly in OA patients [252].

PRG4, despite its low content in SF, constitutes a significant share in boundary lubrication. Its presence in different zones is crucial to the AC friction coefficient. The function of lubricin is to maintain appropriate lubricating properties at the cartilage–synovial fluid interface and to prevent cells from attaching to the joint surfaces [253,254]. Its functions also include facilitating the transport and anchoring of phospholipids to the cartilage surface [255]. Another role of PRG4 is to provide adequate cartilage-protective properties to the AC, which can be enhanced through interaction with the HA by dissipating shear-induced energy [236,246,256–258]. Lubricin, together with the other main components of

SF, is an effective biolubricant agent, whose concentration decreases in acute injury. An increase in this biolubricant was observed in patients undergoing arthrocentesis [259–261].

The most abundant protein in synovial fluid is albumin. It has been shown to improve boundary lubrication by adsorbing to the surface of the joint material, thereby protecting the joint surfaces from wear [249]. Albumin is pH-dependent, while no relationship was shown between albumin and lubricant viscosity at low angular velocity [236]. The function of albumin is to lubricate joint surfaces and also to interact with other components.

Another important protein found in SF is globulin. It has an important role in AC boundary lubrication. Compared to the other components of the synovial fluid, globulin produces thicker layers in tribological tests at different concentrations [262]. Globulin shows a positive effect in artificial joints by blocking the removal of metal ions from the surface layers, which affects the wear resistance of the surface [262,263]. In contrast to albumin, globulin acts independently of the pH value, but only at low velocity. As the velocity increases, its dependence, as a lubricant, on the pH value increases. On the other hand, it has the advantage of achieving mixed or hydrodynamic lubrication.

4.2. Synovial Membrane

The synovial membrane is a highly specialised mesenchymal tissue whose functions are to provide the joints with adequate lubrication and to supply nutrients to the AC [264,265]. It also provides a mechanical barrier that separates the joint cavity from the blood and lymphatic vessels, and is involved in the production and resorption of SF [250]. The structure of the SM consists of two layers: the intima inner layer, and the subintima inner layer [266]. The intima inner layer consists of one or two sheets of macrophages or synoviocytes, which are similar to fibroblasts. The subintima inner layer consists of two or three layers of synoviocytes lying over loose connective tissue containing fibroblasts that secrete collagen and other extracellular matrix proteins [266]. The cells inside the synovial membrane are responsible for the secretion of synovial fluid, providing lubrication to the AC, nutrition and also the activity of the chondrocytes. Type A and B synoviocytes are part of the synovial intima [237].

Type A synoviocytes are the tissue macrophages of the SM, located around the upper lining of the synovial membrane [237,264,266]. Their function is to absorb and degrade extracellular components, as well as joint cavity debris, antigens and microorganisms. These cells have the ability to proliferate under inflammatory conditions. SM macrophages contribute to cartilage destruction under pathological conditions. Chronic production of pro-inflammatory cytokines and osteophyte formation due to the release of transforming growth factor-beta (TGF-β), as well as bone morphogenetic protein BMP-2 and BMP-4, are responsible for this condition [267,268].

Type B synoviocytes, also known as synovial membrane fibroblasts, are located below the type A synoviocytes, on the submental layer, forming the surface of the synovial membrane [269]. Their function is to produce components such as proteoglycans, collagen types III, IV, V, VI, fibronectin, glycosaminoglycans, entactin and laminin [250,269]. In addition, they are responsible for the production of lubricin [237,270]. Characteristic of type B synoviocytes are the dendritic cytoplasmic protrusions observed in SM [269,271]. These cells usually have one or more protrusions that are directed towards the surface of the synovial membrane, either in different directions or parallel to the surface of the membrane, and that overlap to form a plexus [271]. With their cytoplasmic protrusions, type B synoviocytes reach deep into the joint cavity to analyse and control the composition of the SF [250].

Despite the leaky structure of the synovial membrane containing 1-µm-diameter pores between synoviocytes, it ensures that proper quality SF is maintained [264]. The

structure of the intercellular matrix is mainly responsible for the resistance of the SM against water leakage from the joint cavity [272]. This process depends on the concentration of proteoglycans, glycosaminoglycans and glycoproteins between collagen fibrils due to the migration of SF through thin intermolecular spaces [264,273]. SM is also responsible for limiting the efflux of HA from the SF, so that a high concentration of this component is maintained in the joint cavity [272]. In the process of extruding fluid into the joint, HA accumulates on the surface of the synovial membrane, thus creating a buffer layer [274]. When the molecular weight of the HA or its concentration is reduced, there is an increased discharge of HA from the joint cavity [272].

Patients affected by OA experience SM proliferation, resulting in thickening of the SM and remodelling of the tissue architecture [275]. Osteoarthritis is considered a degenerative disease, but inflammatory processes have been shown to be significantly involved at the level of the synovial membrane [237]. Activation of A and B synoviocytes occurs, resulting in increased release of growth factors and inflammatory mediators, which include TNF-α, IL-1β and prostaglandins [237]. There is a process of infiltration of inflammatory cells, particularly macrophages, dendritic cells and T and B lymphocytes, in the synovial membrane of patients affected by OA [275,276]. The resulting infiltrates influence the formation of foci of lymphoid structure that enhance the local immune response [275]. With an increase in pro-inflammatory cytokines, there is degradation of the extracellular matrix in the AC and in the subchondral layer of bone [237]. OA is also associated with a reduction in anti-inflammatory cytokines such as IL-10, while an increase in the concentration of pro-inflammatory factors, including IL-6, IL-8, and matrix metalloproteinases (MMPs), is observed [277]. Persistent inflammation leads to chronic degeneration of the joint [277,278].

4.3. Synovial Fluid—Articular Cartilage Interactions

Articular cartilage does not contain blood vessels, so nutrient delivery is ensured by transport from the SF by diffusion or by convective transport during mechanical loading [123,138,279]. Transport of macromolecules and nutrients in the form of oxygen, glucose and fatty acids takes place by penetrating deep into the tissue via the cartilage surface zone. These components are then used by chondrocytes in metabolic processes [280]. This process is dependent on the structure and the degree of hydration of the extracellular matrix, which provides a porous environment for migrating molecules [138]. The effectiveness of cartilage nutrition depends on the conditions of the joint environment, as changes in osmotic pressure and pH modify the flow of ions and metabolites [279]. Passive transport of molecules occurs in unloaded cartilage, although in the case of rhythmic loads or physical activity, mechanical compression occurs, which results in squeezing fluid towards the surface from deep zones and vice versa, which positively affects the convective flow of nutrients [281]. It has been shown that even a small movement of the joint affects the sliding of the cartilage surface, which leads to improved penetration of molecules into the matrix. This is a particularly important process, as it supports chondrocyte metabolism and also helps to limit degeneration [281]. Dynamic loading also has the effect of increasing the pressure gradients between the deep zones and the surface, resulting in increased fluid exchange and thus the delivery of nutrients [282]. In patients affected by OA, the matrix structure is damaged, thereby reducing the ability of the tissue to retain water. This translates into a reduction in the efficiency of nutrient transport, thereby exacerbating metabolic deficiencies in cells, accelerating degeneration [283].

The interaction between AC and SF is particularly important in the biomechanics of the joint, especially in the context of loading and unloading [123]. AC metabolism and homeostasis are significantly influenced by the mechanisms of mechanical transport of nutrients and removal of metabolites [123]. Articular cartilage obtains nutrients mainly

from synovial fluid, which is transported to the cartilage by diffusion and convection, and these processes are assisted by cyclical loading and relaxation of the joint [121]. The ingredient that plays a special role in these processes is HA. As a result of mechanical loading of the joint, there is an increase in pressure within the AC and compression of the extracellular matrix, resulting in fluid from within the AC entering the joint cavity [284]. The mechanism of fluid expulsion is consistent with the principles of poroelasticity, which assumes that the tough collagen-proteoglycan matrix acts as a skeleton, while the displaced fluid acts as a flow phase [157]. When the joint is no longer under load, there is a diastolic phase in which the pressure in the tissue is reduced, resulting in the SF being sucked back into the AC [138]. Urban et al. described this type of mechanism as a "mechanical pump", whereby waste products in the form of unnecessary metabolic products are removed in addition to nutrient transport [279]. Joints subjected to cyclical physiological loads increase the efficiency of this process [285]. Diffusion and fluid motion-assisted convection are influenced by the structural integrity of the AC. Proteoglycans contribute to water binding and water flow control [286]. In older people and those affected by OA, matrix components are degraded, with the result that AC reduces the capacity for effective fluid exchange [287]. In the case of prolonged non-loading, fluid transport is impaired, leading to hypoxia of the chondrocytes, resulting in their apoptosis and matrix degeneration [288]. In order to restore fluid flow, proper mechanical stimulation of the joint should be ensured, which will influence the metabolic activation of the chondrocytes and provide a protective effect on the AC structure [289]. Systematic fluid exchange due to loading and unloading is important for maintaining joint homeostasis, as well as for the biological functions of the AC.

Synovial fluid plays an important role in maintaining the mechanical function of the AC, with nutritional and lubricating functions. Changes in its biochemical composition can contribute to the formation or development of pathological changes in articular cartilage. A description of the processes leading to AC degradation, as well as their impact on biomechanics, is presented in the next section.

5. Degradation of Articular Cartilage

AC can succumb to a variety of pathologies, from rare disease entities to one of the most common: osteoarthritis [290,291]. OA is considered a disease of the entire knee joint, which includes cartilage degradation as well as subchondral bone remodelling, fibrosis and inflammation of the SM, degenerative changes to the meniscus and ligaments and pathological changes to the subchondral fat pad [292–296]. The main risk factors for OA are gender, genetic predisposition, age, joint injury, obesity and diabetes [297–299]. Currently, there are no effective disease-modifying therapies; the only known therapeutic option is joint endoprosthesis at an advanced stage of the disease [300]. One of the main factors limiting the quality of life of patients affected by OA is pain as a consequence of mechanopathology and chronic inflammation [301,302].

In the progression of osteoarthritis, one of the earliest changes is a disruption of the molecular structure and a change in the composition of the extracellular matrix, due to mechanical stress, genetic predisposition or chronic inflammation [287,303–305]. Even in the early stages of OA, a decrease in AC stiffness and an increase in its permeability are observed, which may contribute to an acceleration of the degradation process [306]. Initial changes include a loss of proteoglycans, as well as an increase in tissue hydration. Damage to the matrix induces proliferation and increased chondrocyte synthesis activity, thus enabling temporary maintenance or partial restoration of AC structure in some cases [306]. Under physiological conditions, chondrocytes are metabolically dormant, whereas in OA, they become active and adopt a hypertrophic phenotype [291]. This results in the deregulation of pro-inflammatory and catabolic genes, and in consequence, upregu-

lation of MMPs production [307]. Catabolic activity can be exacerbated by changes in key signalling pathways (TGF-β, Wnt/β-catenin, Notch, Ihh, FGF), as well as by mutations in genes encoding extracellular matrix components [308]. Overproduction of ECM-degrading enzymes consequently leads to irreversible damage to its structure and function [309].

AC degradation is not always irreversible; in some cases, the synovial joint may show the ability to partially rebuild the cartilaginous surface [306,310]. Although the incidence of such a regenerative response is not clearly defined, clinical studies have shown the possibility of spontaneous AC restoration in patients with complete AC loss [306]. In contrast, this phenomenon requires further study, mainly focusing on identifying the determinants of such a response.

A characteristic feature of OA is the destruction of AC resulting from a disruption of homeostasis, with catabolic activity predominating [291]. This process results in proliferation, hypertrophy and apoptosis of chondrocytes, increased angiogenesis, as well as matrix calcification and pathological replication of flow markers [304,307,311,312]. The main cellular phenomena include loosening and degradation of the ECM due to mechanical damage and increased MMP activity, which affects the initiation of the inflammatory cascade and denaturation of mainly collagen II, while loss of elasticity is also noticeable, as is the formation of ruptures and loss of proteoglycans [305,307]. As the disease progresses, the collagen/aggrecan ratio is disrupted, and the composition of collagen changes from type II to type I, which negatively affects collagen networks, weakening them [291]. A reduction in the water content with increased cross-linking of collagen in the matrix compromises the mechanical properties of the tissue. The decrease in stiffness and mechanical strength of the AC makes it more susceptible to damage and promotes the development of degenerative changes [313–316]. Proteoglycan aggregates become smaller, and the aggregate molecules become shorter and less numerous within the aggregates [317–320]. The lesions formed in the superficial zone of the AC extend into the deeper layers, resulting in the formation of vertical fissures, increased calcification, and the presence of doubled flow markers.

Osteoarthritis leads to significant changes in the mechanical properties of the AC. One of the most important parameters used to assess the biomechanics of this tissue is aggregate modulus. It has been found that in AC affected by OA, the value of this parameter decreases, which may indicate a weakening of the structure of the extracellular matrix, and more precisely, the degradation of proteoglycans and the loss of the ability to transfer loads [291]. Another parameter that decreases with the occurrence of OA is the compressive Young's modulus. The decrease in the value of this parameter is related to the degradation of proteoglycans and increased tissue hydration. As a result, the ECM structure is weakened and the ability to transfer loads is lost. The decrease in E_C is estimated to be about 55–68% compared to healthy AC [321]. Collagen structure damage and loss of matrix integrity are reflected in increased hydraulic permeability values. The literature indicates an increase in this parameter by about 60–80% [322]. A slight increase is also noted in the Poisson's ratio, which may indicate changes in the AC structure as well as increased susceptibility to deformation [12]. During OA, the collagen network is damaged and its tensile strength is lost, which is reflected in a reduction of E_t by up to 90% [152]. E_{eq} is also reduced by about 40–80%, which also confirms the weakening of the collagen structure and its reduced ability to regenerate [323,324]. In the course of OA, the integrity of the collagen network is disturbed, as a result of which the risk of cracks and mechanical damage increases. This is reflected in a decrease in the value of the tensile strength parameter [287]. Reduced values are also observed for the complex shear modulus. It is estimated that this parameter decreases by about 70–80%, which increases the susceptibility to shear deformations and reduces the ability to absorb loads [321]. Progression of OA is associated with a significant reduction in the ability of the AC to withstand long-term shear loads, which compromises

the mechanical stability of the joint. This is reflected by a reduction in G_{eq}. Moreover, OA increases viscosity while reducing AC elasticity, which translates into a reduced ability to transfer mechanical loads and thus increases the shear loss angle. Figure 3 shows a comparison of selected parameters of healthy AC versus AC affected by OA.

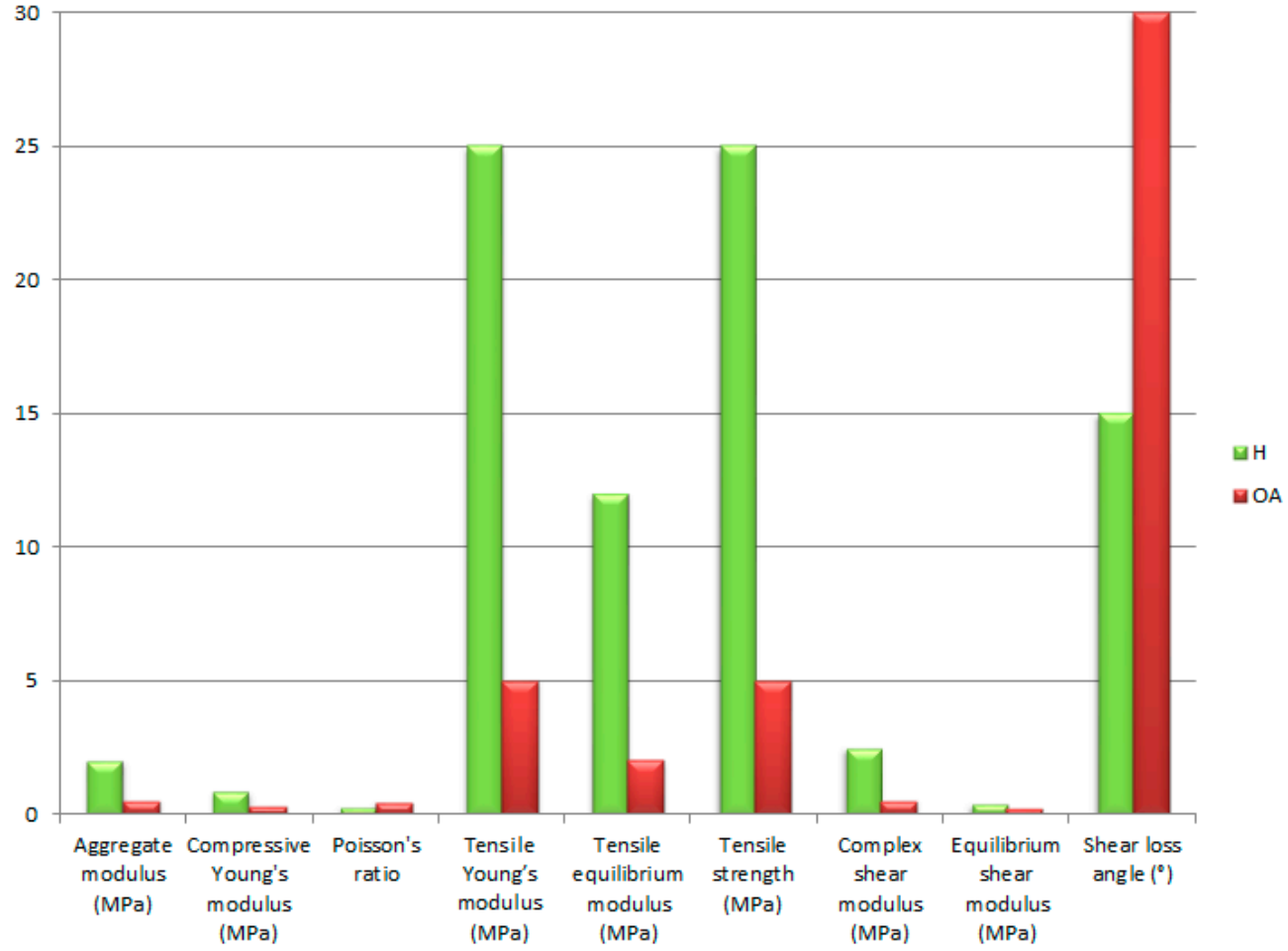

Figure 3. Comparison of selected parameters of healthy AC (H) versus articular cartilage affected by OA.

Age has a significant impact on the composition of the ECM, the spatial organisation of chondrocytes and their response to environmental stimuli, including cytokines [325]. The total number of chondrocytes in the AC does not change, although changes in their distribution within individual zones are observed [2]. With age, the cells tend to disperse in the surface layer, while there is an increased density in the deeper layers. A decrease in the mitotic and synthetic activity of chondrocytes is also observed [129,326]. The response of chondrocytes to anabolic factors in the form of IFG-I is weakened. This may be related to the increased expression of IGF-binding proteins, which limits the availability of the factor for chondrocyte receptors [327,328]. The described changes impair the ability to maintain matrix homeostasis and increase the susceptibility to degradation.

Ageing of AC is associated with a decrease in its hydration, which increases the compressive stiffness of the matrix. The loss of AC's ability to reversibly deform may ultimately lead to greater loads on the underlying subchondral bone. It is therefore crucial to maintain the homeostasis of the extracellular matrix environment for the integrity and function of AC. With age, a decrease in the size of proteoglycan aggregates is observed, which may be the result of limited availability of HA binding sites, as well as proteolytic damage to the connecting proteins and their glycosaminoglycan chains [2]. These changes

may affect the pore size distribution in the matrix and, consequently, its permeability to solutes. An increase in the ratio of keratan sulphate to chondroitin sulphate is also observed, with increased hyaluronan concentration in the ECM. The increase in hyaluronan results from the accumulation of partially degraded molecules in HA [129,327].

The development and progression of OA are supported by chronic, local and systemic low-grade inflammation associated with the secretion of chemokines and cytokines, which regulate the structural and metabolic activity of chondrocytes [308]. In the final stage of osteoarthritis, the AC is completely degraded, exposing the subchondral bone [329].

Figure 4 shows a comparison of MRI images of the healthy knee and the knee with visible degenerative changes. Figure 4A shows a T2-weighted coronal view of a knee joint with full thickness cartilage coverage, no meniscal injury and lack of changes in bone marrow or subchondral bone. In contrast, Figure 4B shows a T2-weighted coronal view of a knee joint with full-thickness cartilage coverage, no meniscal injury and lack of changes in bone marrow or subchondral bone.



Figure 4. MRI of the knee joint: (**A**)—healthy knee, (**B**)—knee with degenerative changes.

Figure 5 shows a comparison of radiographic images of a healthy knee and a knee affected by degenerative changes. Figure 5A shows an AP view of the right knee joint without osteophytes, with a well-preserved joint space. In contrast, 5B shows a long leg standing X-ray with visible joint space narrowing, subchondral sclerosis, marginal osteophytes and alteration in joint line convergence angle.

Figure 6 presents arthroscopic images of a healthy knee and a knee with visible degenerative changes. Figure 6A shows a typical appearance of healthy articular cartilage characterised by a smooth, uniform, and glossy structure. In contrast, Figure 6B depicts an articular surface with irregularities, loss of translucency, and softening of the cartilage, accompanied by superficial fissures and potential focal defects. These findings are consistent with degenerative changes characteristic of osteoarthritis, reflecting compromised cartilage integrity, disruption of surface continuity, and progressive structural deterioration.

Although ageing AC does not necessarily lead to the development of OA, age-related changes lead to an increased risk of degeneration. In older people, there is a several-fold increase in the risk of developing OA after trauma, such as intra-articular fractures [330].

Degenerative processes in the form of proteoglycan loss, collagen degradation or changes in hydration have a direct impact on the reduction of the mechanical properties of AC. It is therefore crucial to detect them at an early stage. The next section includes a description of alternative diagnostic methods that can identify the changes that have occurred at different stages of the disease.

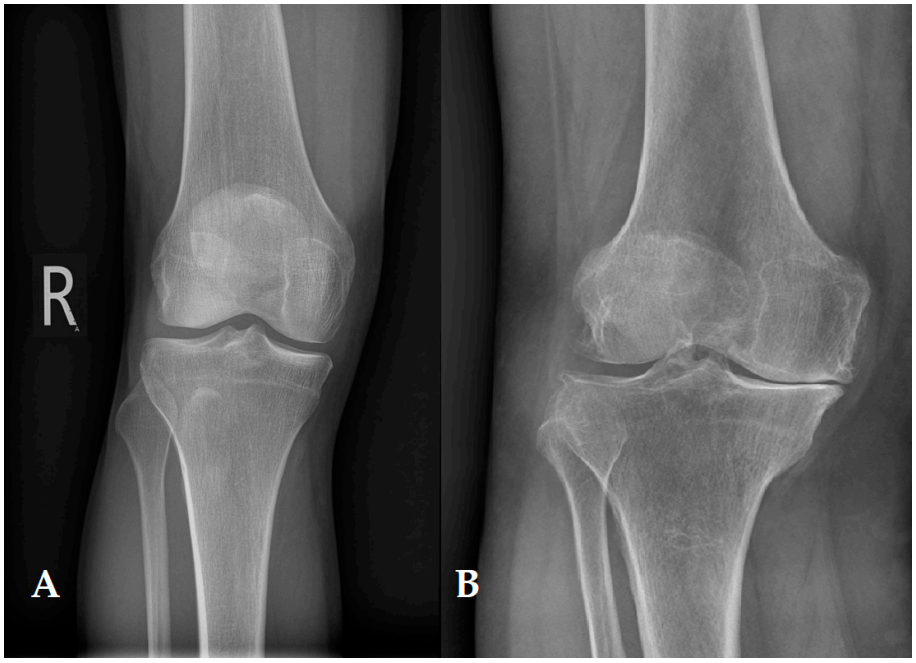

Figure 5. Radiographic image of: (**A**)—healthy knee, (**B**)—knee with degenerative changes.

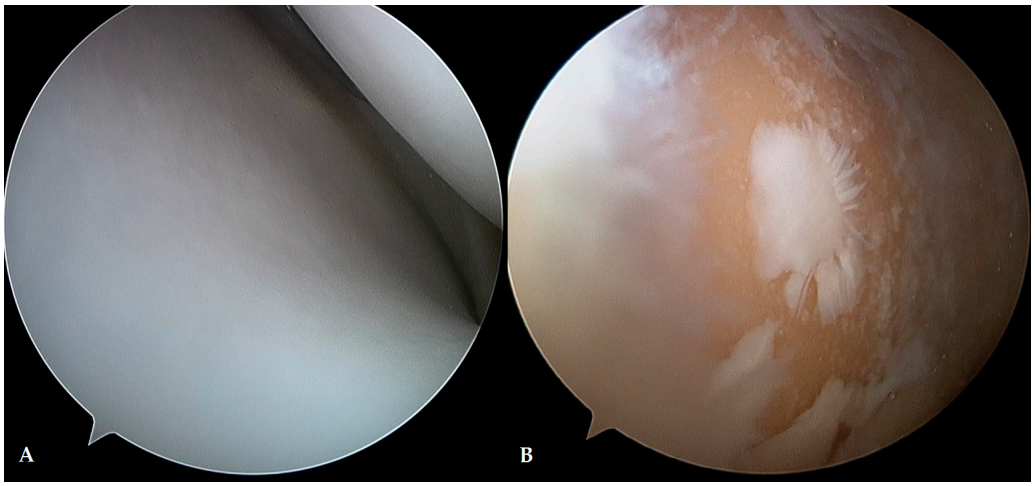

Figure 6. Arthroscopic image of: (**A**)—healthy knee, (**B**)—knee with degenerative changes.

6. Alternative Methods of Articular Cartilage Diagnosis

Modern diagnosis of OA and AC injuries is mainly based on classical imaging techniques, such as MRI and arthroscopy [19]. Although these methods show high accuracy, they also have important limitations, such as invasiveness, high cost and lack of sensitivity to early molecular and biomechanical changes [331]. Alternative diagnostic methods are emerging as the answer to these challenges, making it possible to detect AC degeneration at earlier stages, often even before the onset of clinical symptoms [332].

6.1. MRI with Advanced Imaging Techniques

One of the most relevant imaging modalities for assessing AC is MRI, which has high soft tissue resolution [19]. Advanced techniques in the form of dGEMRIC, T1ρ- or T2-mapping are used to assess the structural and biomechanical properties of the AC before morphological changes occur [331]. Their aim is to detect AC damage at a stage when the changes that have occurred are potentially reversible and there will be no loss of cartilage tissue [331].

The dGEMRIC method, or delayed Gadolinium-Enhanced MRI of Cartilage, is a technique that uses a contrast agent containing negatively charged gadolinium (Gd-DTPA^{2-}), which diffuses into the AC in a proportion inverse to the GAG concentration [32]. In areas where GAG concentrations are low, gadolinium accumulates in greater amounts, resulting in a shortening of the T1ρ relaxation time, making an assessment of AC quality possible [333]. Reduced GAG content and reduced relaxation time due to contrast administration are typical of early degenerative changes [334]. This diagnostic method is considered particularly useful for evaluating the cartilage in the knee and hip.

T1ρ-mapping is a technique based on measuring relaxation in the transverse plane in the presence of a blocking spin, making the method extremely sensitive to changes in proteoglycan content [335]. In AC with degenerative changes, the proteoglycan content decreases, resulting in a prolonged relaxation time [31]. This method has been shown to detect early biomechanical changes in AC before they are visible on standard MRI sequences, hence it shows promise in assessing the progression of OA as well as monitoring the effectiveness of therapy [335]. Another advantage of this method is that it is non-invasive and can be performed without the use of contrast, making it more patient friendly.

T2-mapping is a technique for assessing the orientation and integrity of collagen fibres, as well as the water content of the AC [16]. Collagen fibres in healthy AC are characterised by an ordered structure, which influences the characteristic rather low values of the T2 relaxation time. An increase in T2 values may indicate characteristic degenerative changes, such as disorganisation of the collagen structure or an increase in hydration [16,336]. The use of T2-mapping allows subtle structural changes to be detected before morphological defects appear [336]. The benefits of this method are its non-invasiveness and the lack of a need for contrast.

A modern imaging technique that combines MRI with the analysis of mechanical waves introduced into the tissue to measure its mechanical properties, such as stiffness, is Magnetic Resonance Elastography (MRE) [337]. The use of MRE enables the assessment of AC elasticity and viscosity, which are among the key properties in the diagnosis and monitoring of OA [337]. Lopez et al. [338] used MRE to assess the mechanical properties of hyaline cartilage in vitro, confirming the potential of this method to directly measure the mechanical properties of the tissue. In vitro studies in animal models have also shown the ability to distinguish healthy AC from cartilage with pathological changes, given the differences in stiffness maps [339]. One significant limitation of using this method to assess AC is its limited thickness, thus requiring high spatial resolution as well as precise signal synchronisation [337]. MRE may also find application in monitoring the effectiveness of AC regenerative therapies [339]. However, the answer to this limitation lies in specially developed high-resolution MRE protocols, as well as the use of special mechanical transducers that generate waves at AC-adapted frequencies [337]. Although MRE is currently not a routinely used clinical method to assess AC, the intensive development of this technology offers promising prospects for its use as a diagnostic tool, complementing or even replacing some classical methods [337].

6.2. Vibroarthrography (VAG)

Vibroarthrography is a non-invasive diagnostic method based on the analysis of mechanical vibrations that are generated by a joint during its movement [25,340,341]. The movement of the joint surfaces in a healthy joint is smooth, and the vibroacoustic signals generated are minimal. However, in degenerative lesions, characteristic vibrations that are easier to detect are generated [25]. People struggling with OA are characterised by higher amplitude and variability of VAG signals compared to healthy individuals [342,343]. Through frequency and time analysis of the VAG signals, it is possible to identify char-

acteristic patterns for different stages of cartilage damage. Vibroarthrography, due to its simplicity, low cost and non-invasiveness, can be used as an effective screening tool for the early diagnosis of OA [34,344]. VAG is also characterised by its usefulness in both clinical and population-based screening settings, where there is limited access to advanced imaging techniques [34]. Increasingly accurate sensors and the development of analytical systems based on artificial intelligence are influencing the increasing reliability and accuracy of this method.

Figure 7 shows graphs illustrating vibroarthrography signals recorded during flexion of the healthy knee joint and the knee affected by OA, under two different biomechanical conditions. An open kinematic chain (OCK) and a closed kinematic chain (CKC) were considered. In the two cases mentioned, clear differences in signal characteristics were recorded for the healthy knee joint and the one affected by degenerative changes. The healthy knee joint is characterised by a lower signal amplitude and a more consistent time course, which is related to the smooth sliding of the joint surfaces. In the OA-affected knee, the recorded signals are characterised by higher amplitude and greater irregularity, which is related to increased friction due to unevenness of the articular surfaces as a result of degradation of the articular cartilage.

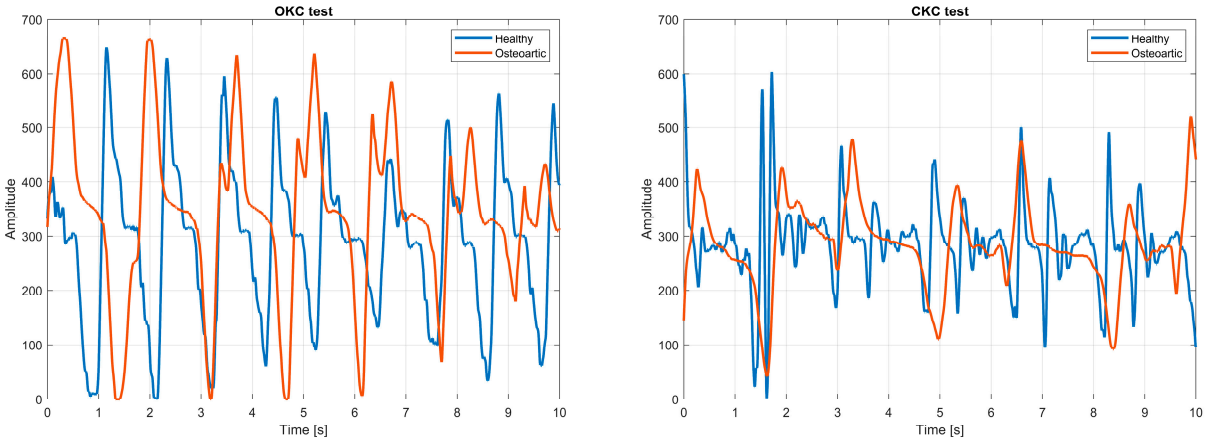

Figure 7. Comparison of vibroarthrographic signals for the healthy and OA knee joint in an open and closed kinematic chain.

6.3. Ultrasound Elastography

Ultrasound elastography is an imaging technique that assesses tissue stiffness based on the speed of shear wave propagation in the tissue [345]. AC is characterised by complex biomechanical properties, showing changes in elasticity during its degeneration. The use of elastography allows information to be obtained about both the structure of the AC and its mechanical properties, which is difficult with traditional imaging techniques [345]. AC during the course of OA shows lower stiffness compared to healthy cartilage [345]. Elastography is extremely useful in the diagnostic process of early degenerative changes, when morphological changes are not yet apparent. The advantages of this method are its non-invasiveness and accessibility, making it an alternative to, for example, MRI in a clinical setting.

6.4. Optical Coherence Tomography (OCT)

Another alternative method is optical coherence tomography, an optical imaging technique that uses near-infrared light to generate high-resolution images of internal structures, such as the AC [346]. Its use allows cross-sectional images of the AC microstructure to be obtained with a resolution of 10–20 µm, which favours the detection of early degenerative changes, such as layer disruption or surface delamination [346]. OCT has been shown to

have a higher sensitivity in detecting early degenerative changes in AC compared to MRI or arthroscopy, indicating the potential of this method in the early diagnosis of OA [347]. It has also been shown that this technique makes it possible to identify changes, such as subtle abnormalities in the collagen fibre system, compared to at least ultrasonography [346]. OCT can also be used during surgical procedures to assess the condition of the AC, increasing its clinical value [348]. Another advantage of OCT is its relatively low invasiveness in contrast to biopsy and classical histopathological methods.

6.5. Modal Analysis

Modal analysis is used to identify properties of mechanical structures, such as vibration modes and damping, as well as natural frequencies, finding application in AC condition assessment [37]. It can be used as an indirect method by which changes in the elastic properties and stiffness of the AC are detected from changes in the dynamic response of the joint [349]. Modal analysis can detect even small changes in the structure of the AC affecting its dynamic response [184]. Local differences in stiffness and damping may be related to the degree of AC damage [350]. Numerical simulations and mechanical experiments can support this method, so it is possible to obtain an accurate representation of the AC response to dynamic loads [351]. The use of modal analysis is particularly useful in the context of AC diagnosis due to the sensitivity of this method [352]. The combination of modal analysis and high-resolution imaging techniques allows the structure and mechanical properties of AC to be assessed at the microscopic level [353]. Nevertheless, the application of this method in clinical practice is still in the research phase [354]. There is a need for further development of modal analysis, focusing on its combination with modern measurement technologies and computer modelling, which may have a positive impact on expanding its diagnostic possibilities.

6.6. Raman Spectroscopy

A promising technique for investigating OA is Raman spectroscopy, which can provide information on the subtle molecular changes in joint tissues as the disease progresses [355]. An important advantage of this method is its non-invasiveness, as well as the direct analysis of well-hydrated tissues, such as AC, in an almost in vivo state [355]. Raman spectroscopy has high spatial resolution and requires little sample processing, making it a suitable method for use in ex vivo AC experiments. Casal-Beiroa et al. [356] described that the analysis of AC samples using this method showed a significant decrease in GAG- and proteoglycan-related signals, with a concomitant increase in the collagen disintegration rate as degenerative changes increased. At the same time, there was also a decrease in the ratio of bands corresponding to GAG versus hydroxyapatite, with an increase in the hydroxyapatite/collagen ratio with OA progression. Correlations of the spectral markers with the biochemical content of GAG and collagen in the tissue were confirmed, proposing them as optical biomarkers of OA. Mason et al. [357] used Raman multivariate curve resolution (MCR) to analyse the cartilage surface, and the results showed that Raman MCR allows accurate quantification of the distribution of AC subcomponents across the surface, down to a depth of 0.5 mm. Jensen et al. [358] demonstrated that polarised Raman spectroscopy can distinguish the different orientations of collagen fibres in different AC layers. The practical potential of the method has been confirmed by screening and classification studies. Shehata et al. [36] described that machine-learning models based on Raman spectra enable healthy AC to be distinguished from damaged AC with high accuracy, and also allow structural, biochemical and biomechanical properties to be estimated. The use of Raman spectroscopy could complement classical imaging methods as well as clinical

examination, influencing the early detection of degenerative changes and tracing the course of OA at the molecular level [36,355].

6.7. Numerical Methods and Artificial Intelligence

Numerical methods and Artificial Intelligence (AI) are becoming the answer to the increasing demand for early, non-invasive and accurate diagnosis [359,360]. The use of numerical methods, especially finite element analysis (FEA), enables precise mapping of the biomechanics of the knee joint. These models take into account the complex biomechanical properties of tissues, including non-linear mechanical behaviour, anisotropies, or structural porosity [361]. Combining these approaches is an important step toward non-invasive and modern diagnosis of degenerative diseases [362,363]. Current AC biomechanical models include single-phase elastic structures, as well as advanced multiphase models [364]. Mohammadi et al. [364] extensively reviewed such models, pointing out their usefulness for analysing the distribution of stresses and displacements under dynamic loading conditions. Smith et al. [365] created a nonlinear, three-dimensional poroelastic model to simulate fluid flow, as well as pressure changes within tissues.

In the work of Peña et al. [362], a three-dimensional FEA model of cartilage, meniscus and ligaments was developed, allowing the local stress distribution to be assessed under physiological conditions. In turn, Mononen et al. [363], using poroelastic properties and fibril-reinforced cartilage, proposed the implementation of gait cycle data into an FEA model, which contributed to a realistic simulation of loading during walking. Such models should be further extended to simulate how mechanical stimuli propagate as vibroacoustic signals, making it possible to investigate the effects of AC degeneration on signal characteristics.

Changes in the mechanical properties of AC, such as a decrease in elastic modulus, affect the way mechanical waves propagate through the joint. The output from a poroelastic model, such as contact displacement or varying pressure, can be used as a source of mechanical vibrations, and then analysed in the time–frequency domain to obtain a synthetic acoustic signal. This approach makes it possible to investigate the effect of changes in AC properties on the spectral characteristics of the recorded signals, which may be of reference in the clinical application of vibroarthrography [366].

The data generated using the models described above can be used as a training base for artificial intelligence models. It is possible to teach machine learning algorithms to classify the degree of AC degeneration based on acoustic features [366]. Reconstruction of mechanical properties can be assisted by neural networks, based on recorded signals, and deep learning algorithms can be used to analyse time-frequency signals showing high sensitivity to structural changes.

There has also been significant development in AI applications, particularly deep neural networks, used in medical image analysis. Segmentation of AC from MRI images is challenging due to its low thickness as well as low signal contrast in T1 and T2 sequences. In such cases, U-Net neural networks and their variants are highly effective, enabling high precision with Dice Similarity Coefficient (DSC) above 0.90 [367,368].

Another example of the use of AI with qualitative analysis is the CartiMorph tool, which aims to integrate deep learning-based segmentation with automated depth and AC volume measurements. The study by Yao et al. [369] showed very high precision, with a correlation >0.95 and a DSC >0.90.

An interesting approach is the analysis of multimodal data, such as Quantitative Susceptibility Mapping (QSM) images combined with nnU-Net segmentation. The use of this method allows for structural and biochemical assessment of AC, obtaining AUC (Area Under the Curve) values exceeding 0.94 [370].

In addition to structural imaging, methods using vibroacoustic signals are emerging. In the work of Karpiński et al. [371], a vibroarthrography method was used to analyse the vibration of the knee joint and classify the AC condition using artificial neural networks, such as the Multilayer Perceptron (MLP) and Radial Basis Function Network (RBF). By applying feature selection using neighbourhood component analysis (NCA), a classification efficiency of >95% was achieved. The use of vibroacoustic methods provides information complementary to structural imaging. In particular, insights gained from FEA-based biomechanical models can provide input for generating or interpreting a synthetic signal.

The combination of numerical methods and AI makes it possible to create clinical decision support systems (CDSS) using both imaging and clinical and biomechanical data to recommend therapies, as well as predict OA progression [372]. Such systems can benefit from the synthetic data that are generated by numerical models. The benefit of this approach is to streamline the training of AI tools for limited clinical data.

In the context of tissue engineering, the use of FEA models supports the design of scaffolds and the simulation of biomaterial–tissue interactions, while AI finds application in the generative design of microstructures with optimal mechanical as well as biological properties [373].

Thus, the integration of numerical methods and AI contributes to new perspectives for more effective diagnosis of AC diseases. The combination of these technologies with modern imaging techniques, biomechanical analysis and tissue engineering approaches offers the potential to develop diagnostic tools with improved accuracy and precision, reproducibility and predictive ability, which may be reflected in improved quality and efficacy of therapy.

Despite the promising nature of advanced diagnostic techniques for articular cartilage assessment, each modality possesses specific limitations that constrain its clinical or research utility. For instance, Optical Coherence Tomography (OCT), while offering near-histological resolution, is limited in in vivo applications by shallow penetration depth and the need for intra-articular access. Similarly, Magnetic Resonance Elastography (MRE) and T1ρ or T2 mapping require specialised sequences and long acquisition times, which may reduce their feasibility in routine practice. Raman spectroscopy, despite its potential for molecular analysis, suffers from high sensitivity to motion artefacts and signal attenuation in deeper tissues. A concise overview of the key advantages and limitations of each modality is presented in Table 4 to assist clinicians and researchers in selecting the appropriate diagnostic tool depending on the clinical scenario or research focus.

Table 4. Advantages and limitations of alternative methods of articular cartilage diagnosis.

Modality	Main Strengths	Key Limitations
MRI	High-resolution soft tissue imaging; good for cartilage morphology; non-invasive	Limited sensitivity to early biochemical changes; long scan times; expensive
CT-Arthrography	Excellent surface detail; useful in patients with MRI contraindications	Radiation exposure; requires contrast agent; not suitable for repeated use
Ultrasound	Low cost; widely available; real-time assessment	Low spatial resolution; operator dependent; limited to surface evaluation
MRE	Quantitative stiffness mapping; non-invasive biomechanical insight	Specialised sequences required; limited availability; long acquisition times

Table 4. *Cont.*

Modality	Main Strengths	Key Limitations
T2/T1ρ/dGEMRIC MRI	Sensitive to biochemical changes; useful for early OA detection	Requires special protocols or contrast agents; expensive; time-consuming
Ultrasound Elastography	Provides mechanical property estimates; fast	Surface-limited; low penetration; operator-dependent
Vibroarthrography (VAG)	Functional, real-time mechanical assessment; simple setup	Low spatial specificity; experimental; signal variability
OCT	Micron-level resolution; near-histological visualisation	Shallow penetration depth; limited to intra-articular or open procedures
Raman Spectroscopy	Molecular composition profiling; label-free biochemical insights	Low depth penetration; motion sensitive; experimental
Modal Analysis	Provides dynamic mechanical parameters; sensitive to tissue degradation	High experimental complexity; limited to research applications

Given the growing number of available diagnostic techniques—both conventional and emerging—it is important to systematise their key characteristics in a comparative manner. Although individual methods differ in terms of clinical maturity, cost, diagnostic performance, and capacity to detect early degenerative changes, their complementary value should be emphasised.

To facilitate a clearer understanding of the advantages and limitations of each modality, Table 5 provides a comparative overview of selected imaging and functional diagnostic techniques used in the assessment of articular cartilage. The comparison includes criteria such as diagnostic accuracy, invasiveness, operator dependence, clinical readiness, and ability to assess biomechanical or biochemical tissue properties. This synthetic summary may serve as a practical reference in clinical decision-making and future research planning.

Table 5. Comparative analysis of alternative methods of articular cartilage diagnosis.

Modality	Diagnostic Accuracy	Invasiveness	Operator Dependence	Clinical Readiness	Ability to Assess Biomechanics	Other Notes
MRI	High for structure, moderate for early OA	Non-invasive	Low	Widely available	Indirect (via advanced protocols)	High cost; long exam duration; sensitive to motion artifacts
CT-Arthrography	High for surface integrity	Minimally invasive (contrast + radiation)	Low	Available, especially when MRI is contraindicated	No	Risk of infection, allergic reaction; repeated use limited due to radiation

Table 5. *Cont.*

Modality	Diagnostic Accuracy	Invasiveness	Operator Dependence	Clinical Readiness	Ability to Assess Biomechanics	Other Notes
Ultrasound	Low-moderate (surface only)	Non-invasive	High	Widely available	No	Inexpensive; real-time imaging; limited depth penetration
MRE	Emerging; promising for stiffness maps	Non-invasive	Moderate	Limited clinical use	Yes (shear stiffness mapping)	Requires advanced MRI hardware and postprocessing
T2/T1ρ/dGEMRIC MRI	High (biochemical properties)	Non-invasive	Low	Research settings	Indirect (composition-based)	Enables early detection of degeneration; requires contrast (dGEMRIC)
Ultrasound Elastography	Moderate (surface stiffness)	Non-invasive	Moderate	Limited clinical use	Yes (local stiffness)	Operator-dependent; resolution limitations
Vibroarthrography (VAG)	Moderate (early degeneration detection)	Non-invasive	Moderate	Experimental	Yes (mechanical friction detection)	Simple to use; promising for dynamic functional assessment
OCT	High (microscopic structure)	Minimally invasive (intra-articular)	High	Experimental	No	High-resolution imaging; limited to accessible joints (e.g., during arthroscopy)
Raman Spectroscopy	High (biochemical markers)	Minimally invasive	Moderate	Experimental	Indirect (molecular composition)	Promising for collagen/proteoglycan content analysis
Modal Analysis	Moderate (mechanical dynamics)	Non-invasive	High	Experimental	Yes (dynamic stiffness)	Requires controlled loading; research-stage tool

In summary, alternative diagnostic methods of AC are an ever-evolving area of research aimed at the early detection of degenerative changes. The techniques discussed above show an increasingly precise view of the AC condition, taking into account the structural, biochemical and biomechanical aspects. Modern vibratory and quantitative imaging techniques enable the non-invasive identification of subtle changes in the composition and properties of AC, thus detecting pathological changes before morphologically visible symptoms of OA develop. A decrease in Young's modulus, disorganisation of collagen fibres, or an increase in permeability are directly reflected in the results obtained by a number of diagnostic techniques. An increase in T2 relaxation time, an increase in T1ρ, or a decrease in dGEMRIC indices have been shown to be associated with a deterioration in the mechanical properties of AC [374,375]. The use of advanced spectroscopic methods or

artificial intelligence algorithms has the positive effect of enhancing both the diagnostic and prognostic potential of these techniques. However, the focus should be on the further development of alternative diagnostic methods of AC in order to implement them in daily clinical practice. These measures will positively improve the efficiency of early diagnosis of degenerative changes, improving patients' quality of life. Further research on the standardisation and validation of these solutions is therefore crucial so that they can be implemented in the care of patients affected by OA.

7. Summary

Articular cartilage is a specialised connective tissue that covers the articular surfaces of bones in synovial joints. It is composed mainly of chondrocytes located in the ECM, type II collagen, proteoglycans, and water. Due to the lack of vascularisation, innervation, and lymphatic vessels, the process of chondrocyte nutrition occurs through fusion with synovial fluid, which significantly limits the ability for self-repair [376].

The function of AC is to absorb and distribute mechanical loads and, above all, to ensure joint movement with minimised friction. The organisation of collagen fibres and the content of proteoglycans in the ECM affect the biomechanical properties of AC, more specifically its elasticity and shear resistance [377].

Degeneration of articular cartilage results in a loss of both structural and functional integrity. Degradation of ECM leads to a loss of proteoglycans and type II collagen. As a result, there is a decrease in AC thickness, crack formation, and exposure of subchondral bone [378]. In the course of OA, the AC structure degrades, which significantly changes its mechanical properties, such as a decrease in the modulus of elasticity, an increase in the coefficient of friction, or a loss of structural integrity. As a result, the cushioning and protective functions of the joint cartilage deteriorate.

Traditional diagnostic methods, such as radiological imaging and magnetic resonance imaging, are used to assess advanced structural changes in cartilage. However, the early stages of degeneration are often not visible using these techniques. Therefore, alternative methods are gaining increasing importance, especially the analysis of vibroacoustic signals generated during joint movement. Changes in the mechanical properties of cartilage can affect the characteristics of acoustic signals, due to which this method can be used for the early detection of degeneration.

Therapies for damaged AC include symptomatic, reparative, and regenerative treatment. Symptomatic treatment is focused on relieving pain and anti-inflammatory medications, as well as intra-articular injections [379]. The aim of repair methods is to stimulate AC regeneration through microfractures or osteochondral grafts [380,381].

The mechanical properties of AC and their changes are important in the pathogenesis and diagnosis of joint diseases. The combination of classical and alternative diagnostic methods may result in earlier diagnosis of pathological changes and more precise monitoring of the effectiveness of the applied therapies. However, further research is needed in this area to enable the development of effective diagnostic and therapeutic strategies in the treatment of degenerative joint diseases.

8. Conclusions

Articular cartilage is a highly specialised connective tissue with a unique structure. The mechanical properties of AC result from the complex organisation of the extracellular matrix, in which type II collagen and proteoglycans play an important role, ensuring the appropriate stiffness and elasticity of the tissue. The mechanical properties of AC play a key role in ensuring its correct biomechanical functions, as the cartilage's function is to provide movement with minimal friction and to transmit and dissipate mechanical

loads. Osteoarthritis leads to a progressive deterioration of these properties, as well as the structure of the AC. In the course of OA, the AC structure degrades, which significantly changes its mechanical properties, such as a decrease in the modulus of elasticity, an increase in the coefficient of friction, or a loss of structural integrity. As a result, the cushioning and protective functions of the joint cartilage deteriorate. These changes are caused by mechanical and biochemical factors that affect the degeneration of collagen and proteoglycans, as well as disturbances in cellular homeostasis. Evaluation of the mechanical properties of AC is possible via classical as well as alternative diagnostic methods.

Typical diagnostic methods mainly provide information on the thickness and morphology of the AC. MRI is characterised by high imaging resolution, making it possible to detect cartilage defects, while visible lesions are only seen at an advanced stage of OA. Arthroscopy is an invaluable method for direct assessment, but its main limitation is its invasiveness, which can result in numerous complications. A quick and accessible method is ultrasound, although this method cannot be used to assess the full structure of the AC, which reduces its diagnostic quality [34]. In addition, the assessment is dependent on the radiologist performing the examination.

Enhanced MRI techniques allow indirect imaging of AC matrix composition. The T2 relaxation time is related to the collagen network structure and water content, while T1ρ shows sensitivity to the proteoglycan content. T1ρ can detect early biochemical changes in OA before the changes are visible on T2 [382]. Nissi et al. [383] showed that T1 ρ and T2 relaxations are related to AC elasticity depending on tissue type. Elastographic techniques, on the other hand, allow in vivo measurements of AC stiffness. Ex vivo tests have confirmed the effect of proteoglycan degradation on lowering the velocity of wave propagation in articular cartilage, reflecting a reduction in its stiffness [345]. Georgas et al. [345] demonstrated that with shear wave ultrasound elastography, it is possible to distinguish typical mechanical changes for different stages of AC damage. In addition, in vivo MRE tests indicated an increase in stiffness as the regenerated AC matured [339]. Vibroarthrography provides dynamic data and can show even subtle biomechanical abnormalities of the AC. While the literature describes the higher diagnostic sensitivity of VAG in contrast to ultrasound, the lack of standardised testing protocols prevents this method from being implemented in everyday clinical practice [34]. Krakowski et al. [322] emphasised the importance of the mechanical and tribological properties of AC in the context of the development and treatment of OA. The effectiveness of repair methods, such as autologous chondrocyte implantation or tissue engineering techniques, is dependent on the reconstruction of the structure and restoration of the appropriate mechanical properties of the tissue. Analysis of vibroacoustic signals can therefore be a valuable tool for monitoring the effectiveness of therapy and for assessing the progression of the disease. A method to assess the chemical composition of the AC matrix, such as the collagen or proteoglycan content, is Raman spectroscopy. Preliminary studies show that there is a correlation between Raman spectral markers and mechanical parameters of AC. Modal analysis provides information on the global structural stiffness of the joint. Nevertheless, both methods require further research. Therefore, a combination of typical and alternative diagnostic methods could enable a more comprehensive assessment of the AC status in OA [382].

In addition to improving early-stage detection, advanced diagnostic modalities hold promise as integral tools in regenerative medicine. The ability to non-invasively assess the structural, mechanical, and biochemical state of articular cartilage may provide critical input for the design and optimisation of bioengineered implants and scaffolds. Recent advances in biofabrication technologies, such as those highlighted by Bini et al. [384], demonstrate how imaging-derived data can inform personalised osteochondral repair strategies, ensuring proper tissue integration and mimicking native zonal architecture.

Bridging diagnostic insights with next-generation therapeutic solutions represents a crucial direction in the evolution of precision musculoskeletal medicine.

Understanding of the mechanical properties of healthy and damaged AC is extremely important in the context of designing biomaterials and scaffolds for joint regeneration. It is necessary to adjust the stiffness and viscoelastic characteristics of the material appropriately so that they can imitate real AC. Knowledge of the mechanical properties of AC may also be useful in clinical practice to assess the efficacy of regenerative therapies. The use of MRE and ultrasound elastography could enable the assessment of the quality of regenerated AC without the need for biopsy [385]. Information on AC mechanics may also increase the effectiveness of selecting implant biomaterials that are resistant to significant compressive loads [229].

There is a need for research on the standardisation of methods for measuring AC biomechanics in vivo. Protocols for measurements using techniques such as VAG should be developed. Researchers should also focus on developing reference values of stiffness and viscosity for healthy and diseased articular cartilage. At present, knowledge about the correlation between mechanical parameters and clinical outcomes is limited. Future studies should focus on the relationship between stiffness or viscosity changes and patient symptoms and the progression of osteoarthritis. It is also worth noting that the use of artificial intelligence and multi-scale analysis to combine imaging, biomechanical and biomarker data is a promising direction.

Author Contributions: Conceptualisation, R.K. and A.P.; methodology, R.K. and A.P.; validation, R.K., K.J., J.B., M.P. and P.K.; formal analysis, R.K., J.B., P.K., K.J., S.R. and M.P.; resources, A.P. and R.K.; data curation, R.K. and A.P.; writing—original draft preparation, A.P. and R.K.; writing—review and editing, R.K., J.B., P.K., S.R. and M.P.; visualisation, R.K., J.B., P.K., S.R. and M.P.; supervision, R.K., J.B., K.J., P.K., S.R. and M.P. All authors have read and agreed to the published version of the manuscript.

Funding: This research received no external funding.

Conflicts of Interest: The authors declare no conflicts of interest.

Abbreviations

AC articular cartilage, **OA** osteoarthritis, **X-ray** radiography, **MRI** magnetic resonance imaging, **CT-arthrography** computed tomography with arthrography, **MRE** magnetic resonance elastography, **dGEMRIC** delayed gadolinium-enhanced MRI of cartilage, **VAG** vibroarthrography, **OCT** optical coherence tomography, **ECM** extracellular matrix, **COL** collagen, **ACAN** aggrecan, **BMSCs** mesenchymal stem cells, **COL2A1** alpha-1 type collagen gene, **Runx2** runt-related transcription factor 2, **PRG4** proteoglycan-4, **Sox9** SRY-Box transcription factor, **TGF-β** transforming growth factor-beta, **BMPs** bone morphogenetic proteins, **MAPK** mitogen-activated protein kinase, $\mathbf{H_A}$ aggregate modulus, $\mathbf{E_C}$ compressive Young's modulus, $\mathbf{E_t}$ tensile Young's modulus, υ Poisson's ratio, k hydraulic permeability, $\mathbf{E_{eq}}$ equilibrium tensile modulus, $\mathbf{G_{eq}}$ equilibrium shear modulus, δ shear loss angle, **GAG** glycosaminoglycans, **SF** synovial fluid, **PSB** phosphate buffer medium, **SM** synovial membrane, **SAPL** surfactant phospholipids, **HA** hyaluronate, **MCR** Raman curve resolution, **AI** Artificial Intelligence, **FEA** finite element analysis, **DSC** Dice Similarity Coefficient, **AUC** Area Under the Curve, **MLP** Multilayer Perceptron, **RBF** Radial Basis Function Network, **NCA** neighbourhood component analysis, OCK open kinematic chain, **CKC** closed kinematic chain.

References

1. Nachtsheim, J.; Dursun, G.; Markert, B.; Stoffel, M. Chondrocyte Colonisation of a Tissue-Engineered Cartilage Substitute under a Mechanical Stimulus. *Med. Eng. Phys.* **2019**, *74*, 58–64. [CrossRef] [PubMed]
2. Sophia Fox, A.J.; Bedi, A.; Rodeo, S.A. The Basic Science of Articular Cartilage: Structure, Composition, and Function. *Sports Health A Multidiscip. Approach* **2009**, *1*, 461–468. [CrossRef] [PubMed]
3. Sajewicz, E. *Wprowadzenie Do Biotribologii*; Oficyna Wydawnicza Politechniki Białostockiej: Białystok, Poland, 2011; ISBN 978-83-62582-13-6.
4. Eschweiler, J.; Horn, N.; Rath, B.; Betsch, M.; Baroncini, A.; Tingart, M.; Migliorini, F. The Biomechanics of Cartilage—An Overview. *Life* **2021**, *11*, 302. [CrossRef]
5. Buckwalter, J.A.; Mankin, H.J.; Grodzinsky, A.J. Articular Cartilage and Osteoarthritis. *Instr. Course Lect.* **2005**, *54*, 465–480.
6. Weber, J.F.; Perez, R.; Waldman, S.D. Mechanobioreactors for Cartilage Tissue Engineering. In *Cartilage Tissue Engineering*; Doran, P.M., Ed.; Methods in Molecular Biology; Springer: New York, NY, USA, 2015; Volume 1340, pp. 203–219. ISBN 978-1-4939-2937-5.
7. Liu, Y.; Shah, K.M.; Luo, J. Strategies for Articular Cartilage Repair and Regeneration. *Front. Bioeng. Biotechnol.* **2021**, *9*, 770655. [CrossRef]
8. Lu, X.L.; Mow, V.C. Biomechanics of Articular Cartilage and Determination of Material Properties. *Med. Sci. Sports Exerc.* **2008**, *40*, 193–199. [CrossRef]
9. Chiang, H.; Jiang, C.-C. Repair of Articular Cartilage Defects: Review and Perspectives. *J. Formos. Med. Assoc.* **2009**, *108*, 87–101. [CrossRef] [PubMed]
10. Iwamoto, M.; Ohta, Y.; Larmour, C.; Enomoto-Iwamoto, M. Toward Regeneration of Articular Cartilage. *Birth Defects Res. Part C* **2013**, *99*, 192–202. [CrossRef]
11. Borrelli, J.; Olson, S.A.; Godbout, C.; Schemitsch, E.H.; Stannard, J.P.; Giannoudis, P.V. Understanding Articular Cartilage Injury and Potential Treatments. *J. Orthop. Trauma* **2019**, *33*, S6–S12. [CrossRef]
12. Petitjean, N.; Canadas, P.; Royer, P.; Noël, D.; Le Floc'h, S. Cartilage Biomechanics: From the Basic Facts to the Challenges of Tissue Engineering. *J. Biomed. Mater. Res.* **2023**, *111*, 1067–1089. [CrossRef]
13. Meftah, M.; Ranawat, A.S.; Ranawat, C.S. The Natural History of Anterior Knee Pain in 2 Posterior-Stabilized, Modular Total Knee Arthroplasty Designs. *J. Arthroplast.* **2011**, *26*, 1145–1148. [CrossRef] [PubMed]
14. Mow, V.C.; Gu, W.; Chen, F.H. Structure and Function of Articular Cartilage and Meniscus. In *Basic Orthopaedic Biomechanics & Mechano-Biology*; Lippincott Williams & Wilkins: Philadelphia, PA, USA, 2005.
15. Rubin, D.A.; Maas, M. Imaging of the Knee. In *Musculoskeletal Diseases 2013–2016: Diagnostic Imaging and Interventional Techniques*; Springer: Milan, Italy, 2013; pp. 59–66.
16. Mosher, T.J.; Dardzinski, B.J. Cartilage MRI T2 Relaxation Time Mapping: Overview and Applications. *Semin. Musculoskelet. Radiol.* **2004**, *8*, 355–368. [CrossRef] [PubMed]
17. Saarakkala, S.; Laasanen, M.S.; Jurvelin, J.S.; Töyräs, J. Quantitative Ultrasound Imaging Detects Degenerative Changes in Articular Cartilage Surface and Subchondral Bone. *Phys. Med. Biol.* **2006**, *51*, 5333. [CrossRef] [PubMed]
18. Hunter, D.J.; Eckstein, F. Exercise and Osteoarthritis. *J. Anat.* **2009**, *214*, 197–207. [CrossRef]
19. Guermazi, A.; Hayashi, D.; Eckstein, F.; Hunter, D.J.; Duryea, J.; Roemer, F.W. Imaging of Osteoarthritis. *Rheum. Dis. Clin. N. Am.* **2013**, *39*, 67–105. [CrossRef]
20. Nieminen, M.T.; Rieppo, J.; Töyräs, J.; Hakumäki, J.M.; Silvennoinen, J.; Hyttinen, M.M.; Helminen, H.J.; Jurvelin, J.S. T_2 Relaxation Reveals Spatial Collagen Architecture in Articular Cartilage: A Comparative Quantitative MRI and Polarized Light Microscopic Study. *Magn. Reson. Med.* **2001**, *46*, 487–493. [CrossRef]
21. Omoumi, P.; Mourad, C.; Ledoux, J.-B.; Hilbert, T. Morphological Assessment of Cartilage and Osteoarthritis in Clinical Practice and Research: Intermediate-Weighted Fat-Suppressed Sequences and Beyond. *Skelet. Radiol.* **2023**, *52*, 2185–2198. [CrossRef]
22. Omoumi, P.; Berg, B.C.V.; Lecouvet, F.E. Value of CT Arthrography in the Assessment of Cartilage Pathology. In *Cartilage Imaging*; Link, T.M., Ed.; Springer: New York, NY, USA, 2011; pp. 37–48. ISBN 978-1-4419-8437-1.
23. Kellgren, J.H.; Lawrence, J.S. Radiological Assessment of Osteo-Arthrosis. *Ann. Rheum. Dis.* **1957**, *16*, 494–502. [CrossRef]
24. Bonnin, M.; Chambat, P. (Eds.) *Osteoartritis of the Knee*; Approche pratique en orthopédie-traumatologie; Springer: Paris, France; Berlin, Germany, 2008; ISBN 978-2-287-74174-6.
25. Befrui, N.; Elsner, J.; Flesser, A.; Huvanandana, J.; Jarrousse, O.; Le, T.N.; Müller, M.; Schulze, W.H.W.; Taing, S.; Weidert, S. Vibroarthrography for Early Detection of Knee Osteoarthritis Using Normalized Frequency Features. *Med. Biol. Eng. Comput.* **2018**, *56*, 1499–1514. [CrossRef]
26. Hayashi, D.; Roemer, F.W.; Guermazi, A. Imaging of Osteoarthritis by Conventional Radiography, MR Imaging, PET–Computed Tomography, and PET–MR Imaging. *PET Clin.* **2019**, *14*, 17–29. [CrossRef]
27. Richette, P.; Latourte, A. Osteoarthritis: Value of imaging and biomarkers. *Rev. Prat.* **2019**, *69*, 507–509. [PubMed]
28. Iagnocco, A. Imaging the Joint in Osteoarthritis: A Place for Ultrasound? *Best. Pract. Res. Clin. Rheumatol.* **2010**, *24*, 27–38. [CrossRef]

29. Grassi, W.; Salaffi, F.; Filippucci, E. Ultrasound in Rheumatology. *Best. Pract. Res. Clin. Rheumatol.* **2005**, *19*, 467–485. [CrossRef] [PubMed]
30. Muthupillai, R.; Lomas, D.J.; Rossman, P.J.; Greenleaf, J.F.; Manduca, A.; Ehman, R.L. Magnetic Resonance Elastography by Direct Visualization of Propagating Acoustic Strain Waves. *Science* **1995**, *269*, 1854–1857. [CrossRef] [PubMed]
31. Li, X.; Benjamin Ma, C.; Link, T.M.; Castillo, D.-D.; Blumenkrantz, G.; Lozano, J.; Carballido-Gamio, J.; Ries, M.; Majumdar, S. In Vivo T1ρ and T2 Mapping of Articular Cartilage in Osteoarthritis of the Knee Using 3T MRI. *Osteoarthr. Cartil.* **2007**, *15*, 789–797. [CrossRef]
32. Bashir, A.; Gray, M.L.; Burstein, D. Gd-DTPA^{2-} as a Measure of Cartilage Degradation. *Magn. Reson. Med.* **1996**, *36*, 665–673. [CrossRef]
33. Doyley, M.M. Model-Based Elastography: A Survey of Approaches to the Inverse Elasticity Problem. *Phys. Med. Biol.* **2012**, *57*, R35-73. [CrossRef]
34. Karpiński, R.; Prus, A.; Jonak, K.; Krakowski, P. Vibroarthrography as a Noninvasive Screening Method for Early Diagnosis of Knee Osteoarthritis: A Review of Current Research. *Appl. Sci.* **2024**, *15*, 279. [CrossRef]
35. Drexler, W.; Fujimoto, J.G. *Optical Coherence Tomography: Technology and Applications*; Springer Science & Business Media: Berlin, Germany, 2008; ISBN 3-540-77550-1.
36. Shehata, E.; Nippolainen, E.; Shaikh, R.; Ronkainen, A.-P.; Töyräs, J.; Sarin, J.K.; Afara, I.O. Raman Spectroscopy and Machine Learning Enables Estimation of Articular Cartilage Structural, Compositional, and Functional Properties. *Ann. Biomed. Eng.* **2023**, *51*, 2301–2312. [CrossRef]
37. Ewins, D.J. *Modal Testing: Theory, Practice and Application*; John Wiley & Sons: Hoboken, NJ, USA, 2009; ISBN 0-86380-218-4.
38. Shepherd, D.E.T.; Seedhom, B.B. Thickness of Human Articular Cartilage in Joints of the Lower Limb. *Ann. Rheum. Dis.* **1999**, *58*, 27–34. [CrossRef]
39. Wayne, J.S.; Brodrick, C.W.; Mukherjee, N. Measurement of Articular Cartilage Thickness in the Articulated Knee. *Ann. Biomed. Eng.* **1998**, *26*, 96–102. [CrossRef] [PubMed]
40. Kuettner, K.E.; Cole, A.A. Cartilage Degeneration in Different Human Joints. *Osteoarthr. Cartil.* **2005**, *13*, 93–103. [CrossRef] [PubMed]
41. Buckwalter, J.A.; Mankin, H.J. Articular Cartilage: Tissue Design and Chondrocyte-Matrix Interactions. *Instr. Course Lect.* **1998**, *47*, 477–486.
42. Doran, P.M. (Ed.) *Cartilage Tissue Engineering: Methods and Protocols*; Methods in Molecular Biology; Springer: New York, NY, USA, 2015; Volume 1340, ISBN 978-1-4939-2937-5.
43. Grässel, S.; Aszódi, A. (Eds.) *Cartilage*; Springer International Publishing: Cham, Switzerland, 2016; ISBN 978-3-319-29566-4.
44. Xu, W.; Zhu, J.; Hu, J.; Xiao, L. Engineering the Biomechanical Microenvironment of Chondrocytes towards Articular Cartilage Tissue Engineering. *Life Sci.* **2022**, *309*, 121043. [CrossRef]
45. Mansour, J.M. Biomechanics of Cartilage. *Kinesiol. Mech. Pathomechanics Hum. Mov.* **2003**, *2*, 66–79.
46. Redler, I.; Mow, V.C.; Zimny, M.L.; Mansell, J. The Ultrastructure and Biomechanical Significance of the Tidemark of Articular Cartilage. *Clin. Orthop. Relat. Res.* **1975**, *112*, 357–362. [CrossRef]
47. Eggli, P.S.; Herrmann, W.; Hunziker, E.B.; Schenk, R.K. Matrix Compartments in the Growth Plate of the Proximal Tibia of Rats. *Anat. Rec.* **1985**, *211*, 246–257. [CrossRef] [PubMed]
48. Guilak, F.; Mow, V.C. The Mechanical Environment of the Chondrocyte: A Biphasic Finite Element Model of Cell-Matrix Interactions in Articular Cartilage. *J. Biomech.* **2000**, *33*, 1663–1673. [CrossRef]
49. Muir, H. The Chondrocyte, Architect of Cartilage. Biomechanics, Structure, Function and Molecular Biology of Cartilage Matrix Macromolecules. *BioEssays* **1995**, *17*, 1039–1048. [CrossRef]
50. Szirmai, J. Aging of Connective and Skeletal Tissue. *Struct. Cartil.* **1969**, 163–184.
51. Mow, V.C.; Guo, X.E. Mechano-Electrochemical Properties Of Articular Cartilage: Their Inhomogeneities and Anisotropies. *Annu. Rev. Biomed. Eng.* **2002**, *4*, 175–209. [CrossRef] [PubMed]
52. Alford, J.W.; Cole, B.J. Cartilage Restoration, Part 1: Basic Science, Historical Perspective, Patient Evaluation, and Treatment Options. *Am. J. Sports Med.* **2005**, *33*, 295–306. [CrossRef]
53. Chen, H.; Tan, X.-N.; Hu, S.; Liu, R.-Q.; Peng, L.-H.; Li, Y.-M.; Wu, P. Molecular Mechanisms of Chondrocyte Proliferation and Differentiation. *Front. Cell Dev. Biol.* **2021**, *9*, 664168. [CrossRef] [PubMed]
54. Jiang, Y.; Tuan, R.S. Origin and Function of Cartilage Stem/Progenitor Cells in Osteoarthritis. *Nat. Rev. Rheumatol.* **2015**, *11*, 206–212. [CrossRef]
55. Chijimatsu, R.; Saito, T. Mechanisms of Synovial Joint and Articular Cartilage Development. *Cell. Mol. Life Sci.* **2019**, *76*, 3939–3952. [CrossRef]
56. Lane Smith, R.; Trindade, M.; Ikenoue, T.; Mohtai, M.; Das, P.; Carter, D.; Goodman, S.; Schurman, D. Effects of Shear Stress on Articular Chondrocyte Metabolism. *Biorheology* **2000**, *37*, 95–107. [CrossRef] [PubMed]

57. Bačenková, D.; Trebuňová, M.; Demeterová, J.; Živčák, J. Human Chondrocytes, Metabolism of Articular Cartilage, and Strategies for Application to Tissue Engineering. *Int. J. Mol. Sci.* **2023**, *24*, 17096. [CrossRef]
58. Lin, Z.; Willers, C.; Xu, J.; Zheng, M.-H. The Chondrocyte: Biology and Clinical Application. *Tissue Eng.* **2006**, *12*, 1971–1984. [CrossRef]
59. Rim, Y.A.; Nam, Y.; Ju, J.H. The Role of Chondrocyte Hypertrophy and Senescence in Osteoarthritis Initiation and Progression. *Int. J. Mol. Sci.* **2020**, *21*, 2358. [CrossRef]
60. Kozhemyakina, E.; Lassar, A.B.; Zelzer, E. A Pathway to Bone: Signaling Molecules and Transcription Factors Involved in Chondrocyte Development and Maturation. *Development* **2015**, *142*, 817–831. [CrossRef]
61. Liu, C.-F.; Samsa, W.E.; Zhou, G.; Lefebvre, V. Transcriptional Control of Chondrocyte Specification and Differentiation. *Semin. Cell Dev. Biol.* **2017**, *62*, 34–49. [CrossRef] [PubMed]
62. Fischer, J.; Knoch, N.; Sims, T.; Rosshirt, N.; Richter, W. Time-dependent Contribution of BMP, FGF, IGF, and HH Signaling to the Proliferation of Mesenchymal Stroma Cells during Chondrogenesis. *J. Cell. Physiol.* **2018**, *233*, 8962–8970. [CrossRef]
63. Akiyama, H.; Chaboissier, M.-C.; Martin, J.F.; Schedl, A.; De Crombrugghe, B. The Transcription Factor Sox9 Has Essential Roles in Successive Steps of the Chondrocyte Differentiation Pathway and Is Required for Expression of *Sox5* and *Sox6*. *Genes Dev.* **2002**, *16*, 2813–2828. [CrossRef]
64. Soetjahjo, B.; Hidayat, M.; Sujuti, H.; Fibrianto, Y. Immunohistochemistry Evaluation of TGF-B1, SOX-9, Type II Collagen and Aggrecan in Cartilage Lesions Treated with Conditioned Medium of Umbilical Cord Mesencyhmal Stem Cells in Wistar Mice (Rattus Novergicus). *J. Trop. Life Sci.* **2018**, *8*, 21–27. [CrossRef]
65. Stegen, S.; Rinaldi, G.; Loopmans, S.; Stockmans, I.; Moermans, K.; Thienpont, B.; Fendt, S.-M.; Carmeliet, P.; Carmeliet, G. Glutamine Metabolism Controls Chondrocyte Identity and Function. *Dev. Cell* **2020**, *53*, 530–544.e8. [CrossRef]
66. Zhao, Q.; Eberspaecher, H.; Lefebvre, V.; De Crombrugghe, B. Parallel Expression ofSox9 andCol2a1 in Cells Undergoing Chondrogenesis. *Dev. Dyn.* **1997**, *209*, 377–386. [CrossRef]
67. Akiyama, H.; Lyons, J.P.; Mori-Akiyama, Y.; Yang, X.; Zhang, R.; Zhang, Z.; Deng, J.M.; Taketo, M.M.; Nakamura, T.; Behringer, R.R.; et al. Interactions between Sox9 and β-Catenin Control Chondrocyte Differentiation. *Genes Dev.* **2004**, *18*, 1072–1087. [CrossRef]
68. Chen, H.; Ghori-Javed, F.Y.; Rashid, H.; Adhami, M.D.; Serra, R.; Gutierrez, S.E.; Javed, A. Runx2 Regulates Endochondral Ossification Through Control of Chondrocyte Proliferation and Differentiation. *J. Bone Miner. Res.* **2014**, *29*, 2653–2665. [CrossRef]
69. Komori, T. Roles of Runx2 in Skeletal Development. In *RUNX Proteins in Development and Cancer*; Groner, Y., Ito, Y., Liu, P., Neil, J.C., Speck, N.A., Van Wijnen, A., Eds.; Advances in Experimental Medicine and Biology; Springer: Singapore, 2017; Volume 962, pp. 83–93. ISBN 978-981-10-3231-8.
70. Ding, M.; Lu, Y.; Abbassi, S.; Li, F.; Li, X.; Song, Y.; Geoffroy, V.; Im, H.; Zheng, Q. Targeting Runx2 Expression in Hypertrophic Chondrocytes Impairs Endochondral Ossification during Early Skeletal Development. *J. Cell. Physiol.* **2012**, *227*, 3446–3456. [CrossRef]
71. Jiang, Q.; Qin, X.; Yoshida, C.A.; Komori, H.; Yamana, K.; Ohba, S.; Hojo, H.; Croix, B.S.; Kawata-Matsuura, V.K.S.; Komori, T. Antxr1, Which Is a Target of Runx2, Regulates Chondrocyte Proliferation and Apoptosis. *Int. J. Mol. Sci.* **2020**, *21*, 2425. [CrossRef]
72. Kamekura, S.; Kawasaki, Y.; Hoshi, K.; Shimoaka, T.; Chikuda, H.; Maruyama, Z.; Komori, T.; Sato, S.; Takeda, S.; Karsenty, G.; et al. Contribution of Runt-related Transcription Factor 2 to the Pathogenesis of Osteoarthritis in Mice after Induction of Knee Joint Instability. *Arthritis Rheum.* **2006**, *54*, 2462–2470. [CrossRef] [PubMed]
73. Heinegård, D. Fell-Muir Lecture: Proteoglycans and More–from Molecules to Biology. *Int. J. Exp. Path* **2009**, *90*, 575–586. [CrossRef] [PubMed]
74. Tseng, C.-C.; Chen, Y.-J.; Chang, W.-A.; Tsai, W.-C.; Ou, T.-T.; Wu, C.-C.; Sung, W.-Y.; Yen, J.-H.; Kuo, P.-L. Dual Role of Chondrocytes in Rheumatoid Arthritis: The Chicken and the Egg. *Int. J. Mol. Sci.* **2020**, *21*, 1071. [CrossRef] [PubMed]
75. Cancedda, R.; Cancedda, F.D.; Castagnola, P. Chondrocyte Differentiation. *Int. Rev. Cytol.* **1995**, *159*, 265–358.
76. Ecke, A.; Lutter, A.-H.; Scholka, J.; Hansch, A.; Becker, R.; Anderer, U. Tissue Specific Differentiation of Human Chondrocytes Depends on Cell Microenvironment and Serum Selection. *Cells* **2019**, *8*, 934. [CrossRef]
77. Camper, L.; Hellman, U.; Lundgren-Åkerlund, E. Isolation, Cloning, and Sequence Analysis of the Integrin Subunit A10, a B1-Associated Collagen Binding Integrin Expressed on Chondrocytes. *J. Biol. Chem.* **1998**, *273*, 20383–20389. [CrossRef] [PubMed]
78. Loeser, R.F. Integrins and Chondrocyte–Matrix Interactions in Articular Cartilage. *Matrix Biol.* **2014**, *39*, 11–16. [CrossRef]
79. Lundgren-Åkerlund, E.; Aszòdi, A. Integrin A10β1: A Collagen Receptor Critical in Skeletal Development. *Adv. Exp. Med. Biol.* **2014**, *819*, 61–71. [PubMed]
80. Knudson, W.; Casey, B.; Nishida, Y.; Eger, W.; Kuettner, K.E.; Knudson, C.B. Hyaluronan Oligosaccharides Perturb Cartilage Matrix Homeostasis and Induce Chondrocytic Chondrolysis. *Arthritis Rheum.* **2000**, *43*, 1165. [CrossRef]
81. Aguiar, D.J.; Knudson, W.; Knudson, C.B. Internalization of the Hyaluronan Receptor CD44 by Chondrocytes. *Exp. Cell Res.* **1999**, *252*, 292–302. [CrossRef]

82. Ishida, O.; Tanaka, Y.; Morimoto, I.; Takigawa, M.; Eto, S. Chondrocytes Are Regulated by Cellular Adhesion Through CD44 and Hyaluronic Acid Pathway. *J. Bone Miner. Res.* **1997**, *12*, 1657–1663. [CrossRef] [PubMed]
83. Burt, D.W.; Law, A.S. Evolution of the Transforming Growth Factor-Beta Superfamily. *Prog. Growth Factor. Res.* **1994**, *5*, 99–118. [CrossRef] [PubMed]
84. De Caestecker, M. The Transforming Growth Factor-β Superfamily of Receptors. *Cytokine Growth Factor. Rev.* **2004**, *15*, 1–11. [CrossRef]
85. Mantel, P.-Y.; Schmidt-Weber, C.B. Transforming Growth Factor-Beta: Recent Advances on Its Role in Immune Tolerance. In *Suppression and Regulation of Immune Responses*; Cuturi, M.C., Anegon, I., Eds.; Methods in Molecular Biology; Humana Press: Totowa, NJ, USA, 2010; Volume 677, pp. 303–338. ISBN 978-1-60761-868-3.
86. Yang, D.; Dai, F.; Yuan, M.; Zheng, Y.; Liu, S.; Deng, Z.; Tan, W.; Chen, L.; Zhang, Q.; Zhao, X.; et al. Role of Transforming Growth Factor-B1 in Regulating Fetal-Maternal Immune Tolerance in Normal and Pathological Pregnancy. *Front. Immunol.* **2021**, *12*, 689181. [CrossRef] [PubMed]
87. Van Osch, G.J.V.M.; Van Der Veen, S.W.; Buma, P.; Verwoerd-Verhoef, H.L. Effect of Transforming Growth Factor-β on Proteoglycan Synthesis by Chondrocytes in Relation to Differentiation Stage and the Presence of Pericellular Matrix. *Matrix Biol.* **1998**, *17*, 413–424. [CrossRef]
88. Puolakkainen, P.A.; Twardzik, D.R.; Ranchalis, J.E.; Pankey, S.C.; Reed, M.J.; Gombotz, W.R. The Enhancement in Wound Healing by Transforming Growth Factor-B1 (TGF-B1) Depends on the Topical Delivery System. *J. Surg. Res.* **1995**, *58*, 321–329. [CrossRef]
89. Critchlow, M.A.; Bland, Y.S.; Ashhurst, D.E. The Effect of Exogenous Transforming Growth Factor-B2 on Healing Fractures in the Rabbit. *Bone* **1995**, *16*, 521–527. [CrossRef]
90. Woo, S.L.; Buckwalter, J.A. Injury and Repair of the Musculoskeletal Soft Tissues. Savannah, Georgia, June 18–20, 1987. *J. Orthop. Res.* **1988**, *6*, 907–931. [CrossRef]
91. Eyre, D. Articular Cartilage and Changes in Arthritis: Collagen of Articular Cartilage. *Arthritis Res. Ther.* **2001**, *4*, 30–35. [CrossRef]
92. Mankin, H.J. Articular Cartilage, Cartilage Injury, and Osteoarthritis. *Patellofemoral Jt.* **1993**, *1993*, 13–45.
93. Kelly, D.J.; Crawford, A.; Dickinson, S.C.; Sims, T.J.; Mundy, J.; Hollander, A.P.; Prendergast, P.J.; Hatton, P.V. Biochemical Markers of the Mechanical Quality of Engineered Hyaline Cartilage. *J. Mater. Sci. Mater. Med.* **2007**, *18*, 273–281. [CrossRef]
94. Eyre, D.R.; Weis, M.A.; Wu, J.-J. Articular Cartilage Collagen: An Irreplaceable Framework. *Eur. Cell Mater.* **2006**, *12*, 57–63. [CrossRef]
95. Wu, J.-J.; Woods, P.E.; Eyre, D.R. Identification of Cross-Linking Sites in Bovine Cartilage Type IX Collagen Reveals an Antiparallel Type II-Type IX Molecular Relationship and Type IX to Type IX Bonding. *J. Biol. Chem.* **1992**, *267*, 23007–23014. [CrossRef]
96. Mwale, F.; Tchetina, E.; Wu, C.W.; Poole, A.R. The Assembly and Remodeling of the Extracellular Matrix in the Growth Plate in Relationship to Mineral Deposition and Cellular Hypertrophy: An in Situ Study of Collagens II and IX and Proteoglycan. *J. Bone Miner. Res.* **2002**, *17*, 275–283. [CrossRef]
97. Muragaki, Y.; Mariman, E.C.; van Beersum, S.E.; Perälä, M.; van Mourik, J.B.; Warman, M.L.; Olsen, B.R.; Hamel, B.C. A Mutation in the Gene Encoding the A2 Chain of the Fibril-Associated Collagen IX, COL9A2, Causes Multiple Epiphyseal Dysplasia (EDM2). *Nat. Genet.* **1996**, *12*, 103–105. [CrossRef]
98. Opolka, A.; Ratzinger, S.; Schubert, T.; Spiegel, H.-U.; Grifka, J.; Bruckner, P.; Probst, A.; Grässel, S. Collagen IX Is Indispensable for Timely Maturation of Cartilage during Fracture Repair in Mice. *Matrix Biol.* **2007**, *26*, 85–95. [CrossRef]
99. Gregory, K.E.; Oxford, J.T.; Chen, Y.; Gambee, J.E.; Gygi, S.P.; Aebersold, R.; Neame, P.J.; Mechling, D.E.; Bächinger, H.P.; Morris, N.P. Structural Organization of Distinct Domains within the Non-Collagenous N-Terminal Region of Collagen Type XI. *J. Biol. Chem.* **2000**, *275*, 11498–11506. [CrossRef]
100. Poole, C.A.; Ayad, S.; Schofield, J.R. Chondrons from Articular Cartilage: I. Immunolocalization of Type VI Collagen in the Pericellular Capsule of Isolated Canine Tibial Chondrons. *J. Cell Sci.* **1988**, *90*, 635–643. [CrossRef]
101. Responte, D.J.; Natoli, R.M.; Athanasiou, K.A. Collagens of Articular Cartilage: Structure, Function, and Importance in Tissue Engineering. *Crit. Rev. Biomed. Eng.* **2007**, *35*, 363–411. [CrossRef]
102. Guilak, F.; Alexopoulos, L.G.; Upton, M.L.; Youn, I.; Choi, J.B.; Cao, L.; Setton, L.A.; Haider, M.A. The Pericellular Matrix as a Transducer of Biomechanical and Biochemical Signals in Articular Cartilage. *Ann. N. Y. Acad. Sci.* **2006**, *1068*, 498–512. [CrossRef]
103. Darling, E.M.; Athanasiou, K.A. Rapid Phenotypic Changes in Passaged Articular Chondrocyte Subpopulations. *J. Orthop. Res.* **2005**, *23*, 425–432. [CrossRef]
104. Kirsch, T.; von der Mark, K. Isolation of Human Type X Collagen and Immunolocalization in Fetal Human Cartilage. *Eur. J. Biochem.* **1991**, *196*, 575–580. [CrossRef]
105. Morrison, E.; Ferguson, M.; Bayliss, M.; Archer, C. The Development of Articular Cartilage: I. The Spatial and Temporal Patterns of Collagen Types. *J. Anat.* **1996**, *189*, 9.
106. Walker, G.D.; Fischer, M.; Gannon, J.; Thompson, R.C., Jr.; Oegema, T.R., Jr. Expression of type-X Collagen in Osteoarthritis. *J. Orthop. Res.* **1995**, *13*, 4–12. [CrossRef]

107. Girkontaite, I.; Frischholz, S.; Lammi, P.; Wagner, K.; Swoboda, B.; Aigner, T.; von der Mark, K. Immunolocalization of Type X Collagen in Normal Fetal and Adult Osteoarthritic Cartilage with Monoclonal Antibodies. *Matrix Biol.* **1996**, *15*, 231–238. [CrossRef]
108. Espanha, M.M. Articular cartilage: Structure and histochemical composition. *Acta Reum. Port.* **2010**, *35*, 424–433.
109. Benninghoff, A. Form Und Bau Der Gelenkknorpel in Ihren Beziehungen Zur Funktion: Zweiter Teil: Der Aufbau Des Gelenkknorpels in Seinen Beziehungen Zur Funktion. *Z. Für Zellforsch. Und Mikrosk. Anat.* **1925**, *2*, 783–862. [CrossRef]
110. Wong, M.; Carter, D. Articular Cartilage Functional Histomorphology and Mechanobiology: A Research Perspective. *Bone* **2003**, *33*, 1–13. [CrossRef]
111. Moger, C.; Barrett, R.; Bleuet, P.; Bradley, D.; Ellis, R.; Green, E.; Knapp, K.; Muthuvelu, P.; Winlove, C. Regional Variations of Collagen Orientation in Normal and Diseased Articular Cartilage and Subchondral Bone Determined Using Small Angle X-Ray Scattering (SAXS). *Osteoarthr. Cartil.* **2007**, *15*, 682–687. [CrossRef]
112. Långsjö, T.K.; Hyttinen, M.; Pelttari, A.; Kiraly, K.; Arokoski, J.; Helminen, H.J. Electron Microscopic Stereological Study of Collagen Fibrils in Bovine Articular Cartilage: Volume and Surface Densities Are Best Obtained Indirectly (from Length Densities and Diameters) Using Isotropic Uniform Random Sampling. *J. Anat.* **1999**, *195*, 281–293. [CrossRef] [PubMed]
113. Guilak, F.; Jones, W.R.; Ting-Beall, H.P.; Lee, G.M. The Deformation Behavior and Mechanical Properties of Chondrocytes in Articular Cartilage. *Osteoarthr. Cartil.* **1999**, *7*, 59–70. [CrossRef]
114. Alexopoulos, L.G.; Haider, M.A.; Vail, T.P.; Guilak, F. Alterations in the Mechanical Properties of the Human Chondrocyte Pericellular Matrix with Osteoarthritis. *J. Biomech. Eng.* **2003**, *125*, 323–333. [CrossRef]
115. Alexopoulos, L.G.; Setton, L.A.; Guilak, F. The Biomechanical Role of the Chondrocyte Pericellular Matrix in Articular Cartilage. *Acta Biomater.* **2005**, *1*, 317–325. [CrossRef]
116. Muir, H. Proteoglycans as Organizers of the Intercellular Matrix. *Biochem. Soc. Trans.* **1983**, *11*, 613–622. [CrossRef]
117. Cohen, N.P.; Foster, R.J.; Mow, V.C. Composition and Dynamics of Articular Cartilage: Structure, Function, and Maintaining Healthy State. *J. Orthop. Sports Phys. Ther.* **1998**, *28*, 203–215. [CrossRef]
118. Buckwalter, J. Articular Cartilage: Composition, Structure, Response to Injury, and Methods of Facilitating Repair. *Articul. Cartil. Knee Jt. Funct. Basic. Sci. Arthrosc.* **1990**, 19–56.
119. Pottenger, L.A.; Lyon, N.B.; Hecht, J.D.; Neustadt, P.M.; Robinson, R.A. Influence of Cartilage Particle Size and Proteoglycan Aggregation on Immobilization of Proteoglycans. *J. Biol. Chem.* **1982**, *257*, 11479–11485. [CrossRef]
120. Maroudas, A. Physicochemical Properties of Articlar Cartilage. In *Adult Articular Cartilage*; Pitman Medical: Tunbridge Wells, UK, 1979.
121. Maroudas, A. Balance between Swelling Pressure and Collagen Tension in Normal and Degenerate Cartilage. *Nature* **1976**, *260*, 808–809. [CrossRef]
122. Lai, W.M.; Hou, J.S.; Mow, V.C. A Triphasic Theory for the Swelling and Deformation Behaviors of Articular Cartilage. *J. Biomech. Eng.* **1991**, *113*, 245–258. [CrossRef] [PubMed]
123. Mow, V.C.; Ratcliffe, A.; Robin Poole, A. Cartilage and Diarthrodial Joints as Paradigms for Hierarchical Materials and Structures. *Biomaterials* **1992**, *13*, 67–97. [CrossRef] [PubMed]
124. Setton, L.A.; Zhu, W.; Mow, V.C. The Biphasic Poroviscoelastic Behavior of Articular Cartilage: Role of the Surface Zone in Governing the Compressive Behavior. *J. Biomech.* **1993**, *26*, 581–592. [CrossRef]
125. Setton, L.A.; Mow, V.C.; Müller, F.J.; Pita, J.C.; Howell, D.S. Mechanical Properties of Canine Articular Cartilage Are Significantly Altered Following Transection of the Anterior Cruciate Ligament. *J. Orthop. Res.* **1994**, *12*, 451–463. [CrossRef]
126. Torzilli, P.A. Influence of Cartilage Conformation on Its Equilibrium Water Partition. *J. Orthop. Res.* **1985**, *3*, 473–483. [CrossRef] [PubMed]
127. Maroudas, A.; Wachtel, E.; Grushko, G.; Katz, E.P.; Weinberg, P. The Effect of Osmotic and Mechanical Pressures on Water Partitioning in Articular Cartilage. *Biochim. Et Biophys. Acta (BBA)-Gen. Subj.* **1991**, *1073*, 285–294. [CrossRef]
128. Mow, V.C.; Kuei, S.C.; Lai, W.M.; Armstrong, C.G. Biphasic Creep and Stress Relaxation of Articular Cartilage in Compression: Theory and Experiments. *J. Biomech. Eng.* **1980**, *102*, 73–84. [CrossRef]
129. Martin, J.A.; Buckwalter, J.A. Telomere Erosion and Senescence in Human Articular Cartilage Chondrocytes. *J. Gerontol. Ser. A Biol. Sci. Med. Sci.* **2001**, *56*, B172–B179. [CrossRef]
130. Buckwalter, J.; Mankin, H. Articular Cartilage: Part I. *J. Bone Jt. Surg.* **1997**, *79*, 600. [CrossRef]
131. Masuda, K.; Sah, R.L.; Hejna, M.J.; Thonar, E.J. A Novel Two-step Method for the Formation of Tissue-engineered Cartilage by Mature Bovine Chondrocytes: The Alginate-recovered-chondrocyte (ARC) Method. *J. Orthop. Res.* **2003**, *21*, 139–148. [CrossRef]
132. Poole, C.A.; Flint, M.H.; Beaumont, B.W. Chondrons in Cartilage: Ultrastructural Analysis of the Pericellular Microenvironment in Adult Human Articular Cartilages. *J. Orthop. Res.* **1987**, *5*, 509–522. [CrossRef]
133. Recht, M.; Bobic, V.; Burstein, D.; Disler, D.; Gold, G.; Gray, M.; Kramer, J.; Lang, P.; McCauley, T.; Winalski, C. Magnetic Resonance Imaging of Articular Cartilage. *Clin. Orthop. Relat. Res.*® **2001**, *391*, S379–S396. [CrossRef]
134. Torzilli, P.A.; Grigiene, R.; Borrelli, J., Jr.; Helfet, D. Effect of Impact Load on Articular Cartilage: Cell Metabolism and Viability, and Matrix Water Content. *J. Biomech. Eng.* **1999**, *121*, 433–441. [CrossRef]

135. Howell, D.S. Pathogenesis of Osteoarthritis. *Am. J. Med.* **1986**, *80*, 24–28. [CrossRef]
136. Buckwalter, J.A. Articular Cartilage: Injuries and Potential for Healing. *J. Orthop. Sports Phys. Ther.* **1998**, *28*, 192–202. [CrossRef]
137. Ateshian, G.A.; Warden, W.H.; Kim, J.J.; Grelsamer, R.P.; Mow, V.C. Finite Deformation Biphasic Material Properties of Bovine Articular Cartilage from Confined Compression Experiments. *J. Biomech.* **1997**, *30*, 1157–1164. [CrossRef]
138. Mow, V.C.; Holmes, M.H.; Michael Lai, W. Fluid Transport and Mechanical Properties of Articular Cartilage: A Review. *J. Biomech.* **1984**, *17*, 377–394. [CrossRef]
139. Mow, V.C. , *Hayes, W.C., Eds. Basic Orthopaedic Biomechanics, 2nd ed*; Lippincott-Raven: Philadelphia, PA, USA, 1997; ISBN 978-0-397-51684-1.
140. Mankin, H. Form and Function of Articular Cartilage. *Orthop. Basic Sci.* **1994**, 1–44.
141. Mow, V.; Ateshian, G.; Ratcliffe, A. Anatomic Form and Biomechanical Properties of Articular Cartilage of the Knee Joint. *Biol. Biomech. Traumatized Synovial Jt. Knee A Model.* **1992**, 55–81.
142. Maroudas, A.; Bullough, P. Permeability of Articular Cartilage. *Nature* **1968**, *219*, 1260–1261. [CrossRef]
143. Frank, E.H.; Grodzinsky, A.J. Cartilage Electromechanics—I. Electrokinetic Transduction and the Effects of Electrolyte pH and Ionic Strength. *J. Biomech.* **1987**, *20*, 615–627. [CrossRef]
144. Mow, V.; Rosenwasser, M. Articular Cartilage: Biomechanics. *Inj. Repair. Musculoskelet. Soft Tissues* **1988**, *1*, 427–463.
145. Woo, S.L.-Y.; Lee, T.Q.; Gomez, M.A.; Sato, S.; Field, F.P. Temperature Dependent Behavior of the Canine Medial Collateral Ligament. *J. Biomech. Eng.* **1987**, *109*, 68–71. [CrossRef]
146. Klika, V.; Gaffney, E.A.; Chen, Y.-C.; Brown, C.P. An Overview of Multiphase Cartilage Mechanical Modelling and Its Role in Understanding Function and Pathology. *J. Mech. Behav. Biomed. Mater.* **2016**, *62*, 139–157. [CrossRef] [PubMed]
147. Simon, B.; Coats, R.; Woo, S. Relaxation and Creep Quasilinear Viscoelastic Models for Normal Articular Cartilage. *J. Biomech. Eng.* **1984**, *106*, 159–164. [CrossRef]
148. Hurschler, C.; Abedian, R. Möglichkeiten Der Biomechanischen Charakterisierung von Knorpelgewebe. *Der Orthopäde* **2013**, *42*, 232–241. [CrossRef]
149. Hayes, W.; Bodine, A. Flow-Independent Viscoelastic Properties of Articular Cartilage Matrix. *J. Biomech.* **1978**, *11*, 407–419. [CrossRef]
150. LY, W.S. Biomechanical Properties of Articular Cartilage. *Handb. Bioeng.* **1988**, *4*, 1–44.
151. Buckwalter, J.A.; Mow, V.C.; Ratcliffe, A. Restoration of Injured or Degenerated Articular Cartilage. *JAAOS-J. Am. Acad. Orthop. Surg.* **1994**, *2*, 192–201. [CrossRef] [PubMed]
152. Akizuki, S.; Mow, V.C.; Müller, F.; Pita, J.C.; Howell, D.S.; Manicourt, D.H. Tensile Properties of Human Knee Joint Cartilage: I. Influence of Ionic Conditions, Weight Bearing, and Fibrillation on the Tensile Modulus. *J. Orthop. Res.* **1986**, *4*, 379–392. [CrossRef]
153. Kempson, G. Mechanical Properties of Articular Cartilage. *Adult Articul. Cartil.* **1979**, 333–414.
154. Roth, V.; Mow, V.C. The Intrinsic Tensile Behavior of the Matrix of Bovine Articular Cartilage and Its Variation with Age. *J. Bone Jt. Surg.* **1980**, *62*, 1102–1117. [CrossRef]
155. Hayes, W.; Mockros, L. Viscoelastic Properties of Human Articular Cartilage. *J. Appl. Physiol.* **1971**, *31*, 562–568. [CrossRef]
156. Setton, L.; Mow, V.C.; Howell, D. Mechanical Behavior of Articular Cartilage in Shear Is Altered by Transection of the Anterior Cruciate Ligament. *J. Orthop. Res.* **1995**, *13*, 473–482. [CrossRef] [PubMed]
157. Mak, A.F. The Apparent Viscoelastic Behavior of Articular Cartilage—The Contributions From the Intrinsic Matrix Viscoelasticity and Interstitial Fluid Flows. *J. Biomech. Eng.* **1986**, *108*, 123–130. [CrossRef]
158. Maier, F.; Drissi, H.; Pierce, D.M. Shear Deformations of Human Articular Cartilage: Certain Mechanical Anisotropies Apparent at Large but Not Small Shear Strains. *J. Mech. Behav. Biomed. Mater.* **2017**, *65*, 53–65. [CrossRef] [PubMed]
159. DiSilvestro, M.R.; Zhu, Q.; Suh, J.-K.F. Biphasic Poroviscoelastic Simulation of the Unconfined Compression of Articular Cartilage: II—Effect of Variable Strain Rates. *J. Biomech. Eng.* **2001**, *123*, 198–200. [CrossRef] [PubMed]
160. Nia, H.T.; Han, L.; Li, Y.; Ortiz, C.; Grodzinsky, A. Poroelasticity of Cartilage at the Nanoscale. *Biophys. J.* **2011**, *101*, 2304–2313. [CrossRef]
161. Park, S.; Hung, C.T.; Ateshian, G.A. Mechanical Response of Bovine Articular Cartilage under Dynamic Unconfined Compression Loading at Physiological Stress Levels. *Osteoarthr. Cartil.* **2004**, *12*, 65–73. [CrossRef]
162. Fung, Y. *Biomechanics: Mechanical Properties of Living Tissues*; Springer Science & Business Media: Berlin, Germany, 2013; ISBN 1-4757-2257-5.
163. Huang, C.-Y.; Soltz, M.A.; Kopacz, M.; Mow, V.C.; Ateshian, G.A. Experimental Verification of the Roles of Intrinsic Matrix Viscoelasticity and Tension-Compression Nonlinearity in the Biphasic Response of Cartilage. *J. Biomech. Eng.* **2003**, *125*, 84–93. [CrossRef]
164. Wilson, W.; Van Donkelaar, C.C.; Van Rietbergen, R.; Huiskes, R. The Role of Computational Models in the Search for the Mechanical Behavior and Damage Mechanisms of Articular Cartilage. *Med. Eng. Phys.* **2005**, *27*, 810–826. [CrossRef]
165. Chen, A.C.; Bae, W.C.; Schinagl, R.M.; Sah, R.L. Depth- and Strain-Dependent Mechanical and Electromechanical Properties of Full-Thickness Bovine Articular Cartilage in Confined Compression. *J. Biomech.* **2001**, *34*, 1–12. [CrossRef]

166. Sun, Y.-L.; Luo, Z.-P.; Fertala, A.; An, K.-N. Stretching Type II Collagen with Optical Tweezers. *J. Biomech.* **2004**, *37*, 1665–1669. [CrossRef] [PubMed]
167. Boschetti, F.; Peretti, G.M. Tensile and Compressive Properties of Healthy and Osteoarthritic Human Articular Cartilage. *Biorheology* **2008**, *45*, 337–344. [CrossRef] [PubMed]
168. Jurvelin, J.S.; Buschmann, M.D.; Hunziker, E.B. Mechanical Anisotropy of the Human Knee Articular Cartilage in Compression. *Proc. Inst. Mech. Eng. H* **2003**, *217*, 215–219. [CrossRef] [PubMed]
169. Wang, C.C.-B.; Hung, C.T.; Mow, V.C. An Analysis of the Effects of Depth-Dependent Aggregate Modulus on Articular Cartilage Stress-Relaxation Behavior in Compression. *J. Biomech.* **2001**, *34*, 75–84. [CrossRef]
170. Huang, C.-Y.; Mow, V.C.; Ateshian, G.A. The Role of Flow-Independent Viscoelasticity in the Biphasic Tensile and Compressive Responses of Articular Cartilage. *J. Biomech. Eng.* **2001**, *123*, 410–417. [CrossRef]
171. Akizuki, S.; Mow, V.C.; Muller, F.; Pita, J.C.; Howell, D.S. Tensile Properties of Human Knee Joint Cartilage. II. Correlations between Weight Bearing and Tissue Pathology and the Kinetics of Swelling. *J. Orthop. Res.* **1987**, *5*, 173–186. [CrossRef]
172. Jurvelin, J.S.; Buschmann, M.D.; Hunziker, E.B. Optical and Mechanical Determination of Poisson's Ratio of Adult Bovine Humeral Articular Cartilage. *J. Biomech.* **1997**, *30*, 235–241. [CrossRef]
173. Mow, V.C.; Gibbs, M.C.; Lai, W.M.; Zhu, W.B.; Athanasiou, K.A. Biphasic Indentation of Articular Cartilage—II. A Numerical Algorithm and an Experimental Study. *J. Biomech.* **1989**, *22*, 853–861. [CrossRef]
174. Williamson, A.K.; Chen, A.C.; Masuda, K.; Thonar, E.J.-M.A.; Sah, R.L. Tensile Mechanical Properties of Bovine Articular Cartilage: Variations with Growth and Relationships to Collagen Network Components. *J. Orthop. Res.* **2003**, *21*, 872–880. [CrossRef]
175. Zhu, W.; Mow, V.C.; Koob, T.J.; Eyre, D.R. Viscoelastic Shear Properties of Articular Cartilage and the Effects of Glycosidase Treatments. *J. Orthop. Res.* **1993**, *11*, 771–781. [CrossRef]
176. LeRoux, M.A.; Guilak, F.; Setton, L.A. Compressive and Shear Properties of Alginate Gel: Effects of Sodium Ions and Alginate Concentration. *J. Biomed. Mater. Res.* **1999**, *47*, 46–53. [CrossRef]
177. Little, C.J.; Bawolin, N.K.; Chen, X. Mechanical Properties of Natural Cartilage and Tissue-Engineered Constructs. *Tissue Eng. Part B Rev.* **2011**, *17*, 213–227. [CrossRef] [PubMed]
178. Mak, A.F.; Lai, W.M.; Mow, V.C. Biphasic Indentation of Articular Cartilage—I. Theoretical Analysis. *J. Biomech.* **1987**, *20*, 703–714. [CrossRef] [PubMed]
179. Moroni, L.; de Wijn, J.R.; Blitterswijk, C.A. van 3D Fiber-Deposited Scaffolds for Tissue Engineering: Influence of Pores Geometry and Architecture on Dynamic Mechanical Properties. *Biomaterials* **2006**, *27*, 974–985. [CrossRef]
180. Jurvelin, J.S.; Arokoski, J.P.A.; Hunziker, E.B.; Helminen, H.J. Topographical Variation of the Elastic Properties of Articular Cartilage in the Canine Knee. *J. Biomech.* **2000**, *33*, 669–675. [CrossRef]
181. Williamson, A.K.; Masuda, K.; Thonar, E.J.-M.A.; Sah, R.L. Growth of Immature Articular Cartilage in Vitro: Correlated Variation in Tensile Biomechanical and Collagen Network Properties. *Tissue Eng.* **2003**, *9*, 625–634. [CrossRef]
182. Korhonen, R.K.; Jurvelin, J.S. Compressive and Tensile Properties of Articular Cartilage in Axial Loading Are Modulated Differently by Osmotic Environment. *Med. Eng. Phys.* **2010**, *32*, 155–160. [CrossRef]
183. Spirt, A.A.; Mak, A.F.; Wassell, R.P. Nonlinear Viscoelastic Properties of Articular Cartilage in Shear. *J. Orthop. Res.* **1989**, *7*, 43–49. [CrossRef]
184. Patel, J.M.; Wise, B.C.; Bonnevie, E.D.; Mauck, R.L. A Systematic Review and Guide to Mechanical Testing for Articular Cartilage Tissue Engineering. *Tissue Eng. Part C Methods* **2019**, *25*, 593–608. [CrossRef]
185. Forster, H.; Fisher, J. The Influence of Loading Time and Lubricant on the Friction of Articular Cartilage. *Proc. Inst. Mech. Eng. Part H J. Eng. Med.* **1996**, *210*, 109–119. [CrossRef]
186. Krishnan, R.; Kopacz, M.; Ateshian, G.A. Experimental Verification of the Role of Interstitial Fluid Pressurization in Cartilage Lubrication. *J. Orthop. Res.* **2004**, *22*, 565–570. [CrossRef] [PubMed]
187. Klein, J. Molecular Mechanisms of Synovial Joint Lubrication. *Proc. Inst. Mech. Eng. Part J J. Eng. Tribol.* **2006**, *220*, 691–710. [CrossRef]
188. Lin, W.; Klein, J. Recent Progress in Cartilage Lubrication. *Adv. Mater.* **2021**, *33*, 2005513. [CrossRef] [PubMed]
189. Wright, V.; Dowson, D. Lubrication and Cartilage. *J. Anat.* **1976**, *121*, 107.
190. Hou, J.; Holmes, M.; Lai, W.; Mow, V. Boundary Conditions at the Cartilage-Synovial Fluid Interface for Joint Lubrication and Theoretical Verifications. *J. Biomech. Eng.* **1989**, *111*, 78–87. [CrossRef]
191. Katta, J.; Jin, Z.; Ingham, E.; Fisher, J. Biotribology of Articular Cartilage—A Review of the Recent Advances. *Med. Eng. Phys.* **2008**, *30*, 1349–1363. [CrossRef]
192. Daniel, M. Boundary Cartilage Lubrication: Review of Current Concepts. *Wien. Med. Wochenschr.* **2014**, *164*, 88–94. [CrossRef]
193. Burris, D.L.; Moore, A.C. Cartilage and Joint Lubrication: New Insights into the Role of Hydrodynamics. *Biotribology* **2017**, *12*, 8–14. [CrossRef]
194. MacConaill, M. The Function of Intra-Articular Fibrocartilages, with Special Reference to the Knee and Inferior Radio-Ulnar Joints. *J. Anat.* **1932**, *66*, 210.

195. Dowson, D. Bio-Tribology. *Faraday Discuss.* **2012**, *156*, 9–30. [CrossRef]
196. Jin, Z.; Dowson, D. Bio-Friction. *Friction* **2013**, *1*, 100–113. [CrossRef]
197. McCutchen, C. Mechanism of Animal Joints: Sponge-Hydrostatic and Weeping Bearings. *Nature* **1959**, *184*, 1284–1285. [CrossRef]
198. McCutchen, C.W. The Frictional Properties of Animal Joints. *Wear* **1962**, *5*, 1–17. [CrossRef]
199. Maroudas, A. Biophysical Chemistry of Cartilaginous Tissues with Special Reference to Solute and Fluid Transport. *Biorheology* **1975**, *12*, 233–248.
200. Dowson, D.; Jin, Z.-M. Micro-Elastohydrodynamic Lubrication of Synovial Joints. *Eng. Med.* **1986**, *15*, 63–65. [CrossRef]
201. Ateshian, G.; Wang, H.; Lai, W. The Role of Interstitial Fluid Pressurization and Surface Porosities on the Boundary Friction of Articular Cartilage. *J. Tribol.* **1998**, *120*, 241–248. [CrossRef]
202. Ateshian, G.A. The Role of Interstitial Fluid Pressurization in Articular Cartilage Lubrication. *J. Biomech.* **2009**, *42*, 1163–1176. [CrossRef] [PubMed]
203. Murakami, T.; Nakashima, K.; Sawae, Y.; Sakai, N.; Hosoda, N. Roles of Adsorbed Film and Gel Layer in Hydration Lubrication for Articular Cartilage. *Proc. Inst. Mech. Eng. Part J J. Eng. Tribol.* **2009**, *223*, 287–295. [CrossRef]
204. Morrell, K.C.; Hodge, W.A.; Krebs, D.E.; Mann, R.W. Corroboration of in Vivo Cartilage Pressures with Implications for Synovial Joint Tribology and Osteoarthritis Causation. *Proc. Natl. Acad. Sci. USA* **2005**, *102*, 14819–14824. [CrossRef]
205. Radin, E.L.; Swann, D.A.; Weisser, P.A. Separation of a Hyaluronate-Free Lubricating Fraction from Synovial Fluid. *Nature* **1970**, *228*, 377–378. [CrossRef]
206. Radin, E.L.; Paul, I.L.; Pollock, D. Animal Joint Behaviour under Excessive Loading. *Nature* **1970**, *226*, 554–555. [CrossRef] [PubMed]
207. Mow, V.C.; Lai, W.M. Recent Developments in Synovial Joint Biomechanics. *SIAM Rev.* **1980**, *22*, 275–317. [CrossRef]
208. Ateshian, G.A.; Chahine, N.O.; Basalo, I.M.; Hung, C.T. The Correspondence between Equilibrium Biphasic and Triphasic Material Properties in Mixture Models of Articular Cartilage. *J. Biomech.* **2004**, *37*, 391–400. [CrossRef] [PubMed]
209. Caligaris, M.; Ateshian, G.A. Effects of Sustained Interstitial Fluid Pressurization under Migrating Contact Area, and Boundary Lubrication by Synovial Fluid, on Cartilage Friction. *Osteoarthr. Cartil.* **2008**, *16*, 1220–1227. [CrossRef]
210. Bonnevie, E.D.; Baro, V.J.; Wang, L.; Burris, D.L. Fluid Load Support during Localized Indentation of Cartilage with a Spherical Probe. *J. Biomech.* **2012**, *45*, 1036–1041. [CrossRef]
211. Krishnan, R.; Mariner, E.N.; Ateshian, G.A. Effect of Dynamic Loading on the Frictional Response of Bovine Articular Cartilage. *J. Biomech.* **2005**, *38*, 1665–1673. [CrossRef]
212. Soltz, M.A.; Ateshian, G.A. Interstitial Fluid Pressurization During Confined Compression Cyclical Loading of Articular Cartilage. *Ann. Biomed. Eng.* **2000**, *28*, 150–159. [CrossRef]
213. Schmidt, T.A.; Gastelum, N.S.; Nguyen, Q.T.; Schumacher, B.L.; Sah, R.L. Boundary Lubrication of Articular Cartilage: Role of Synovial Fluid Constituents. *Arthritis Rheum.* **2007**, *56*, 882–891. [CrossRef]
214. Gleghorn, J.P.; Jones, A.R.C.; Flannery, C.R.; Bonassar, L.J. Boundary Mode Lubrication of Articular Cartilage by Recombinant Human Lubricin. *J. Orthop. Res.* **2009**, *27*, 771–777. [CrossRef]
215. Moore, A.C.; Burris, D.L. Tribological Rehydration of Cartilage and Its Potential Role in Preserving Joint Health. *Osteoarthr. Cartil.* **2017**, *25*, 99–107. [CrossRef]
216. Milner, P.E.; Parkes, M.; Puetzer, J.L.; Chapman, R.; Stevens, M.M.; Cann, P.; Jeffers, J.R.T. A Low Friction, Biphasic and Boundary Lubricating Hydrogel for Cartilage Replacement. *Acta Biomater.* **2018**, *65*, 102–111. [CrossRef] [PubMed]
217. Sun, Z.; Feeney, E.; Guan, Y.; Cook, S.G.; Gourdon, D.; Bonassar, L.J.; Putnam, D. Boundary Mode Lubrication of Articular Cartilage with a Biomimetic Diblock Copolymer. *Proc. Natl. Acad. Sci. USA* **2019**, *116*, 12437–12441. [CrossRef] [PubMed]
218. Smith, D.W.; Gardiner, B.S.; Zhang, L.; Grodzinsky, A.J. *Articular Cartilage Dynamics*; Springer: Singapore, 2019; ISBN 9789811314735.
219. Jay, G.D.; Waller, K.A. The Biology of Lubricin: Near Frictionless Joint Motion. *Matrix Biol.* **2014**, *39*, 17–24. [CrossRef] [PubMed]
220. Chang, D.P.; Guilak, F.; Jay, G.D.; Zauscher, S. Interaction of Lubricin with Type II Collagen Surfaces: Adsorption, Friction, and Normal Forces. *J. Biomech.* **2014**, *47*, 659–666. [CrossRef]
221. Bell, C.J.; Ingham, E.; Fisher, J. Influence of Hyaluronic Acid on the Time-Dependent Friction Response of Articular Cartilage under Different Conditions. *Proc. Inst. Mech. Eng. H* **2006**, *220*, 23–31. [CrossRef]
222. Forsey, R.; Fisher, J.; Thompson, J.; Stone, M.; Bell, C.; Ingham, E. The Effect of Hyaluronic Acid and Phospholipid Based Lubricants on Friction within a Human Cartilage Damage Model. *Biomaterials* **2006**, *27*, 4581–4590. [CrossRef]
223. Seror, J.; Merkher, Y.; Kampf, N.; Collinson, L.; Day, A.J.; Maroudas, A.; Klein, J. Articular Cartilage Proteoglycans as Boundary Lubricants: Structure and Frictional Interaction of Surface-Attached Hyaluronan and Hyaluronan–Aggrecan Complexes. *Biomacromolecules* **2011**, *12*, 3432–3443. [CrossRef]
224. Lee, D.W.; Banquy, X.; Israelachvili, J.N. Stick-Slip Friction and Wear of Articular Joints. *Proc. Natl. Acad. Sci. USA* **2013**, *110*. [CrossRef]

225. Gaisinskaya, A.; Ma, L.; Silbert, G.; Sorkin, R.; Tairy, O.; Goldberg, R.; Kampf, N.; Klein, J. Hydration Lubrication: Exploring a New Paradigm. *Faraday Discuss.* **2012**, *156*, 217. [CrossRef]
226. Kobayashi, S.; Yonekubo, S.; Kurogouchi, Y. Cryoscanning Electron Microscopy of Loaded Articular Cartilage with Special Reference to the Surface Amorphous Layer. *J. Anat.* **1996**, *188 Pt 2*, 311–322.
227. Gleghorn, J.P.; Bonassar, L.J. Lubrication Mode Analysis of Articular Cartilage Using Stribeck Surfaces. *J. Biomech.* **2008**, *41*, 1910–1918. [CrossRef] [PubMed]
228. Cooke, A.F.; Dowson, D.; Wright, V. The Pressure-Viscosity Characteristics of Synovial Fluid. *Biorheology* **1978**, *15*, 129–135. [CrossRef] [PubMed]
229. Makris, E.A.; Hadidi, P.; Athanasiou, K.A. The Knee Meniscus: Structure–Function, Pathophysiology, Current Repair Techniques, and Prospects for Regeneration. *Biomaterials* **2011**, *32*, 7411–7431. [CrossRef]
230. Fox, A.J.S.; Wanivenhaus, F.; Burge, A.J.; Warren, R.F.; Rodeo, S.A. The Human Meniscus: A Review of Anatomy, Function, Injury, and Advances in Treatment. *Clin. Anat.* **2015**, *28*, 269–287. [CrossRef] [PubMed]
231. DiSilvestro, M.R.; Zhu, Q.; Wong, M.; Jurvelin, J.S.; Suh, J.-K.F. Biphasic Poroviscoelastic Simulation of the Unconfined Compression of Articular Cartilage: I—Simultaneous Prediction of Reaction Force and Lateral Displacement. *J. Biomech. Eng.* **2001**, *123*, 191–197. [CrossRef]
232. McCutchen, C.W. Joint Lubrication. *Bull. Hosp. Jt. Dis. Orthop. Inst.* **1983**, *43*, 118–129.
233. Vazquez, K.J.; Andreae, J.T.; Henak, C.R. Cartilage-on-Cartilage Cyclic Loading Induces Mechanical and Structural Damage. *J. Mech. Behav. Biomed. Mater.* **2019**, *98*, 262–267. [CrossRef]
234. Drewniak, E.I.; Jay, G.D.; Fleming, B.C.; Zhang, L.; Warman, M.L.; Crisco, J.J. Cyclic Loading Increases Friction and Changes Cartilage Surface Integrity in Lubricin-mutant Mouse Knees. *Arthritis Rheum.* **2012**, *64*, 465–473. [CrossRef]
235. Zhang, L.; Miramini, S.; Smith, D.W.; Gardiner, B.S.; Grodzinsky, A.J. Time Evolution of Deformation in a Human Cartilage Under Cyclic Loading. *Ann. Biomed. Eng.* **2015**, *43*, 1166–1177. [CrossRef]
236. Ghosh, S.; Choudhury, D.; Das, N.S.; Pingguan-Murphy, B. Tribological Role of Synovial Fluid Compositions on Artificial Joints—A Systematic Review of the Last 10 Years: Tribological role of synovial fluid compositions on artificial joints. *Lubr. Sci.* **2014**, *26*, 387–410. [CrossRef]
237. Scanzello, C.R.; Goldring, S.R. The Role of Synovitis in Osteoarthritis Pathogenesis. *Bone* **2012**, *51*, 249–257. [CrossRef]
238. Kraus, V.B.; Burnett, B.; Coindreau, J.; Cottrell, S.; Eyre, D.; Gendreau, M.; Gardiner, J.; Garnero, P.; Hardin, J.; Henrotin, Y.; et al. Application of Biomarkers in the Development of Drugs Intended for the Treatment of Osteoarthritis. *Osteoarthr. Cartil.* **2011**, *19*, 515–542. [CrossRef] [PubMed]
239. Mobasheri, A.; Henrotin, Y. Biomarkers of (Osteo)Arthritis. *Biomarkers* **2015**, *20*, 513–518. [CrossRef]
240. Carlson, A.K.; Rawle, R.A.; Wallace, C.W.; Brooks, E.G.; Adams, E.; Greenwood, M.C.; Olmer, M.; Lotz, M.K.; Bothner, B.; June, R.K. Characterization of Synovial Fluid Metabolomic Phenotypes of Cartilage Morphological Changes Associated with Osteoarthritis. *Osteoarthr. Cartil.* **2019**, *27*, 1174–1184. [CrossRef]
241. Oliveira, J.M.; Reis, R.L. (Eds.) *Regenerative Strategies for the Treatment of Knee Joint Disabilities*; Studies in Mechanobiology, Tissue Engineering and Biomaterials; Springer International Publishing: Cham, Switzerland, 2017; Volume 21, ISBN 978-3-319-44783-4.
242. Prekasan, D.; Saju, K.K. Review of the Tribological Characteristics of Synovial Fluid. *Procedia Technol.* **2016**, *25*, 1170–1174. [CrossRef]
243. Fournier, R.L. *Basic Transport Phenomena in Biomedical Engineering*; CRC Press: Boca Raton, FL, USA, 2017; ISBN 1-315-12047-X.
244. Tamer, T.M. Hyaluronan and Synovial Joint: Function, Distribution and Healing. *Interdiscip. Toxicol.* **2013**, *6*, 111–125. [CrossRef]
245. Milošev, I.; Levašič, V.; Vidmar, J.; Kovač, S.; Trebše, R. pH and Metal Concentration of Synovial Fluid of Osteoarthritic Joints and Joints with Metal Replacements. *J. Biomed. Mater. Res.* **2017**, *105*, 2507–2515. [CrossRef] [PubMed]
246. Baghdadi, H.A.; Sardinha, H.; Bhatia, S.R. Rheology and Gelation Kinetics in Laponite Dispersions Containing Poly(Ethylene Oxide). *J. Polym. Sci. B Polym. Phys.* **2005**, *43*, 233–240. [CrossRef]
247. Helfet, A.J. (Ed.) *Disorders of the Knee*, 2nd ed.; Lippincott: Philadelphia, PA, USA, 1982; ISBN 978-0-397-50484-8.
248. Benz, M.; Chen, N.; Israelachvili, J. Lubrication and Wear Properties of Grafted Polyelectrolytes, Hyaluronan and Hylan, Measured in the Surface Forces Apparatus. *J. Biomed. Mater. Res.* **2004**, *71A*, 6–15. [CrossRef]
249. Gispert, M.P.; Serro, A.P.; Colaço, R.; Saramago, B. Friction and Wear Mechanisms in Hip Prosthesis: Comparison of Joint Materials Behaviour in Several Lubricants. *Wear* **2006**, *260*, 149–158. [CrossRef]
250. Iwanaga, T.; Shikichi, M.; Kitamura, H.; Yanase, H.; Nozawa-Inoue, K. Morphology and Functional Roles of Synoviocytes in the Joint. *Arch. Histol. Cytol.* **2000**, *63*, 17–31. [CrossRef] [PubMed]
251. Chang, D.P.; Abu-Lail, N.I.; Coles, J.M.; Guilak, F.; Jay, G.D.; Zauscher, S. Friction Force Microscopy of Lubricin and Hyaluronic Acid between Hydrophobic and Hydrophilic Surfaces. *Soft Matter* **2009**, *5*, 3438–3445. [CrossRef]
252. Bernardeau, C.; Bucki, B.; Lioté, F. Acute Arthritis after Intra-Articular Hyaluronate Injection: Onset of Effusions without Crystal. *Ann. Rheum. Dis.* **2001**, *60*, 518–520. [CrossRef] [PubMed]

253. Rees, S.G.; Davies, J.R.; Tudor, D.; Flannery, C.R.; Hughes, C.E.; Dent, C.M.; Caterson, B. Immunolocalisation and Expression of Proteoglycan 4 (Cartilage Superficial Zone Proteoglycan) in Tendon. *Matrix Biol.* **2002**, *21*, 593–602. [CrossRef]
254. Jones, A.R.C.; Gleghorn, J.P.; Hughes, C.E.; Fitz, L.J.; Zollner, R.; Wainwright, S.D.; Caterson, B.; Morris, E.A.; Bonassar, L.J.; Flannery, C.R. Binding and Localization of Recombinant Lubricin to Articular Cartilage Surfaces. *J. Orthop. Res.* **2007**, *25*, 283–292. [CrossRef]
255. Trunfio-Sfarghiu, A.-M.; Berthier, Y.; Meurisse, M.-H.; Rieu, J.-P. Multiscale Analysis of the Tribological Role of the Molecular Assemblies of Synovial Fluid. Case of a Healthy Joint and Implants. *Tribol. Int.* **2007**, *40*, 1500–1515. [CrossRef]
256. Elsaid, K.A.; Fleming, B.C.; Oksendahl, H.L.; Machan, J.T.; Fadale, P.D.; Hulstyn, M.J.; Shalvoy, R.; Jay, G.D. Decreased Lubricin Concentrations and Markers of Joint Inflammation in the Synovial Fluid of Patients with Anterior Cruciate Ligament Injury. *Arthritis Rheum.* **2008**, *58*, 1707–1715. [CrossRef] [PubMed]
257. Lee, S.Y.; Nakagawa, T.; Reddi, A.H. Induction of Chondrogenesis and Expression of Superficial Zone Protein (SZP)/Lubricin by Mesenchymal Progenitors in the Infrapatellar Fat Pad of the Knee Joint Treated with TGF-B1 and BMP-7. *Biochem. Biophys. Res. Commun.* **2008**, *376*, 148–153. [CrossRef]
258. Das, R.H.J.; Jahr, H.; Verhaar, J.A.N.; Van Der Linden, J.C.; Van Osch, G.J.V.M.; Weinans, H. In Vitro Expansion Affects the Response of Chondrocytes to Mechanical Stimulation. *Osteoarthr. Cartil.* **2008**, *16*, 385–391. [CrossRef]
259. Wang, A.; Essner, A.; Schmidig, G. The Effects of Lubricant Composition on in Vitro Wear Testing of Polymeric Acetabular Components. *J. Biomed. Mater. Res.* **2004**, *68B*, 45–52. [CrossRef]
260. Elsaid, K.A.; Jay, G.D.; Warman, M.L.; Rhee, D.K.; Chichester, C.O. Association of Articular Cartilage Degradation and Loss of Boundary-lubricating Ability of Synovial Fluid Following Injury and Inflammatory Arthritis. *Arthritis Rheum.* **2005**, *52*, 1746–1755. [CrossRef] [PubMed]
261. Hui, A.Y.; McCarty, W.J.; Masuda, K.; Firestein, G.S.; Sah, R.L. A Systems Biology Approach to Synovial Joint Lubrication in Health, Injury, and Disease. *WIREs Mech. Dis.* **2012**, *4*, 15–37. [CrossRef] [PubMed]
262. Fan, J.; Myant, C.W.; Underwood, R.; Cann, P.M.; Hart, A. Inlet Protein Aggregation: A New Mechanism for Lubricating Film Formation with Model Synovial Fluids. *Proc. Inst. Mech. Eng. H* **2011**, *225*, 696–709. [CrossRef] [PubMed]
263. Myant, C.; Underwood, R.; Fan, J.; Cann, P.M. Lubrication of Metal-on-Metal Hip Joints: The Effect of Protein Content and Load on Film Formation and Wear. *J. Mech. Behav. Biomed. Mater.* **2012**, *6*, 30–40. [CrossRef]
264. Hyc, A.; Iwan, A.; Moskalewski, S. Morphology and Function of Normal Synovial Membrane. *Reumatologia* **2012**, *50*, 501–506. [CrossRef]
265. Berumen-Nafarrate, E.; Leal-Berumen, I.; Luevano, E.; Solis, F.J.; Muñoz-Esteves, E. Synovial Tissue and Synovial Fluid. *J. Knee Surg.* **2002**, *15*, 46–48.
266. De Sousa, E.B.; Casado, P.L.; Neto, V.M.; Duarte, M.E.L.; Aguiar, D.P. Synovial Fluid and Synovial Membrane Mesenchymal Stem Cells: Latest Discoveries and Therapeutic Perspectives. *Stem Cell Res. Ther.* **2014**, *5*, 112. [CrossRef]
267. Blom, A.B.; Van Lent, P.L.E.M.; Holthuysen, A.E.M.; Van Der Kraan, P.M.; Roth, J.; Van Rooijen, N.; Van Den Berg, W.B. Synovial Lining Macrophages Mediate Osteophyte Formation during Experimental Osteoarthritis. *Osteoarthr. Cartil.* **2004**, *12*, 627–635. [CrossRef]
268. Van Lent, P.L.; Van Den Berg, W.B. Mesenchymal Stem Cell Therapy in Osteoarthritis: Advanced Tissue Repair or Intervention with Smouldering Synovial Activation? *Arthritis Res. Ther.* **2013**, *15*, 112. [CrossRef]
269. Revell, P.A.; al-Saffar, N.; Fish, S.; Osei, D. Extracellular Matrix of the Synovial Intimal Cell Layer. *Ann. Rheum. Dis.* **1995**, *54*, 404–407. [CrossRef]
270. Jay, G.D.; Tantravahi, U.; Britt, D.E.; Barrach, H.J.; Cha, C. Homology of Lubricin and Superficial Zone Protein (SZP): Products of Megakaryocyte Stimulating Factor (MSF) Gene Expression by Human Synovial Fibroblasts and Articular Chondrocytes Localized to Chromosome 1q25. *J. Orthop. Res.* **2001**, *19*, 677–687. [CrossRef] [PubMed]
271. Kitamura, H.P.; Yanase, H.; Kitamura, H.; Iwanaga, T. Unique Localization of Protein Gene Product 9.5 in Type B Synoviocytes in the Joints of the Horse. *J. Histochem. Cytochem.* **1999**, *47*, 343–351. [CrossRef]
272. Sabaratnam, S.; Coleman, P.J.; Mason, R.M.; Levick, J.R. Interstitial Matrix Proteins Determine Hyaluronan Reflection and Fluid Retention in Rabbit Joints: Effect of Protease. *J. Physiol.* **2007**, *578*, 291–299. [CrossRef]
273. Levick, J.R. Flow Through Interstitium and Other Fibrous Matrices. *Exp. Physiol.* **1987**, *72*, 409–437. [CrossRef] [PubMed]
274. Lu, Y.; Levick, J.; Wang, W. The Mechanism of Synovial Fluid Retention in Pressurized Joint Cavities. *Microcirculation* **2005**, *12*, 581–595. [CrossRef]
275. Benito, M.J.; Veale, D.J.; FitzGerald, O.; Van Den Berg, W.B.; Bresnihan, B. Synovial Tissue Inflammation in Early and Late Osteoarthritis. *Ann. Rheum. Dis.* **2005**, *64*, 1263–1267. [CrossRef] [PubMed]
276. De Lange-Brokaar, B.J.E.; Ioan-Facsinay, A.; Van Osch, G.J.V.M.; Zuurmond, A.-M.; Schoones, J.; Toes, R.E.M.; Huizinga, T.W.J.; Kloppenburg, M. Synovial Inflammation, Immune Cells and Their Cytokines in Osteoarthritis: A Review. *Osteoarthr. Cartil.* **2012**, *20*, 1484–1499. [CrossRef]

277. Robinson, W.H.; Lepus, C.M.; Wang, Q.; Raghu, H.; Mao, R.; Lindstrom, T.M.; Sokolove, J. Low-Grade Inflammation as a Key Mediator of the Pathogenesis of Osteoarthritis. *Nat. Rev. Rheumatol.* **2016**, *12*, 580–592. [CrossRef]
278. Kraus, V. Osteoarthritis Year 2010 in Review: Biochemical Markers. *Osteoarthr. Cartil.* **2011**, *19*, 346–353. [CrossRef]
279. Urban, J.P.G.; Hall, A.C.; Gehl, K.A. Regulation of Matrix Synthesis Rates by the Ionic and Osmotic Environment of Articular Chondrocytes. *J. Cell. Physiol.* **1993**, *154*, 262–270. [CrossRef]
280. Buschmann, M.D.; Gluzband, Y.A.; Grodzinsky, A.J.; Hunziker, E.B. Mechanical Compression Modulates Matrix Biosynthesis in Chondrocyte/Agarose Culture. *J. Cell Sci.* **1995**, *108*, 1497–1508. [CrossRef]
281. Graham, B.T.; Moore, A.C.; Burris, D.L.; Price, C. Sliding Enhances Fluid and Solute Transport into Buried Articular Cartilage Contacts. *Osteoarthr. Cartil.* **2017**, *25*, 2100–2107. [CrossRef] [PubMed]
282. Burris, D.; Ramsey, L.; Graham, B.; Price, C.; Moore, A. How Sliding and Hydrodynamics Contribute to Articular Cartilage Fluid and Lubrication Recovery. *Tribol. Lett.* **2019**, *67*, 46. [CrossRef]
283. Sise, C.V.; Petersen, C.A.; Ashford, A.K.; Yun, J.; Zimmerman, B.K.; Vukelic, S.; Hung, C.T.; Ateshian, G.A. A Major Functional Role of Synovial Fluid Is to Reduce the Rate of Cartilage Fatigue Failure under Cyclical Compressive Loading. *Osteoarthr. Cartil.* **2025**, *33*, 94–100. [CrossRef]
284. Soltz, M.A.; Ateshian, G.A. A Conewise Linear Elasticity Mixture Model for the Analysis of Tension-Compression Nonlinearity in Articular Cartilage. *J. Biomech. Eng.* **2000**, *122*, 576–586. [CrossRef] [PubMed]
285. O'hara, B.; Urban, J.; Maroudas, A. Influence of Cyclic Loading on the Nutrition of Articular Cartilage. *Ann. Rheum. Dis.* **1990**, *49*, 536–539. [CrossRef]
286. Eisenberg, S.R.; Grodzinsky, A.J. Swelling of Articular Cartilage and Other Connective Tissues: Electromechanochemical Forces. *J. Orthop. Res.* **1985**, *3*, 148–159. [CrossRef]
287. Buckwalter, J.; Mankin, H. Articular Cartilage: Degeneration and Osteoarthritis, Repair, Regeneration, and Transplantation. *Instr. Course Lect.* **1998**, *47*, 487–504.
288. Mauck, R.L.; Soltz, M.A.; Wang, C.C.; Wong, D.D.; Chao, P.-H.G.; Valhmu, W.B.; Hung, C.T.; Ateshian, G.A. Functional Tissue Engineering of Articular Cartilage through Dynamic Loading of Chondrocyte-Seeded Agarose Gels. *J. Biomech. Eng.* **2000**, *122*, 252–260. [CrossRef]
289. Khan, K.M.; Scott, A. Mechanotherapy: How Physical Therapists' Prescription of Exercise Promotes Tissue Repair. *Br. J. Sports Med.* **2009**, *43*, 247–252. [CrossRef]
290. Krishnan, Y.; Grodzinsky, A.J. Cartilage Diseases. *Matrix Biol.* **2018**, *71–72*, 51–69. [CrossRef] [PubMed]
291. Belluzzi, E.; Todros, S.; Pozzuoli, A.; Ruggieri, P.; Carniel, E.L.; Berardo, A. Human Cartilage Biomechanics: Experimental and Theoretical Approaches towards the Identification of Mechanical Properties in Healthy and Osteoarthritic Conditions. *Processes* **2023**, *11*, 1014. [CrossRef]
292. Englund, M.; Guermazi, A.; Lohmander, S.L. The Role of the Meniscus in Knee Osteoarthritis: A Cause or Consequence? *Radiol. Clin. N. Am.* **2009**, *47*, 703–712. [CrossRef] [PubMed]
293. Martel-Pelletier, J.; Barr, A.J.; Cicuttini, F.M.; Conaghan, P.G.; Cooper, C.; Goldring, M.B.; Goldring, S.R.; Jones, G.; Teichtahl, A.J.; Pelletier, J.-P. Osteoarthritis. *Nat. Rev. Dis. Primers* **2016**, *2*, 16072. [CrossRef]
294. Favero, M.; El-Hadi, H.; Belluzzi, E.; Granzotto, M.; Porzionato, A.; Sarasin, G.; Rambaldo, A.; Iacobellis, C.; Cigolotti, A.; Fontanella, C.G.; et al. Infrapatellar Fat Pad Features in Osteoarthritis: A Histopathological and Molecular Study. *Rheumatology* **2017**, *56*, 1784–1793. [CrossRef]
295. Belluzzi, E.; Macchi, V.; Fontanella, C.; Carniel, E.; Olivotto, E.; Filardo, G.; Sarasin, G.; Porzionato, A.; Granzotto, M.; Pozzuoli, A.; et al. Infrapatellar Fat Pad Gene Expression and Protein Production in Patients with and without Osteoarthritis. *Int. J. Mol. Sci.* **2020**, *21*, 6016. [CrossRef]
296. Sanchez-Lopez, E.; Coras, R.; Torres, A.; Lane, N.E.; Guma, M. Synovial Inflammation in Osteoarthritis Progression. *Nat. Rev. Rheumatol.* **2022**, *18*, 258–275. [CrossRef]
297. Sowers, M. Epidemiology of Risk Factors for Osteoarthritis: Systemic Factors. *Curr. Opin. Rheumatol.* **2001**, *13*, 447–451. [CrossRef]
298. Belluzzi, E.; El Hadi, H.; Granzotto, M.; Rossato, M.; Ramonda, R.; Macchi, V.; De Caro, R.; Vettor, R.; Favero, M. Systemic and Local Adipose Tissue in Knee Osteoarthritis. *J. Cell. Physiol.* **2017**, *232*, 1971–1978. [CrossRef]
299. Olivotto, E.; Belluzzi, E.; Pozzuoli, A.; Cigolotti, A.; Scioni, M.; Goldring, S.R.; Goldring, M.B.; Ruggieri, P.; Ramonda, R.; Grigolo, B.; et al. Do Synovial Inflammation and Meniscal Degeneration Impact Clinical Outcomes of Patients Undergoing Arthroscopic Partial Meniscectomy? A Histological Study. *Int. J. Mol. Sci.* **2022**, *23*, 3903. [CrossRef]
300. Ghouri, A.; Conaghan, P.G. Update on Novel Pharmacological Therapies for Osteoarthritis. *Ther. Adv. Musculoskelet.* **2019**, *11*, 1759720X19864492. [CrossRef] [PubMed]
301. Belluzzi, E.; Stocco, E.; Pozzuoli, A.; Granzotto, M.; Porzionato, A.; Vettor, R.; De Caro, R.; Ruggieri, P.; Ramonda, R.; Rossato, M.; et al. Contribution of Infrapatellar Fat Pad and Synovial Membrane to Knee Osteoarthritis Pain. *BioMed Res. Int.* **2019**, *2019*, 1–18. [CrossRef] [PubMed]
302. Yu, H.; Huang, T.; Lu, W.W.; Tong, L.; Chen, D. Osteoarthritis Pain. *Int. J. Mol. Sci.* **2022**, *23*, 4642. [CrossRef] [PubMed]

303. Loeser, R.F.; Goldring, S.R.; Scanzello, C.R.; Goldring, M.B. Osteoarthritis: A Disease of the Joint as an Organ. *Arthritis Rheum.* **2012**, *64*, 1697–1707. [CrossRef]
304. Xiao, Z.; Su, G.; Hou, Y.; Chen, S.; Lin, D. Cartilage Degradation in Osteoarthritis: A Process of Osteochondral Remodeling Resembles the Endochondral Ossification in Growth Plate? *Med. Hypotheses* **2018**, *121*, 183–187. [CrossRef]
305. Torzilli, P.A.; Allen, S.N. Effect of Articular Surface Compression on Cartilage Extracellular Matrix Deformation. *J. Biomech. Eng.* **2022**, *144*, 091007. [CrossRef]
306. Martin, J.A.; Buckwalter, J.A. Aging, Articular Cartilage Chondrocyte Senescence and Osteoarthritis. *Biogerontology* **2002**, *3*, 257–264. [CrossRef]
307. Goldring, M.B. Articular Cartilage Degradation in Osteoarthritis. *HSS J.® Musculoskelet. J. Hosp. Spec. Surg.* **2012**, *8*, 7–9. [CrossRef]
308. Chen, D.; Shen, J.; Zhao, W.; Wang, T.; Han, L.; Hamilton, J.L.; Im, H.-J. Osteoarthritis: Toward a Comprehensive Understanding of Pathological Mechanism. *Bone Res.* **2017**, *5*, 16044. [CrossRef]
309. Singh, P.; Marcu, K.B.; Goldring, M.B.; Otero, M. Phenotypic Instability of Chondrocytes in Osteoarthritis: On a Path to Hypertrophy. *Ann. N. Y. Acad. Sci.* **2019**, *1442*, 17–34. [CrossRef]
310. Buckwalter, J.A.; Stanish, W.D.; Rosier, R.N.; Schenck, R.C.; Dennis, D.A.; Coutts, R.D. The Increasing Need for Nonoperative Treatment of Patients with Osteoarthritis. *Clin. Orthop. Relat. Res.* **2001**, *385*, 36–45. [CrossRef] [PubMed]
311. Kim, J.-S.; Ali, M.H.; Wydra, F.; Li, X.; Hamilton, J.L.; An, H.S.; Cs-Szabo, G.; Andrews, S.; Moric, M.; Xiao, G.; et al. Characterization of Degenerative Human Facet Joints and Facet Joint Capsular Tissues. *Osteoarthr. Cartil.* **2015**, *23*, 2242–2251. [CrossRef] [PubMed]
312. Statham, P.; Jones, E.; Jennings, L.M.; Fermor, H.L. Reproducing the Biomechanical Environment of the Chondrocyte for Cartilage Tissue Engineering. *Tissue Eng. Part B Rev.* **2022**, *28*, 405–420. [CrossRef]
313. Kempson, G.E. The Mechanical Properties of Articular Cartilage. In *The Joints and Synovial Fluid*; Elsevier: Amsterdam, The Netherlands, 1980; pp. 177–238. ISBN 978-0-12-655102-0.
314. Kempson, G.E. Relationship between the Tensile Properties of Articular Cartilage from the Human Knee and Age. *Ann. Rheum. Dis.* **1982**, *41*, 508–511. [CrossRef]
315. Kempson, G.E. Age-Related Changes in the Tensile Properties of Human Articular Cartilage: A Comparative Study between the Femoral Head of the Hip Joint and the Talus of the Ankle Joint. *Biochim. Et Biophys. Acta (BBA)-Gen. Subj.* **1991**, *1075*, 223–230. [CrossRef]
316. Mow, V. Mechanical Factors in Articular Cartilage and Their Role in Osteoarthritis. *Osteoarthr. Disord.* **1995**.
317. Buckwalter, J.A.; Rosenberg, L.C. Electron Microscopic Studies of Cartilage Proteoglycans. Direct Evidence for the Variable Length of the Chondroitin Sulfate-Rich Region of Proteoglycan Subunit Core Protein. *J. Biol. Chem.* **1982**, *257*, 9830–9839. [CrossRef] [PubMed]
318. Buckwalter, J.A.; Kuettner, K.E.; Thonar, E.J. Age-related Changes in Articular Cartilage Proteoglycans: Electron Microscopic Studies. *J. Orthop. Res.* **1985**, *3*, 251–257. [CrossRef]
319. Buckwalter, J.A.; Roughley, P.J.; Rosenberg, L.C. Age-Related Changes in Cartilage Proteoglycans: Quantitative Electron Microscopic Studies. *Microsc. Res. Tech.* **1994**, *28*, 398–408. [CrossRef]
320. Thonar, E.J.; Buckwalter, J.A.; Kuettner, K.E. Maturation-Related Differences in the Structure and Composition of Proteoglycans Synthesized by Chondrocytes from Bovine Articular Cartilage. *J. Biol. Chem.* **1986**, *261*, 2467–2474. [CrossRef]
321. Lee, H.-S.; Salter, D.M. Biomechanics of Cartilage and Osteoarthritis. In Osteoarthritis-Progress in Basic Research and Treatment; Chen, Q., Ed.; InTech: Hong Kong, China, 2015 ISBN 978-953-51-2136-7.
322. Krakowski, P.; Rejniak, A.; Sobczyk, J.; Karpiński, R. Cartilage Integrity: A Review of Mechanical and Frictional Properties and Repair Approaches in Osteoarthritis. *Healthcare* **2024**, *12*, 1648. [CrossRef] [PubMed]
323. Kleemann, R.U.; Krocker, D.; Cedraro, A.; Tuischer, J.; Duda, G.N. Altered Cartilage Mechanics and Histology in Knee Osteoarthritis: Relation to Clinical Assessment (ICRS Grade). *Osteoarthr. Cartil.* **2005**, *13*, 958–963. [CrossRef]
324. Ebrahimi, M.; Ojanen, S.; Mohammadi, A.; Finnilä, M.A.; Joukainen, A.; Kröger, H.; Saarakkala, S.; Korhonen, R.K.; Tanska, P. Elastic, Viscoelastic and Fibril-Reinforced Poroelastic Material Properties of Healthy and Osteoarthritic Human Tibial Cartilage. *Ann. Biomed. Eng.* **2019**, *47*, 953–966. [CrossRef]
325. Hardingham, T.; Bayliss, M. Proteoglycans of Articular Cartilage: Changes in Aging and in Joint Disease. *Semin. Arthritis Rheum.* **1990**, *20*, 12–33. [CrossRef] [PubMed]
326. Bolton, M.C.; Dudhia, J.; Bayliss, M.T. Age-Related Changes in the Synthesis of Link Protein and Aggrecan in Human Articular Cartilage: Implications for Aggregate Stability. *Biochem. J.* **1999**, *337*, 77–82. [CrossRef]
327. Martin, J.A.; Ellerbroek, S.M.; Buckwalter, J.A. Age-related Decline in Chondrocyte Response to Insulin-like Growth factor-I: The Role of Growth Factor Binding Proteins. *J. Orthop. Res.* **1997**, *15*, 491–498. [CrossRef] [PubMed]
328. Martin, J.A.; Buckwalter, J.A. The Role of Chondrocyte–Matrix Interactions in Maintaining and Repairing Articular Cartilage. *Biorheol. Off. J. Int. Soc. Biorheol.* **2000**, *37*, 129–140. [CrossRef]

329. Li, G.; Yin, J.; Gao, J.; Cheng, T.S.; Pavlos, N.J.; Zhang, C.; Zheng, M.H. Subchondral Bone in Osteoarthritis: Insight into Risk Factors and Microstructural Changes. *Arthritis Res. Ther.* **2013**, *15*, 223. [CrossRef]
330. Volpin, G.; Dowd, G.; Stein, H.; Bentley, G. Degenerative Arthritis after Intra-Articular Fractures of the Knee. Long-Term Results. *J. Bone Jt. Surgery. Br. Vol.* **1990**, *72-B*, 634–638. [CrossRef]
331. Link, T.M.; Stahl, R.; Woertler, K. Cartilage Imaging: Motivation, Techniques, Current and Future Significance. *Eur. Radiol.* **2007**, *17*, 1135–1146. [CrossRef]
332. Goldring, M.B.; Goldring, S.R. Osteoarthritis. *J. Cell. Physiol.* **2007**, *213*, 626–634. [CrossRef]
333. Tiderius, C.J.; Olsson, L.E.; Leander, P.; Ekberg, O.; Dahlberg, L. Delayed Gadolinium-enhanced MRI of Cartilage (dGEMRIC) in Early Knee Osteoarthritis. *Magn. Reson. Med.* **2003**, *49*, 488–492. [CrossRef] [PubMed]
334. Burstein, D.; Bashir, A.; Gray, M.L. MRI Techniques in Early Stages of Cartilage Disease. *Investig. Radiol.* **2000**, *35*, 622–638. [CrossRef] [PubMed]
335. Regatte, R.R.; Akella, S.V.S.; Borthakur, A.; Kneeland, J.B.; Reddy, R. In Vivo Proton MR Three-Dimensional T1ρ Mapping of Human Articular Cartilage: Initial Experience. *Radiology* **2003**, *229*, 269–274. [CrossRef] [PubMed]
336. David-Vaudey, E.; Ghosh, S.; Ries, M.; Majumdar, S. T2 Relaxation Time Measurements in Osteoarthritis. *Magn. Reson. Imaging* **2004**, *22*, 673–682. [CrossRef]
337. Mariappan, Y.K.; Glaser, K.J.; Ehman, R.L. Magnetic Resonance Elastography: A Review. *Clin. Anat.* **2010**, *23*, 497–511. [CrossRef]
338. Lopez, O.; Amrami, K.K.; Manduca, A.; Rossman, P.J.; Ehman, R.L. Developments in Dynamic MR Elastography for in Vitro Biomechanical Assessment of Hyaline Cartilage under High-frequency Cyclical Shear. *J. Magn. Reson. Imaging Off. J. Int. Soc. Magn. Reson. Med.* **2007**, *25*, 310–320. [CrossRef]
339. Khalilzad-Sharghi, V.; Han, Z.; Xu, H.; Othman, S.F. MR Elastography for Evaluating Regeneration of Tissue-engineered Cartilage in an Ectopic Mouse Model. *Magn. Reson. Med.* **2016**, *75*, 1209–1217. [CrossRef]
340. Karpiński, R. Knee joint osteoarthritis diagnosis based on selected acoustic signal discriminants using machine learning. *Appl. Comput. Sci.* **2022**, *18*, 71–85. [CrossRef]
341. Machrowska, A.; Karpiński, R.; Maciejewski, M.; Jonak, J.; Krakowski, P. Application of eemd-dfa algorithms and ann classification for detection of knee osteoarthritis using vibroarthrography. *Appl. Comput. Sci.* **2024**, *20*, 90–108. [CrossRef]
342. Choi, D.; Ahn, S.; Ryu, J.; Nagao, M.; Kim, Y. Knee Acoustic Emission Characteristics of the Healthy and the Patients with Osteoarthritis Using Piezoelectric Sensor. *Sens. Mater.* **2018**, *30*, 1629. [CrossRef]
343. Vatolik, I.; Everington, M.; Hunter, G.; Swann, N.; Augousti, A.T. Development of a Multi-Modal Sensor Network to Detect and Monitor Knee Joint Condition. *Meas. Sens.* **2022**, *24*, 100483. [CrossRef]
344. Machrowska, A.; Karpiński, R.; Maciejewski, M.; Jonak, J.; Krakowski, P.; Syta, A. Multi-Scale Analysis of Knee Joint Acoustic Signals for Cartilage Degeneration Assessment. *Sensors* **2025**, *25*, 706. [CrossRef] [PubMed]
345. Georgas, E.; Rayes, A.; Zhang, J.; Zhou, Q.; Qin, Y.-X. Shear Wave Ultrasound Elastography for Estimating Cartilage Stiffness: Implications for Early Detection of Osteoarthritis. *Med-X* **2024**, *2*, 4. [CrossRef]
346. Zhou, X.; Eltit, F.; Yang, X.; Maloufi, S.; Alousaimi, H.; Liu, Q.; Huang, L.; Wang, R.; Tang, S. Detecting Human Articular Cartilage Degeneration in Its Early Stage with Polarization-Sensitive Optical Coherence Tomography. *Biomed. Opt. Express* **2020**, *11*, 2745. [CrossRef]
347. Chu, C.R.; Williams, A.; Tolliver, D.; Kwoh, C.K.; Bruno, S.; Irrgang, J.J. Clinical Optical Coherence Tomography of Early Articular Cartilage Degeneration in Patients with Degenerative Meniscal Tears. *Arthritis Rheum.* **2010**, *62*, 1412–1420. [CrossRef]
348. Li, X.; Martin, S.; Pitris, C.; Ghanta, R.; Stamper, D.L.; Harman, M.; Fujimoto, J.G.; Brezinski, M.E. High-Resolution Optical Coherence Tomographic Imaging of Osteoarthritic Cartilage during Open Knee Surgery. *Arthritis Res. Ther.* **2005**, *7*, R318. [CrossRef]
349. Korhonen, R.; Laasanen, M.; Töyräs, J.; Rieppo, J.; Hirvonen, J.; Helminen, H.; Jurvelin, J. Comparison of the Equilibrium Response of Articular Cartilage in Unconfined Compression, Confined Compression and Indentation. *J. Biomech.* **2002**, *35*, 903–909. [CrossRef] [PubMed]
350. Ma, Y.; Lin, Q.; Wang, X.; Liu, Y.; Yu, X.; Ren, Z.; Zhang, Y.; Guo, L.; Wu, X.; Zhang, X. Biomechanical Properties of Articular Cartilage in Different Regions and Sites of the Knee Joint: Acquisition of Osteochondral Allografts. *Cell Tissue Bank.* **2024**, *25*, 633–648. [CrossRef] [PubMed]
351. Kabir, W.; Di Bella, C.; Choong, P.F.; O'Connell, C.D. Assessment of Native Human Articular Cartilage: A Biomechanical Protocol. *Cartilage* **2021**, *13*, 427S–437S. [CrossRef]
352. Wang, S.-Z.; Huang, Y.-P.; Saarakkala, S.; Zheng, Y.-P. Quantitative Assessment of Articular Cartilage with Morphologic, Acoustic and Mechanical Properties Obtained Using High-Frequency Ultrasound. *Ultrasound Med. Biol.* **2010**, *36*, 512–527. [CrossRef]
353. Goodwin, M.; Workman, J.; Thambyah, A.; Vanholsbeeck, F. Impact-Induced Cartilage Damage Assessed Using Polarisation-Sensitive Optical Coherence Tomography. *J. Mech. Behav. Biomed. Mater.* **2021**, *117*, 104326. [CrossRef] [PubMed]
354. Catalano, E. Biophysical and Biomechanical Properties of Cartilage. *arXiv* **2023**, arXiv:2305.01529.

355. Pavlou, E.; Zhang, X.; Wang, J.; Kourkoumelis, N. Raman Spectroscopy for the Assessment of Osteoarthritis. *Ann. Jt.* **2018**, *3*, 83. [CrossRef]
356. Casal-Beiroa, P.; Balboa-Barreiro, V.; Oreiro, N.; Pértega-Díaz, S.; Blanco, F.J.; Magalhães, J. Optical Biomarkers for the Diagnosis of Osteoarthritis through Raman Spectroscopy: Radiological and Biochemical Validation Using Ex Vivo Human Cartilage Samples. *Diagnostics* **2021**, *11*, 546. [CrossRef] [PubMed]
357. Mason, D.; Murugkar, S.; Speirs, A.D. Measurement of Cartilage Sub-component Distributions through the Surface by Raman Spectroscopy-based Multivariate Analysis. *J. Biophotonics* **2021**, *14*, e202000289. [CrossRef]
358. Jensen, M.; Horgan, C.C.; Vercauteren, T.; Albro, M.B.; Bergholt, M.S. Multiplexed Polarized Hypodermic Raman Needle Probe for Biostructural Analysis of Articular Cartilage. *Opt. Lett.* **2020**, *45*, 2890–2893. [CrossRef]
359. Li, X.; Majumdar, S. Quantitative MRI of Articular Cartilage and Its Clinical Applications. *Magn. Reson. Imaging* **2013**, *38*, 991–1008. [CrossRef]
360. Park, E.H.; Fritz, J. The Role of Imaging in Osteoarthritis. *Best Pract. Res. Clin. Rheumatol.* **2023**, *37*, 101866. [CrossRef]
361. Mononen, M.E.; Jurvelin, J.S.; Korhonen, R.K. Implementation of a Gait Cycle Loading into Healthy and Meniscectomised Knee Joint Models with Fibril-Reinforced Articular Cartilage. *Comput. Methods Biomech. Biomed. Eng.* **2015**, *18*, 141–152. [CrossRef]
362. Peña, E.; Calvo, B.; Martínez, M.A.; Doblaré, M. A Three-Dimensional Finite Element Analysis of the Combined Behavior of Ligaments and Menisci in the Healthy Human Knee Joint. *J. Biomech.* **2006**, *39*, 1686–1701. [CrossRef]
363. Mononen, M.E.; Tanska, P.; Isaksson, H.; Korhonen, R.K. A Novel Method to Simulate the Progression of Collagen Degeneration of Cartilage in the Knee: Data from the Osteoarthritis Initiative. *Sci. Rep.* **2016**, *6*, 21415. [CrossRef] [PubMed]
364. Mohammadi, H.; Mequanint, K.; Herzog, W. Computational Aspects in Mechanical Modeling of the Articular Cartilage Tissue. *Proc. Inst. Mech. Eng. H* **2013**, *227*, 402–420. [CrossRef] [PubMed]
365. Smith, D.W.; Gardiner, B.S.; Davidson, J.B.; Grodzinsky, A.J. Computational Model for the Analysis of Cartilage and Cartilage Tissue Constructs: Computational Model for Cartilage and Cartilage Tissue Constructs Analysis. *J. Tissue Eng. Regen. Med.* **2016**, *10*, 334–347. [CrossRef]
366. Karpiński, R.; Krakowski, P.; Jonak, J.; Machrowska, A.; Maciejewski, M. Comparison of selected classification methods based on machine learning as a diagnostic tool for knee joint cartilage damage based on generated vibroacoustic processes. *Appl. Comput. Sci.* **2023**, *19*, 136–150. [CrossRef]
367. Ebrahimkhani, S.; Jaward, M.H.; Cicuttini, F.M.; Dharmaratne, A.; Wang, Y.; De Herrera, A.G.S. A Review on Segmentation of Knee Articular Cartilage: From Conventional Methods towards Deep Learning. *Artif. Intell. Med.* **2020**, *106*, 101851. [CrossRef]
368. Isensee, F.; Jaeger, P.F.; Kohl, S.A.A.; Petersen, J.; Maier-Hein, K.H. nnU-Net: A Self-Configuring Method for Deep Learning-Based Biomedical Image Segmentation. *Nat. Methods* **2021**, *18*, 203–211. [CrossRef] [PubMed]
369. Yao, Y.; Zhong, J.; Zhang, L.; Khan, S.; Chen, W. CartiMorph: A Framework for Automated Knee Articular Cartilage Morphometrics. *Med. Image Anal.* **2023**, *91*, 103035. [CrossRef]
370. Liu, F.; Zhou, Z.; Samsonov, A.; Blankenbaker, D.; Larison, W.; Kanarek, A.; Lian, K.; Kambhampati, S.; Kijowski, R. Deep Learning Approach for Evaluating Knee MR Images: Achieving High Diagnostic Performance for Cartilage Lesion Detection. *Radiology* **2018**, *289*, 160–169. [CrossRef]
371. Karpiński, R.; Krakowski, P.; Jonak, J.; Machrowska, A.; Maciejewski, M.; Nogalski, A. Diagnostics of Articular Cartilage Damage Based on Generated Acoustic Signals Using ANN—Part I: Femoral-Tibial Joint. *Sensors* **2022**, *22*, 2176. [CrossRef]
372. Tiulpin, A.; Klein, S.; Bierma-Zeinstra, S.M.A.; Thevenot, J.; Rahtu, E.; Meurs, J.V.; Oei, E.H.G.; Saarakkala, S. Multimodal Machine Learning-Based Knee Osteoarthritis Progression Prediction from Plain Radiographs and Clinical Data. *Sci. Rep.* **2019**, *9*, 20038. [CrossRef]
373. Sharma, B.; Fermanian, S.; Gibson, M.; Unterman, S.; Herzka, D.A.; Cascio, B.; Coburn, J.; Hui, A.Y.; Marcus, N.; Gold, G.E.; et al. Human Cartilage Repair with a Photoreactive Adhesive-Hydrogel Composite. *Sci. Transl. Med.* **2013**, *5*, 167ra6. [CrossRef] [PubMed]
374. Cai, L.; Nauman, E.A.; Pedersen, C.B.W.; Neu, C.P. Finite Deformation Elastography of Articular Cartilage and Biomaterials Based on Imaging and Topology Optimization. *Sci. Rep.* **2020**, *10*, 7980. [CrossRef]
375. Albano, D.; Viglino, U.; Esposito, F.; Rizzo, A.; Messina, C.; Gitto, S.; Fusco, S.; Serpi, F.; Kamp, B.; Müller-Lutz, A.; et al. Quantitative and Compositional MRI of the Articular Cartilage: A Narrative Review. *Tomography* **2024**, *10*, 949–969. [CrossRef]
376. Żylińska, B.; Sobczyńska-Rak, A.; Lisiecka, U.; Stodolak-Zych, E.; Jarosz, Ł.; Szponder, T. Structure and Pathologies of Articular Cartilage. *In Vivo* **2021**, *35*, 1355–1363. [CrossRef] [PubMed]
377. Solanki, K.; Shanmugasundaram, S.; Shetty, N.; Kim, S.-J. Articular Cartilage Repair & Joint Preservation: A Review of the Current Status of Biological Approach. *J. Clin. Orthop. Trauma* **2021**, *22*, 101602. [CrossRef] [PubMed]
378. Sharif, M.U.; Aslam, H.M.; Iftakhar, T.; Abdullah, M. Pathophysiology of Cartilage Damage in Knee Osteoarthritis and Regenerative Approaches toward Recovery. *J. Bone Jt. Dis.* **2024**, *39*, 32–44. [CrossRef]

379. Bannuru, R.R.; Osani, M.; Vaysbrot, E.; Arden, N.; Bennell, K.; Bierma-Zeinstra, S.; Kraus, V.; Lohmander, L.S.; Abbott, J.; Bhandari, M. OARSI Guidelines for the Non-Surgical Management of Knee, Hip, and Polyarticular Osteoarthritis. *Osteoarthr. Cartil.* **2019**, *27*, 1578–1589. [CrossRef]
380. Mithoefer, K.; Williams III, R.J.; Warren, R.F.; Potter, H.G.; Spock, C.R.; Jones, E.C.; Wickiewicz, T.L.; Marx, R.G. The Microfracture Technique for the Treatment of Articular Cartilage Lesions in the Knee: A Prospective Cohort Study. *J. Bone Jt. Surg.* **2005**, *87*, 1911–1920. [CrossRef]
381. Hangody, L.; Füles, P. Autologous Osteochondral Mosaicplasty for the Treatment of Full-Thickness Defects of Weight-Bearing Joints: Ten Years of Experimental and Clinical Experience. *J. Bone Jt. Surg.* **2003**, *85*, 25–32. [CrossRef]
382. Le, J.; Peng, Q.; Sperling, K. Biochemical Magnetic Resonance Imaging of Knee Articular Cartilage: T1rho and T2 Mapping as Cartilage Degeneration Biomarkers. *Ann. N. Y. Acad. Sci.* **2016**, *1383*, 34–42. [CrossRef]
383. Nissi, M.J.; Rieppo, J.; Töyräs, J.; Laasanen, M.S.; Kiviranta, I.; Nieminen, M.T.; Jurvelin, J.S. Estimation of Mechanical Properties of Articular Cartilage with MRI–dGEMRIC, T2 and T1 Imaging in Different Species with Variable Stages of Maturation. *Osteoarthr. Cartil.* **2007**, *15*, 1141–1148. [CrossRef] [PubMed]
384. Bini, F.; D'Alessandro, S.; Pica, A.; Marinozzi, F.; Cidonio, G. Harnessing Biofabrication Strategies to Re-Surface Osteochondral Defects: Repair, Enhance, and Regenerate. *Biomimetics* **2023**, *8*, 260. [CrossRef] [PubMed]
385. Kotecha, M.; Yin, Z.; Magin, R.L. Magnetic Resonance in the Assessment of Tissue Engineered Cartilage. In *Biophysics and Biochemistry of Cartilage by NMR and MRI*; Xia, Y., Momot, K., Eds.; The Royal Society of Chemistry: London, UK, 2016; pp. 529–551. ISBN 978-1-78262-133-1.

Disclaimer/Publisher's Note: The statements, opinions and data contained in all publications are solely those of the individual author(s) and contributor(s) and not of MDPI and/or the editor(s). MDPI and/or the editor(s) disclaim responsibility for any injury to people or property resulting from any ideas, methods, instructions or products referred to in the content.